Robust investment strategies for electricity distribution network expansion:

Applying Robust Decision Making method and EMA to address future grid congestion in the Netherlands

EPA2942: Master thesis EPA

Maryvonne Marang

TU Delft

Robust investment strategies for electricity distribution network expansion:

Applying Robust Decision Making method and EMA to address future grid congestion in the Netherlands

Master thesis research by

Maryvonne Marang

to obtain the degree of Master of Science
at the Delft University of Technology
Faculty of Technology, Policy and Management

To be defended publicly on Tuesday July 9, 2025 at 1:30 PM.

The simulation model and analysis code developed for this thesis ae available on GitHub: https://github.com/mmarang/Thesis
Access is possible under certain conditions.

First supervisor:	Igor Nikolic
Second supervisor:	Jan Kwakkel
External supervisor:	Arjan van Voorden
External supervisor:	Ton Wurth
Project Duration:	February 13, 2025 - July 9, 2025
MSc programme:	Engineering Policy Analysis

Cover: Müller, R. (2024, April 3). *Grid congestion: What is it and how do we solve it?* Tibo Energy. https://tibo.energy/blog/grid-congestion-explained/

TU Delft

STEDIN.NET

Preface

With this thesis, I conclude my two-year master's in Engineering Policy Analysis (EPA) at TU Delft. It marks the final step of my academic journey, which began with a bachelor's degree in Management, Society & Technology. Over the years, I have had numerous opportunities to develop both my knowledge and skills, and my time at TU Delft has been instrumental in preparing me for the next chapter of my career. My passion for sustainability has been the driving force behind my academic and professional choices. While I did not choose the Energy & Industry track during my bachelor's, my minor was focused on sustainability, which solidified my interest in this field. Throughout my studies, I engaged in various projects related to sustainability, and my interest in data-driven decision-making grew. Although I had some experience with coding from my bachelor's, my skills developed significantly during my master's. It was during the course 'Model-Based Decision Making' that I was introduced to the EMA Workbench and Jan Kwakkel's work. I had already envisioned incorporating simulation into my thesis, but this course confirmed my desire to apply the EMA Workbench to real-world energy challenges.

This thesis would not have been possible without the guidance and support of several individuals. I would like to thank Alexander Verbraeck, who played a crucial role in helping me find the right direction for my thesis. His advice led me to Igor Nikolic, my first supervisor, who introduced me to this project. From the moment I learned about it, I knew it was the perfect fit for me. I would also like to express my appreciation to Ton Wurth, who was always available to answer my questions and provided invaluable support during the initial phases of my research. A special thanks goes to my Stedin supervisor, Arjan van Voorden, as well as the entire team at Stedin, for their warm welcome and for sharing their knowledge and data, which were essential to this study. Lastly, I would like to thank my friends, family, and everyone who has supported me throughout this journey. I am happy to end this chapter of my life and I look forward to what comes next.

Maryvonne Marang
The Hague, June 2025

Summary

The Netherlands is undergoing a major transformation in its energy landscape as it pursues ambitious climate goals, including achieving climate neutrality by 2050 [50]. Central to this transition is a rapid shift towards electrification and the decentralization of energy production, with households, businesses, and industries increasingly relying on electricity from renewable sources such as solar and wind [53]. However, this transformation has placed significant stress on the existing electricity grid. Grid congestion has become a pressing concern, already affecting nine out of twelve Dutch provinces [35]. It delays new business connections, hinders housing development, and threatens to stall progress on national climate targets [53].

At the core of this issue lies a misalignment between the evolving demands on the electricity grid and its physical and operational capacity. The Dutch electricity grid, particularly at the medium- and low-voltage distribution level, was never designed to handle such dynamic, bidirectional flows of power [30]. Adding to this challenge is the high degree of uncertainty surrounding future developments in electricity demand, technology adoption, and policy direction. Factors such as the rate of electric vehicle (EV) uptake, the adoption of electric heating systems, and the pace of solar photovoltaic (PV) deployment introduce complexity and unpredictability that traditional planning methods—based largely on deterministic forecasts—struggle to accommodate.

This thesis addresses a critical gap in current grid planning approaches: the absence of a structured method for incorporating deep uncertainty into long-term investment strategies for medium-voltage distribution networks. While Robust Decision Making (RDM) has been explored in the context of transmission expansion and national-level energy planning [57], no peer-reviewed studies to date have applied RDM to distribution network expansion planning. This represents a significant research gap, especially given the increasing congestion and complexity at the distribution level due to decentralized energy resources. Traditional planning methods—such as deterministic or stochastic models—often rely on historical data and predefined probabilities, making them ill-suited to handle the deep uncertainty surrounding future demand, technology adoption, and infrastructure delays [19]. To address this, the present study applies RDM, supported by the Exploratory Modeling and Analysis (EMA) Workbench, to stress-test and improve the robustness of Stedin's distribution network investment plan. In doing so, it provides the first academic application of RDM in this context and introduces an adaptive, scenario-based framework for planning under uncertainty.

The central research question of this thesis is: **How robust is Stedin's investment plan for distribution network expansion under deep uncertainty?** To answer this question, three sub-questions guided the research:

1. What are the key characteristics of long-term uncertainty in distribution network expansion planning?
2. What is the design of a simulation model that can effectively stress-test a distribution network expansion plan across multiple scenarios?
3. What actionable advice can stress-testing provide for Stedin's investment decisions?

Through a combination of literature review and a focus group with professionals from Stedin, eleven critical uncertainties were identified. These included behavioral variables (e.g., EV charging patterns), technological developments (e.g., shore power and rooftop solar), and infrastructural variables (e.g., delays in ring relocation). These uncertainties were structured using the XLRM framework, which helped categorize the relationships between uncertainties (X), decision levers (L) like relocation of rings and adding a new substation, system relationships (R), and the performance metrics (M) capacity risk and cost.

Following the identification of key uncertainties, a simulation model was developed and implemented in the EMA Workbench to replicate the behavior of a representative medium-voltage distribution network in Stedin's service area. The model incorporated a baseline of existing infrastructure, projected demand profiles, and Stedin's proposed investment levers, including substation construction and ring relocation. To explore how the network performs under diverse future conditions, the model was calibrated with real-world data and evaluated by randomly sampling discrete scenario pathways. This approach enabled the generation of thousands of plausible scenarios by systematically varying the identified uncertainties, providing a comprehensive basis for stress-testing the robustness of the investment plan. The primary outcomes evaluated by the simulation model are capacity risk and cost. Here, capacity risk refers to the risk of insufficient grid capacity to meet future electricity demand due to deep uncertainties in demand growth, technology adoption, and infrastructure delays. These metrics enable a robust assessment of how well Stedin's investment plan can perform under a broad spectrum of uncertain futures.

The simulation results revealed that Stedin's original investment plan was not robust: the current substation experienced capacity risks in 100% of simulated scenarios. Significant vulnerabilities emerged in the mid-term—particularly around 2034 and 2037—as well as in the long-term years 2049 and 2052, highlighting the plan's inability to cope with a wide range of uncertain futures. To better understand these weaknesses, the Patient Rule Induction Method (PRIM) was used to identify clusters of high-risk scenarios. Based on these insights, a second iteration of the investment plan was developed. This revised plan involved realizing the new substation as early as 2025—rather than relying on a demand threshold trigger—and ensuring that upcoming solar parks would be connected exclusively to the new substation, rather than adding further load to the existing one. This adjusted strategy demonstrated a marked improvement in robustness across simulated futures. On the basis of these results, a set of prioritized recommendations for Stedin was developed using the MoSCoW framework.

1. **Must-have**
   These are the most urgent and impactful actions that should be prioritized:
   - Start construction of the new substation in 2025, independent of the original 40,000 kW demand threshold. Early construction addresses sharp demand increases expected after 2028 and significantly reduces capacity risks peaking in 2034 and 2037.
   - Manage rooftop solar PV growth on industrial buildings proactively by:
     - Conducting detailed grid impact studies before approving new rooftop solar projects on industrial buildings, especially in vulnerable areas.
     - Promoting co-located battery energy storage systems to absorb excess generation and mitigate reverse power flows.
2. **Should-have**
   These actions support the effectiveness of the must-haves and reduce the risk of failure:
   - Ensure timely delivery of the new substation through robust project management, contingency planning, and active stakeholder coordination. Delays of even one to two years significantly increase capacity risks in 2031 and 2034.
3. **Could-have**
   These are beneficial long-term actions that can enhance future robustness:
   - Plan for additional capacity expansions after 2046, such as a potential third substation or upgrades to existing infrastructure.
   - Explore flexible operational strategies, like dynamic load management, to accommodate future rooftop solar PV expansion and improve grid robustness.
4. **Won't-have**
   These are actions outside Stedin's scope or with limited influence:
   - Avoid interventions focused on societal developments such as air conditioning adoption rates or heat transition rollout speed, as these are largely outside Stedin's direct influence.

In conclusion, the second iteration of Stedin's investment plan marks a meaningful improvement in robustness compared to the original threshold-based plan. The proportion of scenarios in which the new substation faces no capacity risk remains relatively stable—around 46.6%—but the current substation sees a notable improvement, rising from 0% in the original plan to 23.4% in the updated plan. However, the analysis also reveals that capacity risks remain in the majority of simulated futures, indicating that even the updated plan does not yet meet the threshold for full robustness. Temporal analysis shows mid-term vulnerabilities at the current substation, especially in 2031 and 2034, largely driven by delays in infrastructure delivery. Meanwhile, risks at the new substation emerge primarily in the long term (2049 and 2052), driven by high levels of decentralized solar PV generation. These patterns suggest that infrastructure investments alone will not be sufficient. Strengthening the robustness of the distribution network expansion plan will require timely execution of critical upgrades alongside targeted, non-infrastructure measures—particularly around rooftop solar management. While the revised plan is a significant step forward, further adaptive actions are essential to ensure robust and reliable grid performance across a deeply uncertain energy future.

Contents

List of abbreviations

Abbreviations

Abbreviation	Definition
EV	Electric vehicle
PV	Photovoltaic
DSOs	Distributed System Operators
RDM	Robust Decision Making
EMA	Exploratory Modeling and Analysis
EPA	Engineering and Policy Analysis
EDA	Exploratory data analysis
DERs	Distributed energy resources
VPPs	Virtual Power Plants
DRO	Distributionally robust optimization
PRIM	Patient Rule Induction Method
eHP	Electric heat pump
HHP	Hybrid heat pump
Airco	Air conditioning
NPV	Net Present Value

List of Figures

List of Tables

1 Introduction

1.1. Background

The Netherlands is facing a growing electricity grid crisis as it accelerates towards its 2050 climate neutrality goal [50]. Businesses are being told they must wait years for new electricity connections, while housing developments are delayed due to limited grid capacity [53]. Grid congestion is no longer a distant concern—it is already slowing the energy transition and threatening economic growth.

Currently, nine out of twelve provinces in the Netherlands are experiencing grid congestion, causing delays in connecting new businesses, homes, and clean energy projects [35]. These challenges are expected to intensify as electric vehicle (EV) adoption, heat pump installations, and solar photovoltaic (PV) systems realization continue to accelerate [14]. Demand peaks—such as mass EV charging and home heating on cold evenings—combined with the intermittent nature of renewables, introduce volatility that the grid was never designed to manage [30]. If these trends continue, up to 1.5 million households could be affected by congestion by 2030 [35].

At the core of this crisis lies a profound shift in how electricity is produced and consumed—marked by decentralization, electrification, and variability. Households, industries, and transportation rapidly electrify, while fossil fuels are being phased out in favor of renewable sources such as wind and solar [53]. To meet European climate targets—such as a 55% CO_2 reduction by 2030 and the broader ambitions of the European Green Deal—the Dutch energy system must undergo a large-scale, accelerated transition [36, 33]. This transformation is pushing the electricity grid far beyond what it was originally designed to handle. The system, once built for predictable, one-directional energy flows from large, centralized power plants, must now absorb growing and fluctuating demand from electrified households, industries, and vehicles. At the same time, it must accommodate large volumes of renewable electricity—much of it generated locally through decentralized sources such as rooftop solar and onshore wind. These shifts were not anticipated when much of today's infrastructure was developed—and adapting to them is neither straightforward nor quick [15]. As a result, grid operators and policymakers face difficult decisions about how, where, and when to invest in expansion, often without clear guidance on which strategies will remain effective in the face of ongoing change.

The Dutch electricity grid consists of a high-voltage transmission network managed by TenneT and medium- and low-voltage distribution networks operated by Distributed System Operators (DSOs) such as Stedin and Alliander. TenneT oversees the bulk transport of electricity across the country, while the DSOs ensure that electricity reaches households, businesses, and other end users through local substations [51]. Historically, this system has delivered reliable power. However, today's surge in electricity demand and the decentralized growth of renewable generation create severe capacity bottlenecks, particularly at the distribution level [36].

Long-term grid expansion strategies are essential to address the growing risk of grid congestion and ensure the energy system can support future demands. Recognizing the need for urgent action, the Dutch government launched the National Grid Congestion Action Program, focusing on accelerating grid expansion, optimizing infrastructure, and enhancing energy flexibility [36]. While there is a system-

atic approach to grid planning, Alliander (2023) stresses the need for long-term solutions, including grid expansion and strategic investments. However, existing planning approaches do not adequately account for the deep uncertainties surrounding demand growth, technology adoption, and policy changes, which could result in either underinvestment or overinvestment. Therefore, a more robust and flexible framework for long-term grid investment planning is crucial to ensure the grid can meet the demands of a rapidly changing energy landscape [29].

1.2. Problem definition

A key barrier to adequately plan grid expansions is the deep uncertainty surrounding the future of electricity demand and renewable energy development. The energy transition is transforming both the scale and shape of electricity use, but the exact trajectory of this transformation is inherently difficult to predict [37]. Yet, grid planning in the Netherlands relies predominantly on deterministic forecasts, single-scenario projections that assume a stable and predictable evolution of demand and supply [56]. This approach offers limited insight into the wide range of possible futures facing the grid.

The sources of uncertainty for grid expansion planning are numerous and interconnected. On the demand side, growth depends, among others, on the rate of EV and heat pump adoption and the extent to which industry electrifies its operations [5]. These trends are shaped by consumer behavior, market developments, and policy interventions—each of which can change rapidly. On the supply side, the expansion of renewable energy is influenced by subsidies, permitting processes, and spatial constraints. The variable output of solar and wind energy adds further complexity to grid planning [7].

Emerging technologies offer potential solutions—but also introduce new uncertainty. Large-scale batteries, vehicle-to-grid integration, and demand-side flexibility could significantly reshape grid dynamics, yet their timing, scalability, and regulatory integration remain unclear [59]. Policy adds an additional layer of unpredictability: national decarbonization goals, local zoning regulations, and financial incentives may shift with political priorities, creating instability in long-term planning [12]. Finally, local and regional developments often deviate from expectations. Housing construction, industrial expansion, and regional economic trends can diverge from official projections, creating unforeseen pressure points in distribution networks [7].

These factors create a planning environment defined by deep uncertainty. This type of uncertainty arises when future developments lack known probability distributions and when decisions impact stakeholders with conflicting values and objectives [25]. Grid expansion decisions affect a wide range of actors, including network operators, policymakers, consumers, industries, and local communities, each with potentially conflicting interests and risk perceptions. In such a context, traditional planning methods that optimize for a “most likely” future are no longer adequate. Instead, ensuring the long-term robustness of the electricity grid requires adaptive and forward-looking planning approaches: methods capable of identifying vulnerabilities of a plan across a wide range of scenarios, incorporating diverse stakeholder perspectives, and enabling decisions that can adapt as conditions and interests evolve.

1.3. Research objective and question

This study adopts an unbundled market perspective, in which developments such as rooftop PV deployment are considered external uncertainties rather than controllable variables for infrastructure planners. This research focuses on the expansion planning for a medium voltage distribution network operated by Stedin, specifically the area served by substations A (50/13 kV). In this region, electricity demand and renewable energy developments are expected to grow substantially in the coming years. As a result, there is a risk that the existing grid infrastructure will become inadequate to meet future capacity requirements. To address this challenge, Stedin has developed an investment plan aimed at expanding and reinforcing the network. However, given the deep uncertainties surrounding future demand growth, renewable energy adoption, and technological developments, it is crucial to assess whether this plan is sufficiently robust under a wide range of possible futures.

This study applies the Robust Decision Making (RDM) method to evaluate alternative rerouting strategies. RDM is a decision-support approach designed to identify investment strategies that perform well across many plausible future scenarios, rather than relying on a single forecast or best estimate [57]. By stress-testing plans under uncertainty, RDM helps identify potential vulnerabilities, ultimately enhancing the robustness and performance of the plans.

The analysis will employ the Exploratory Modeling and Analysis (EMA) Workbench. This tool allows

grid planners to simulate thousands of future scenarios and assess the performance of alternative expansion strategies [21]. The research question that will be addressed is:

How robust is Stedin's investment plan for distribution network expansion under deep uncertainty?

1.4. EPA relevance

This study aligns with the mission of the Engineering and Policy Analysis (EPA) program by addressing a key societal challenge, ensuring robust electricity networks amidst growing demand and uncertainty. The complexity of electricity grid expansion planning extends beyond technical challenges as many stakeholders are affected. Effective long-term planning must balance the needs of policymakers, businesses, and consumers, ensuring equitable energy access and avoiding situations where certain groups face disadvantages such as delays in connection or higher costs. Importantly, capacity shortages can also hinder the energy transition itself. Without sufficient infrastructure, households and businesses may be unable to adopt sustainable technologies such as electric heat pumps, EV charging systems, or even connect new assets to the grid. This can exacerbate regional disparities and delay decarbonization efforts. Congestion is already unevenly distributed across the Netherlands, with certain regions and sectors being hit harder than others. For example, in some residential areas with long, thin low-voltage cables, rooftop solar panels are frequently disconnected without warning due to voltage congestion [24]. Homes located farther from the local transformer are typically the first to be affected, while those closer to the transformer continue operating normally. As a result, some households lose out on solar earnings more often than their neighbors—despite living on the same street. This uneven impact highlights not only the technical limitations of the grid, but also raises broader concerns about fairness and energy justice. By applying RDM in this context, this research integrates technical, economic, and social considerations into grid planning. The approach helps identify strategies that perform well across a wide range of possible future developments. In doing so, it supports decisions that are robust, adaptable, and fair—ensuring that investments in the electricity grid contribute not only to energy security and climate goals, but also to social equity. This contribution is closely aligned with the EPA program's broader goal of supporting policy-relevant decision-making under deep uncertainty.

1.5. Outline

This chapter has outlined the problem this research aims to address and formulated the research objective and question to achieve this goal. Chapter 2 reviews the state of the art in distribution network expansion planning, with a focus on how long-term uncertainties are addressed. Key research gaps are identified, highlighting the need for change. Chapter 3 outlines the research design, detailing the methodological approach used to answer the research questions. A flow diagram illustrates the overall research process, and each sub-question is paired with the specific method used to address it. In Chapter 4, the first sub-question is discussed and the conceptualization of the distribution network is presented, forming the foundation for subsequent analysis. Chapter 5 covers the data preparation and cleaning procedures, followed by an exploratory data analysis (EDA) to identify key patterns and trends. Chapter 6 centers on model implementation, explaining the development and application of the simulation model. Chapter 7 presents the simulation results, upon which a PRIM analysis is performed to evaluate the influence of various variables. Key trigger points that may require adjustments are identified, and the model is rerun with the updated investment plan to test its adaptability under different scenarios. Chapter 8 offers practical advice on how to improve the investment plan. The thesis concludes with a discussion in Chapter 9 and final conclusions in Chapter 10.

2

Literature review

2.1. Literature search strategy

The aim of this literature review is to support the central research question: **How robust is Stedin's investment plan for distribution network expansion under deep uncertainty?** To structure the search, three key concepts were derived directly from the research question:

- **Distribution network expansion** captures the technical and strategic challenges of scaling electricity infrastructure to meet future demand
- **Planning under deep uncertainty** relates to how unpredictable developments—such as fluctuating demand, renewable energy integration, and policy changes—affect long-term infrastructure decisions
- **Robustness of investment plans** refers to approaches for testing whether long-term plans remain effective across a wide range of uncertain future conditions

These three concepts informed the development of search keywords and variations, which were used in an iterative and exploratory literature search using Google Scholar as the primary tool. Google Scholar was chosen for its broad coverage of peer-reviewed academic publications, including journal articles, conference papers, and theses.

Search terms were used both individually and in combination—for instance, pairing "distribution expansion planning" with "uncertainty" or combining "robust decision-making" with "electricity grid"—to reflect different dimensions of the research question. Table 2.1 summarizes how each concept was translated into keywords, along with representative sources.

After receiving the search results, an initial screening was conducted by reviewing the titles and publication dates of the articles to ensure topical relevance and a balance between foundational literature and more recent developments. For titles that appeared relevant, the abstract was read. If the abstract aligned with the focus of the literature review, the article was read in more depth. Articles were included based on their contribution to the understanding of uncertainty in electricity grid expansion, planning methods, and scenario-based approaches.

Keywords / concepts	Selected sources
Deep uncertainty	[54]
Adaptive and robust planning in grid distribution expansion	[58, 26]
Smart grids and renewables	[34]
Distribution expansion planning with uncertainty	[27]
Uncertainties in distribution grid expansion	[3]
Distribution grid planning	[19]
Multi stage optimization distribution grid planning	[40]

Table 2.1: Overview of concepts and related sources

In addition to general academic sources, targeted searches focused on the Dutch context. For example, searches such as “grid congestion in the Netherlands” led to the inclusion of a relevant master thesis by Michiel van Dalsum. This source was used for snowball sampling, which brought in additional relevant works including [14] and a report by [31] on Dutch grid constraints.

To ensure inclusion of key contributions in the field of planning under deep uncertainty, targeted searches were conducted for publications by Jan Kwakkel, a leading researcher in this domain. Kwakkel is known for his extensive work on robust decision-making, adaptive policy design, and exploratory modeling. He is also the primary developer of the EMA Workbench, an open-source tool widely used for scenario discovery and decision support under conditions of deep uncertainty. As such, his publications represent a significant portion of the methodological foundation for this review. Relevant works identified through this targeted search include [21, 23], along with joint publications by Kwakkel and Haasnoot and Shavazipour et al. published in 2021 and 2025, which offer valuable insights into the use of modeling, simulation, and decision frameworks for electricity grid planning under uncertainty.

Lastly, literature related to the application of RDM within the Gridmaster project was identified through a direct Google search. This search was based on prior knowledge that the RDM approach had been applied in this context. The search led to the inclusion of [57], a publication that documents the use of RDM in electricity grid planning.

2.2. Definition of core concepts

Before analyzing the state of the art in grid planning, it is essential to define the three key concepts that underpin the challenges and solutions discussed in this chapter: grid congestion, deep uncertainty, and adaptive and robust planning.

Grid congestion occurs when electricity flows in the distribution network exceed the technical limits of the infrastructure, such as thermal ratings of cables or transformers, or voltage tolerances. Grid congestion is not simply a matter of demand exceeding supply. It occurs when conditions such as thermal overloads, voltage instability, or forced curtailment of generation or demand create operational constraints that compromise the reliable functioning of the grid [3]. Traditional electricity grids were designed for centralized power generation with predictable power flows [31]. However, the increasing integration of distributed energy resources (DERs)—such as PV systems, wind turbines, EVs, and battery storage—has fundamentally altered this landscape. These DERs introduce bidirectional power flows and heightened variability in supply and demand, creating localized congestion issues that require new planning methodologies [14].

A major challenge in addressing congestion is deep uncertainty, a concept introduced in the previous chapter to describe situations where future developments are highly unpredictable and difficult to quantify [54]. Conventional risks, while uncertain, are often situations where possible outcomes and their probabilities can be estimated based on historical data or well-understood models. For example, equipment failure rates represent conventional risks that can typically be quantified using probabilistic forecasting based on historical data. In contrast, deep uncertainty arises when key variables, relationships, or external conditions are not well understood or are subject to rapid and unprecedented change. This means that not only are the outcomes unknown, but the probabilities themselves cannot be reliably assigned or may change over time. In the context of electricity grid planning, this includes uncertainties related to technological innovation, policy shifts, or societal changes that could dramatically alter future demand and supply patterns. Because these factors are not easily modeled or predicted, standard probabilistic methods fall short. Instead, planners must rely on robust and adaptive strategies—approaches designed to perform well across many plausible futures and to accommodate the perspectives of multiple stakeholders with potentially conflicting interests, without relying on precise probability estimates.

To navigate these challenges, planners are increasingly turning to approaches that are both robust and adaptive. Robust planning aims to ensure acceptable performance across a wide range of plausible futures, rather than optimizing for a single predicted scenario [38]. Adaptive planning, on the other hand, enables decisions to evolve over time in response to new information or changing conditions [57]. While traditional grid investments—such as cable reinforcements and substation upgrades—are often seen as rigid and capital-intensive, they too can be made adaptive. For example, a ring configuration

can be designed to convert into a new substation once demand surpasses a certain threshold. When planned with flexibility in timing or scale, such physical infrastructure can contribute to both robustness and adaptivity under deep uncertainty. Smart grid technologies—like sensors, automation, and real-time energy management—further enhance adaptivity by enabling short-term operational flexibility [34]. By combining these physical and digital strategies, and embedding both robust and adaptive principles across investment types, planners can better manage long-term uncertainty while ensuring system reliability.

2.3. State of the art

Building on the foundational concepts of congestion, deep uncertainty, and adaptive and robust planning, this section reviews the latest approaches to distribution network expansion planning under long-term uncertainty.

2.3.1. Current approaches to long-term grid expansion planning under deep uncertainty

Traditional grid planning methods rely primarily on deterministic or probabilistic approaches that use historical data to forecast future conditions [19]. However, these methods struggle under deep uncertainty, where future developments cannot be reliably predicted. Many existing approaches attempt to address uncertainty using stochastic methods, which model it through probability distributions derived from past data [26]. While this can be effective in stable environments with well-understood risks, it becomes problematic in dynamic contexts like the energy transition, where probabilities are difficult to define and emerging risks may not follow historical patterns. As a result, these models may offer a false sense of precision and fail to account for disruptive or unknown developments. Moreover, they often fail to capture systemic risks, such as cascading failures, which can be triggered by high-impact, low-probability events. While these operational risks are important considerations in grid security, the focus of this research is on long-term capacity challenges driven by structural developments in the energy transition. Therefore, operational risk management falls outside the scope of this study.

One major driver of uncertainty is the rapid transition from fossil fuels to renewable energy sources, particularly PV systems and wind turbines. These DERs introduce volatility into the grid, leading to challenges such as voltage instability, reverse power flows, and overloading of grid components [3]. While research has explored proactive control strategies—such as optimal controller placement to manage voltage fluctuations—these solutions alone may not be sufficient to address long-term uncertainties [3].

Another critical challenge lies in balancing long-term investment decisions with short-term operational constraints. Renewable energy sources, with their fluctuating outputs, introduce significant variability. If this variability is not incorporated into planning, it can lead to inefficiencies. To effectively manage both short-term variability and deep long-term uncertainty, multistage planning frameworks have gained traction. These frameworks enable phased investments and adaptive adjustments over time, allowing planners to respond flexibly as conditions and information evolve [27]. This approach enhances decision quality by delaying costly infrastructure upgrades until they are truly necessary, thereby reducing financial risks associated with uncertain energy transitions.

An example of this approach is the multi-stage co-optimization framework proposed by [40], which integrates long-term infrastructure investments—such as the addition of distributed generation and new feeders—with operational strategies like network reconfiguration. Their model demonstrates how staged investments can be optimized alongside flexible operations, allowing the grid to adapt more effectively to evolving conditions and deep uncertainty.

At the same time, emerging technologies in the smart grid landscape—such as Virtual Power Plants (VPPs) and community-based prosumer networks—offer complementary solutions to the challenges posed by distributed energy integration. VPPs aggregate distributed energy resources, storage, and controllable loads, enabling decentralized optimization of energy flows and improving market responsiveness [34]. Prosumer communities, by sharing and trading energy within localized grids, contribute to local balancing. While these models primarily focus on operational flexibility and market dynamics, they also play a key role in adaptive grid planning strategies. By enhancing the grid's ability to cope

with variability, they support traditional infrastructure investments and provide a dynamic response to the uncertainties faced in long-term planning.

These emerging models show that decentralized coordination is both feasible and impactful. However, much of the existing research on smart grids and microgrids remains narrowly focused. Many studies emphasize localized technical robustness without adequately addressing the broader, large-scale challenges of distribution network expansion—particularly in the context of long-term uncertainty and diverse stakeholder interests. At the same time, network planning for both transmission and distribution networks continue to struggle with future uncertainties. Transmission expansion planning is more mature, with established frameworks for long-term capacity forecasting and investment decision-making. However, these frameworks still face significant challenges in managing deep structural uncertainty, particularly as energy systems become increasingly complex and decentralized. Distribution network planning, on the other hand, faces additional complexities, such as localized congestion and high penetration of distributed energy resources, yet it also lacks robust methods to incorporate uncertainty into strategic decision-making. These gaps underscore the need for systematic, data-driven approaches that integrate stakeholder perspectives and address long-term uncertainty at scale.

2.3.2. Integrating adaptive and robust planning in grid expansion

To overcome the limitations of traditional planning, researchers increasingly incorporate adaptive and robust planning principles into grid expansion strategies. As discussed earlier, these approaches focus on maintaining flexibility and performance across a range of uncertain futures.

In practice, adaptive planning enables decision-makers to revise investment strategies in response to real-time indicators. For example, trigger-based mechanisms can activate grid upgrades when specific thresholds—such as rising DER adoption or increased peak loads—are crossed. Robust planning, in turn, focuses on identifying strategies that perform reasonably well across multiple plausible futures, mitigating the risks of stranded assets or unmet demand if reality deviates from forecasts.

To address the challenges of uncertainty and limited coordination in unbundled electricity markets, recent studies propose integrating distributionally robust optimization (DRO) into grid expansion planning. For example, [58] develop a two-stage DRO-based model for joint planning of electric vehicle charging systems and distribution networks. Their approach explicitly models uncertainties in distributed generation and EV charging demand without relying on centralized control or perfect foresight. The method achieves reliable investment decisions by balancing economic costs with reliability benefits quantified through failure rate–based metrics. By embedding uncertainty directly into the planning framework, the model offers robust performance across a range of plausible futures and remains applicable within regulatory constraints of unbundled systems.

While this approach significantly improves robustness over deterministic methods, it still relies on a predefined uncertainty set and lacks mechanisms for iterative, adaptive adjustment as new information emerges. This is where RDM offers complementary benefits, by enabling planners to examine a broader space of possible futures and to embed adaptive triggers more dynamically, as discussed in the next section.

2.3.3. RDM in grid expansion planning

RDM has been proposed as a promising approach for managing long-term uncertainties in grid expansion planning. Unlike traditional static methods, RDM focuses on stress-testing investment strategies across a broad range of possible futures to identify vulnerabilities and robust solutions [55]. One key feature of RDM is the use of trigger conditions—specific indicators that signal when an adjustment to the expansion strategy is needed [57]. For instance, the Gridmaster project identified eleven key drivers that could serve as triggers for adaptive investments to prevent capacity bottlenecks.

A core component of RDM is large-scale scenario stress-testing. By evaluating investment pathways under thousands of potential futures, RDM can identify weaknesses in grid expansion strategies that might not be apparent when relying on a limited set of predefined scenarios. For example, the Gridmaster project analyzed 10,000 scenarios to assess the robustness of various investment plans, suggesting potential advantages over conventional planning methods that typically rely on only three to four scenarios [57].

The EMA Workbench is a key tool supporting RDM by enabling planners to assess the robustness of different strategies through structured, large-scale simulation of diverse uncertainty scenarios [21, 23]. By systematically identifying vulnerabilities and opportunities, EMA facilitates the development of flexi-

ble and robust investment strategies for long-term grid expansion planning.

Despite its advantages, the practical application of RDM in decision-making remains limited. While it has been successfully applied in one exploratory case (Gridmaster), real-world adoption has been slow due to its complexity and the cognitive burden it places on decision-makers [39]. Planners must weigh trade-offs across thousands of uncertain futures—an overwhelming task without intuitive, user-friendly tools. This cognitive load can hinder engagement and limit the accessibility of RDM in practical distribution planning contexts. These challenges are particularly pronounced in distribution network planning, where localized congestion issues and uncertainty about DERs require adaptive decision-making. While RDM has been explored in the context of transmission expansion, no peer-reviewed studies to date have applied RDM to distribution network expansion planning. This represents a significant research gap.

Additionally, many studies focus on methodological advancements rather than direct engagement with decision-makers, limiting their practical impact. Integrating interactive frameworks, where decision-makers actively contribute to solution generation, could improve confidence in the strategies chosen and enhance implementation success [39]. This is particularly relevant in distribution networks, where ongoing adaptation is needed as grid conditions and energy sources evolve.

2.4. Knowledge gap

While the literature on distribution network expansion planning has advanced considerably, a critical gap remains: no existing methodology robustly incorporates deep uncertainty into distribution network planning. This absence means that current strategies are ill-equipped to address the fundamental unpredictability surrounding the pace, scale, and spatial distribution of DERs, as well as other critical factors such as consumer behavior, new housing developments, and battery adoption. Although some studies have used stochastic programming or scenario-based approaches, these rely on historical data and predefined probabilities, which are insufficient when uncertainties are deep and cannot be reliably quantified.

Distribution networks face unique challenges compared to transmission systems, particularly more localized congestion and increasing complexity introduced by a variety of factors—including, among others, DER integration, evolving user behavior, spatial development patterns, and emerging technologies such as batteries. These networks require planning approaches that can accommodate bidirectional power flows, temporal variability, and spatial unpredictability. However, much of the existing research focuses on microgrids and smart grid systems, which operate at smaller scales and under different constraints. These studies typically overlook the systemic impacts of large-scale DER integration on congestion and the corresponding need for flexible, scalable planning strategies.

Another significant gap lies in the lack of peer-reviewed studies applying the RDM framework to distribution network planning. While RDM has shown promise in industrial contexts and long-term policy design, and has been applied in one non-peer-reviewed report (Gridmaster) for energy infrastructure expansion, its application to distribution networks—particularly in the built environment—remains absent from academic literature.

Most existing planning approaches remain static, offering limited capacity to adapt as future conditions evolve. By introducing RDM into this context, this study offers a novel contribution: it is the first to systematically explore how robust and adaptive planning can be applied to distribution network expansion under deep uncertainty. They also rarely involve comprehensive stress-testing across thousands of plausible futures, leaving investment plans vulnerable to unforeseen developments in demand, technology adoption, and regulatory environments. This research addresses these limitations by using the EMA Workbench, which enables simulation and evaluation across a wide uncertainty space. The tool supports adaptive planning through trigger-based strategies and facilitates detailed analysis of trade-offs between robustness and cost-efficiency. By doing so, this study provides a systematic and actionable framework for informed decision-making under deep and persistent uncertainty in distribution network planning.

By bridging these gaps, this research contributes not only to practice but also to theoretical and methodological advancements in the field of energy infrastructure expansion planning. It enhances understanding of how deep uncertainty impacts grid congestion, and how RDM can be used to design more robust

and adaptive infrastructure strategies at the distribution level. Based on these gaps, this research seeks to address the following question: **How robust is Stedin's investment plan for distribution network expansion under deep uncertainty?**

To address this, the study explores the following sub-questions:

1. What are the key characteristics of long-term uncertainty in distribution network expansion planning?
2. What is the design of a simulation model that can effectively stress-test a distribution network expansion plan across multiple scenarios?
3. What actionable advice can stress-testing provide for Stedin's investment decisions?

3

Study design

This chapter outlines the methodology used to address the research question, employing RDM to evaluate investment decisions through scenario-based simulations.

3.1. Research design

This research applied RDM to identify investment strategies for distribution network expansion that yielded robust outcomes across diverse scenarios. To operationalize RDM, the EMA Workbench was used, which enabled the exploration of multiple possible futures [21]. This tool is particularly well-suited for the study, as it facilitates scenario-based simulations and allows for the stress-testing of the investment plan under a variety of future conditions.

The primary performance measure is capacity risk, defined as the risk of insufficient grid capacity to meet future demand due to uncertainties. The robustness of the investment strategies was evaluated based on their ability to mitigate this risk across a wide range of scenarios, specifically assessing how well they managed uncertainty in both electricity demand and supply. In addition to capacity risk, cost served as a secondary performance measure to evaluate the economic feasibility of the strategies. Together, these measures allowed for an assessment of the trade-offs between financial investment and the extent to which each strategy maintains robust across a wide range of uncertain futures.

While alternative methods such as static optimization or deterministic forecasting have historically played an important role in grid planning, they were considered limited for this study due to their inability to guide decisions under deep uncertainty. These methods typically optimize for a single expected future, making them vulnerable to unforeseen developments [4]. In contrast, RDM proved well-suited to the research goals, as it did not rely on probabilistic forecasts. Instead, it systematically explores a broad range of plausible futures to identify strategies that remain effective under varying conditions. This shifts the focus from predicting the future to preparing for it—an approach especially relevant in the context of rapidly evolving and uncertain energy systems. Although multistage optimization frameworks aim to introduce more flexibility by incorporating phased decision-making, they often rely on predefined scenario trees and fixed decision points. This limits their responsiveness to emerging developments [57]. RDM, on the other hand, enables dynamic adaptation by identifying vulnerabilities in plans and facilitating responsive, context-specific decisions. As a result, RDM is not only more adaptive in theory but also more actionable in practice—particularly when combined with tools like the EMA Workbench, which supports interactive stress-testing and stakeholder engagement. Therefore, this study adopted RDM not just as a theoretical lens, but as a practical method for developing robust and flexible investment strategies for distribution network expansion.

3.2. Sub-question 1

To address the first sub-question—**What are the key characteristics of long-term uncertainty in distribution network expansion planning?**—the XLRM framework was used [9]. The XLRM framework was chosen because it offers a structured way to frame complex decision problems under deep

uncertainty, which is central to RDM. Each component of the framework plays a specific role in guiding the analysis: Uncertainties (X) describe external factors beyond Stedin's control, such as demand or renewable energy growth fluctuations. Policy levers (L) represent investment choices that Stedin can influence. Relationships (R) define how uncertainties and levers interact within the system—essential for building the simulation model. Metrics (M) determine how the system's performance is evaluated, such as capacity risk and cost. By clearly organizing the decision problem into these dimensions, the XLRM framework supports both the conceptual understanding of the system and the practical implementation of scenario-based modeling and policy evaluation in subsequent phases of the research. In this phase of the study, the focus was on identifying and characterizing the uncertainties relevant to distribution network planning. However, the full XLRM structure was used to guide the broader study design, with other elements—such as investment levers, performance metrics, and system relationships—defined to support the simulation model developed in sub-question 2.

The identification of uncertainties began with a literature review of common drivers of uncertainty in grid expansion. These included increasing electricity demand due to EV adoption, the variability and intermittency of renewable energy generation and emerging technological innovations. Foundational insights were drawn from academic literature, including peer-reviewed articles, conference papers, and books accessed via academic databases such as Google Scholar and ScienceDirect.

However, as the context of Stedin's distribution network involved additional or uniquely expressed uncertainties, academic literature alone did not capture the full range of relevant factors. To address this, a focus group was conducted with five professionals from Stedin, including grid planners, asset managers, and operations managers. This group was selected to ensure a comprehensive and practice-based understanding of the uncertainty landscape specific to Stedin's geographic, infrastructural, and regulatory context.

The focus group session was recorded and analyzed, and a summary of key findings was compiled. This summary identified the most critical uncertainties as perceived by practitioners, offering real-world validation and refinement of the uncertainty parameters derived from the literature. By combining these two sources—academic theory and practitioner insight—the basis for the uncertainty component of the XLRM framework was created. The remaining XLRM elements were defined based on Stedin's current investment plan (levers), system logic used in simulation modeling (relationships), and relevant performance indicators cost and capacity risk (metrics). These components are further elaborated in the next section, which focuses on the development of the simulation model.

3.3. Sub-question 2

To address the second sub-question—**What is the design of a simulation model that can effectively stress-test a distribution network expansion plan across multiple scenarios?**—a simulation model was developed to represent the evolution of the considered system over time, based on Stedin's investment plan and a range of future scenarios. This model integrated the uncertainty factors identified through the XLRM framework in sub-question 1, combining general trends from the academic literature with contextualized insights from Stedin's professional focus group. These uncertainties formed the basis for generating diverse and plausible future scenarios within the EMA Workbench.

To ensure the simulations were grounded in real-world conditions, the model was calibrated using historical performance data from Stedin's network. This included time-series data on energy consumption patterns, demand fluctuations, and supply reliability. These data points helped align the model with observed grid behavior and ensure that the simulated system responses accurately reflected the operational characteristics of Stedin's distribution network.

Furthermore, a baseline model representing the current state of Stedin's network was incorporated to serve as the foundation for all scenario simulations. This model included information on current grid infrastructure, topology, and operating constraints. In addition, Stedin's investment plan was embedded within the simulation to reflect planned infrastructure upgrades, expansion projects, and long-term investment priorities. This ensured that all simulated strategies remained aligned with Stedin's strategic direction and policy context.

By applying RDM in combination with a calibrated simulation model in the EMA Workbench, this study provided an in-depth assessment of the long-term performance of Stedin's investment plan. The analysis focused on the plan's ability to mitigate the capacity risk, while also incorporating cost as a secondary metric to evaluate the financial impact of competing strategies. This methodology ensured that

proposed solutions are not only technically viable, but also economically sound under a wide spectrum of future conditions.

3.4. Sub-question 3

To address the third sub-question—**What actionable advice can stress-testing provide for Stedin's investment decisions?**—this study analyzed the results from stress-testing of a candidate expansion plan. The aim was to translate performance insights into concrete, prioritized advice that support a robust and adaptive plan.

The primary data source for this sub-question consisted of the quantitative analysis of simulation results, which included performance metrics capacity risk and cost across diverse future scenarios. To interpret these results, the Patient Rule Induction Method (PRIM) was used to identify clusters of scenarios—i.e., specific combinations of uncertain input variables—that are associated with either high or low performance outcomes. This method supports the exploration of vulnerable and robust regions in the uncertainty space, helping to uncover qualitative patterns or ”if–then” relationships (e.g., certain conditions that consistently lead to capacity bottlenecks).

When the analysis revealed specific conditions under which the investment plan failed—such as excessive demand growth or specific renewable capacity growth—trigger conditions were developed and introduced into the model. These triggers served as early warning signals, indicating when certain pre-defined actions should be taken to prevent system stress or failure. The corresponding actions were drawn from the policy levers identified in the XLRM framework (sub-question 1), ensuring alignment between strategic responses and the uncertainties they were meant to address. The revised model, now incorporating these adaptive triggers, underwent an additional round of stress-testing to assess whether the changes enhanced robustness.

To translate the analytical findings into concrete advice for improving Stedin's investment plan, a structured prioritization process was applied. The MoSCoW method (Must-have, Should-have, Could-have, Won't-have) was used to organize proposed changes based on their urgency and expected impact. Advice classified as “Must-have” are prioritized for implementation, as they address urgent vulnerabilities in the investment plan—such as grid sections at high risk of capacity shortages. “Should-have” modifications focus on improving cost-efficiency without compromising robustness and are considered next in line. “Could-have” items offer beneficial enhancements that are desirable but not essential, while “Won't-have” suggestions were deprioritized due to limited added value or feasibility concerns.

These recommended adjustments to the investment plan were informed by both quantitative and qualitative input. Quantitatively, the PRIM analyses highlighted which uncertainty conditions most significantly influenced performance and where the existing plan fell short. These insights pointed to specific future conditions where the plan required reinforcement or flexibility. Qualitatively, the recommendations were reviewed in consultation with the responsible grid planner at Stedin, whose operational expertise helped assess the practicality and priority of proposed changes.

By combining analytical results with structured prioritization and practitioner input, this approach ensured that the advice was not only grounded in rigorous analysis but also feasible and aligned with Stedin's operational realities. The result was a set of actionable proposals for adapting the investment plan to better withstand a wide range of future uncertainties.

3.5. Research flow diagram

The diagram below visualizes the research process described in the preceding chapters, distinguishing between data inputs, methodological steps, and key outputs using color-coded elements.

- **Yellow boxes** represent the primary inputs feeding into the research process. These include both qualitative sources—such as the literature review and focus group—as well as quantitative inputs like historical performance data, the current network model, and Stedin's investment plan.
- **Green cloud shapes** denote the analytical methods and modeling tools applied throughout the study. These range from the XLRM framework used to structure uncertainties, to stress-testing, and PRIM analysis used in simulation and result evaluation.
- **Diamond shapes** signal decision points or transitional steps in the process, such as identifying uncertainties or analyzing results, which lead to subsequent phases in model development and

evaluation.

- **Blue circles** highlight the key outputs of the sub-questions, which include the refined uncertainties, the stress-tested simulation model, and the actionable advice for the investment plan.

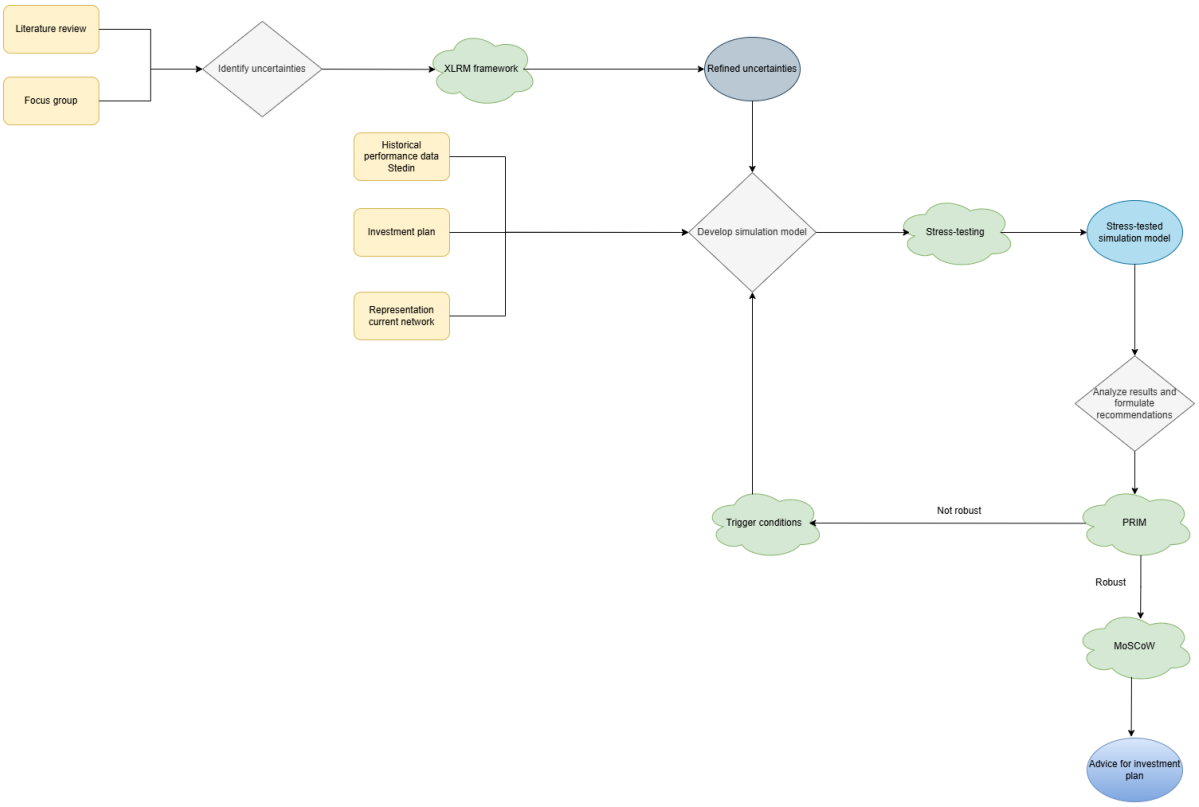

Figure 3.1: Research flow diagram

4

Conceptualization

This chapter addresses the first sub-question: **What are the key characteristics of long-term uncertainty in distribution network expansion planning?** It begins by identifying key uncertainties through a review of academic literature, supplemented by a focus group with professionals from Stedin. These insights informed the conceptualization of the decision environment, which was structured using the XLRM framework introduced in Chapter 3. This provided a systematic way to define uncertainties, identify relevant policy levers, describe system dynamics, and select performance metrics. The chapter concludes with a high-level conceptual model of the energy system under study. This model translates the abstract decision environment into a simplified representation of Stedin's distribution network. It is structured using sector-based building blocks—such as residential and industrial areas—reflecting the observation that many key uncertainties are likely to manifest differently across sectors. This conceptualization serves as a foundation for applying the decision framework to a concrete network setting and supports the development of the simulation model in the next chapter.

4.1. Case description

The focus of this thesis is on a specific 13 kV distribution network, here referred to as substation A. Power is delivered through substation A, which contains three transformers that step down voltage from 50 kV to 13 kV. These transformers supply electricity to different sections of the network, which are further interconnected. Within each section, ring networks distribute power to several distribution rooms, where voltage is typically reduced from 13 kV to 400 V for most end users. However, certain large consumers—such as solar parks or industrial facilities—are often connected directly to the 13 kV network and do not require further voltage reduction. Some rings in the network are also connected to other substations outside network A, creating additional interconnections that increase both the system's complexity and its operational flexibility. To make this real-world complexity manageable in simulation, it was necessary to abstract and simplify the network layout.

The area supplied by substation A includes a small harbor, several industrial zones, a substantial agricultural sector—particularly greenhouse horticulture—and a built environment.

To support future demand growth and avoid anticipated congestion at substation A, an investment plan has been proposed. This plan involves constructing a new 21 kV substation (substation B) within the existing distribution area of network A, alongside the relocation of specific rings from the current 13 kV substation to the new one. Figure 4.1 provides a stylized illustration of this concept. While the figure shows only four rings for simplicity, the actual network contains more. In the proposed plan, a subset of these rings—selected based on their load profiles and spatial location—will be reassigned to substation B. This reconfiguration is intended to relieve capacity stress at substation A and better accommodate projected demand growth in the area. The specific building blocks that are relocated will be discussed in more detail in Chapter 6.3.

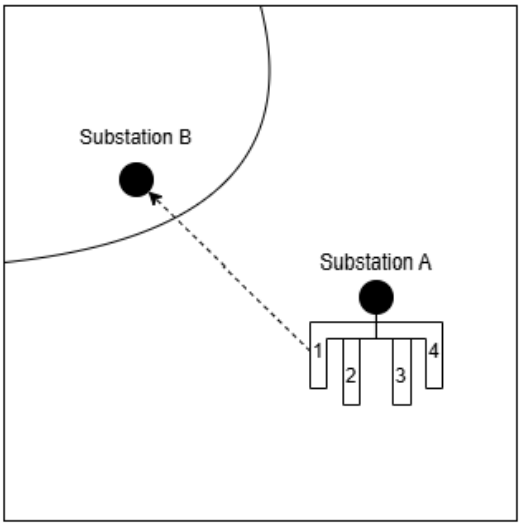

Figure 4.1: Current distribution network with investment plan

4.2. Identifying key uncertainties

4.2.1. Literature

Long-term uncertainty in electricity demand growth is widely recognized as a critical factor in distribution network expansion planning. Studies such as Muñoz-Delgado et al. (2021) highlight that the unpredictability of future demand presents major challenges for the design of robust and cost-effective grid infrastructure, particularly over multi-decade planning horizons. The accuracy of such expansion plans depends heavily on assumptions about how electricity consumption patterns will evolve, making it essential to understand the primary factors that drive changes in demand.

A review of relevant literature reveals a number of interrelated uncertainties that influence electricity demand in the long term. One of the most significant areas of uncertainty is technological change, especially related to the transition in heating and cooling systems [20]. The uptake of electric heat pumps is expected to increase as fossil-fuel-based heating systems are replaced. This trend contributes to higher overall electricity consumption and also reshapes the seasonal and daily demand profiles. Also, rising temperatures due to climate change are expected to increase the use of technologies like air conditioning, particularly in southern Europe, leading to higher electricity demand for cooling. At the same time, milder winters in northern regions may slightly reduce heating needs [10].

Electrification in other sectors, particularly in industry and agriculture, further adds to the complexity of demand forecasting. Koreneff et al. (2009) identify the electrification of greenhouses, livestock farms, and various industrial processes—especially for heating, ventilation, and lighting—as emerging contributors to increased electricity use. These changes are regionally dependent, introducing spatial variation that must be accounted for in distribution planning.

Another major factor is the adoption of EVs, which not only raises total electricity demand but also introduces uncertainty regarding the timing and concentration of load. EV-related demand is highly sensitive to charging behavior—whether it follows smart charging practices or occurs in an uncontrolled manner [20]. Additionally, the expansion of EV charging infrastructure, both public and private, has the potential to create localized peaks in demand that necessitates targeted grid reinforcement.

Kan et al. (2021) highlight that alongside changes in overall demand, there is increasing uncertainty in demand patterns, especially regarding seasonal and daily variability. For example, future peaks could shift from winter to summer due to widespread use of air conditioning, or experience sharper intraday swings due to EV charging habits. These demand variations are particularly significant in electricity systems with a high share of renewable energy, where matching supply and demand becomes more complex [17]. The study also notes that new buildings and evolving patterns of energy use—driven by sector coupling and climate adaptation—may alter the shape of future load curves.

Several supply-side developments—such as the increasing adoption of rooftop solar PV systems, the expansion of utility-scale solar parks, and the integration of wind energy—are also expected to

significantly influence demand patterns. These sources contribute to local energy generation, reduce reliance on the central grid during peak production hours, and reshape the residual demand curve that distribution networks must manage.

4.2.2. Focus group

Following the literature review, a focus group was conducted in which the identified uncertainties were discussed and further insights were gathered from professionals at Stedin. One key uncertainty raised during the session was the potential use of shore power. Since the distribution area includes a small harbour, there is a possibility that ships could connect to the electricity grid while docked. The estimated average instantaneous power demand for a container ship while connected to shore power is approximately 600 kW [41], meaning that widespread adoption of shore power could place significant additional demand on the network.

Another topic of discussion was the development of a planned solar park within the network area. The size and scope of this project remains uncertain, as does the possibility of future expansions, which introduces variability in the amount of electricity that may be fed back into the grid. In addition, the installation of solar panels on large rooftops—such as those of schools or industrial buildings—was highlighted as another factor that could substantially influence local demand and supply patterns.

Lastly, participants noted that while there are general expectations regarding the time required to construct or reconfigure parts of the distribution network (such as relocating a ring), delays may occur due to permit issues or shortages in skilled labor. These potential delays introduce further planning uncertainty and should be taken into consideration. Further details from the focus group discussion are available in the summary provided in Appendix A.

4.3. Structuring the decision problem: XLRM framework

A list of all the identified uncertainties can be found in Appendix B. Based on these, an XLRM framework was constructed to analyze how various factors influence grid planning under uncertainty (see Figure 4.2). To enhance readability, closely related elements were grouped together. At the top of the diagram, the two key metrics are shown: capacity risks (M1) and costs (M2). M1 refers to the risk of insufficient grid capacity to meet future demand due to uncertainties. It reflects the vulnerability of the energy system to shifts in consumption and production patterns. M2 represents the financial implications of different investment strategies, providing insight into their economic feasibility.

The levers box (L) contains measures that can be implemented to influence the system. These levers reflect the core elements of Stedin's proposed investment plan and include the relocation of rings, the construction of new rings, and the development of new substations. These interventions are intended to mitigate capacity risks but also involve significant financial costs, thereby affecting both M1 and M2. In the first iteration of running the simulation model, only two of these levers—relocating rings and constructing a new substation—are implemented, corresponding to Stedin's initial investment strategy. The option to construct entirely new rings is considered as an additional lever for later adaptive adjustments if required. The full implementation details, including technical assumptions and cost parameters, are described in Chapter 6.

In the middle section of the diagram are the uncertainties derived from the literature and focus group. These include developments such as the heat and cooling transition of buildings, the expansion of EV infrastructure, industrial and greenhouse transitions, and the deployment of solar systems (both rooftop and solar parks). Most of these uncertainties increase M1, either by directly raising demand or by introducing more variable and unpredictable usage patterns. The exceptions are solar panels, solar parks, and the implementation of levers, which can help reduce capacity risks by contributing to decentralized generation or by relieving stress on the grid. M2, on the other hand, is only driven by the implementation of levers, which require substantial investments.

Dashed arrows in the figure indicate interdependencies or dynamic relationships between uncertainties. For example, the growth in EVs determines the required number of charging points, while the behavior of people charging their vehicles affects the timing and magnitude of electricity demand. These variations lead to more fluctuating and less predictable load patterns on the grid, increasing uncertainty in both demand peaks and troughs. Consequently, this reduces the stability of the grid and raises capacity risk, as the system must be prepared to handle sudden or unexpected changes in electricity consumption.

This diagram offers a structured overview of how multiple variables interact to shape the two main outcomes: capacity risk and cost. It underscores the complexity and interconnectedness of the energy transition, where technical, behavioral, and infrastructural changes must be aligned to ensure a robust, reliable, and cost-effective energy system under a wide range of future scenarios. A detailed explanation of the full diagram can be found in Appendix C.

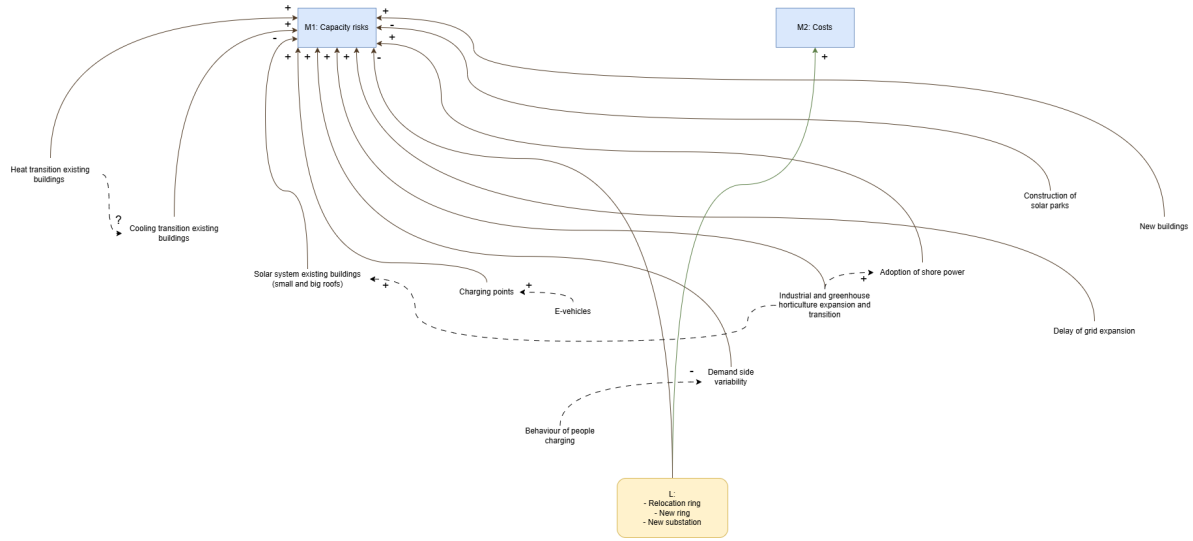

Figure 4.2: XLRM framework

4.4. Conceptual model of the distribution network

The conceptualization process used sectors—such as industry, greenhouses, and residential buildings—as the primary classification criteria. Based on geographic and functional data provided by Stedin and visualized in PowerFactory, entire rings or parts of rings were grouped into coherent units referred to as building blocks. These building blocks serve as the core analytical elements in the simulation model. From this point onward, the term building blocks will be used in place of rings to reflect this abstraction.

Figure 4.3 illustrates this conceptual structure of the network. It shows how transformers supply grouped building blocks through sectioned busbars and how certain parts of the network connect to external substations. While simplified, the diagram preserves the essential relationships and power flow paths needed to evaluate how different demand patterns and investment decisions impact substation capacity and network costs.

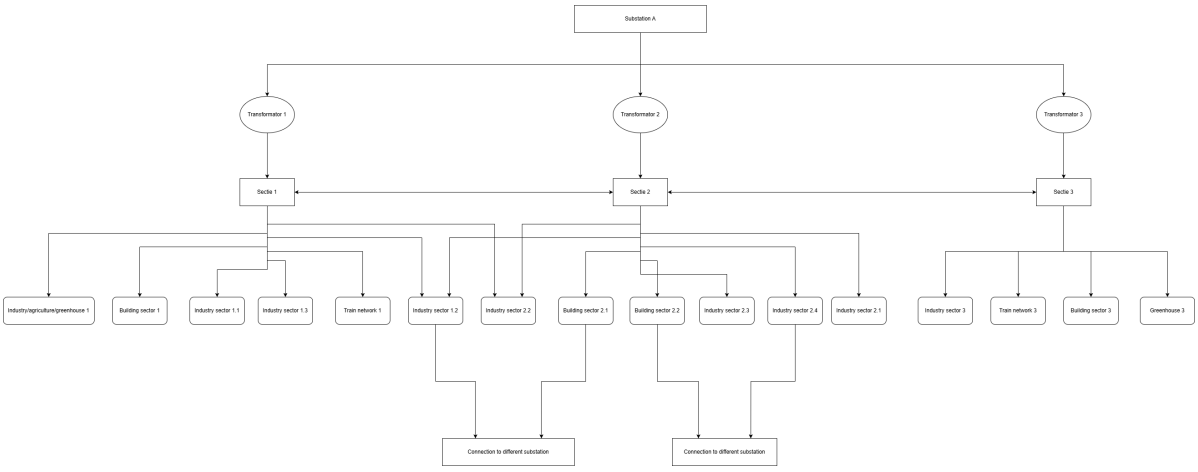

Figure 4.3: Conceptual model of distribution network

5

Data preparation & exploration

5.1. Data preparation

To model the distribution network of the current substation accurately, several types of data are essential. One of the most important is the capacity of the distribution network, as this determines when a new substation needs to be built or when a potential capacity risk may arise. Equally important is the hourly load of the distribution network from 2025 to 2050. This hourly load is based on scenario projections developed by Stedin, making it a valuable benchmark for comparison. Since the simulation in this thesis is based on defined building blocks, it is particularly important to obtain the hourly load data of individual distribution rooms for the year 2025, which serves as the primary input for the model.

In addition to these core datasets, supplementary data specific to the current substation was also collected. This includes the capacity and voltage levels of the medium-voltage rails and transformers connected to the substation, as well as hourly load data for its medium-voltage transformers TR1 and TR2 over the same time period. Unfortunately, data for transformer TR3 was not available. Additional datasets cover the number of connections and distribution rooms within the substation's service area, along with customer-level energy consumption data from 2021 to 2025. All data was provided by Stedin and delivered in CSV format. To ensure privacy and comply with data-sharing requirements, the datasets have been anonymised before being included in the publicly accessible GitHub repository. The complete collection of anonymised datasets is stored in the "Data" directory of the repository accompanying this thesis.

To prepare the data for analysis, several cleaning and transformation steps were applied. Irrelevant columns were removed, data types were verified and converted where necessary, missing values were addressed, column names were adjusted for clarity, and duplicate entries were eliminated. During this process, several discrepancies were identified and resolved.

First, the number of distribution rooms in the dataset did not match the expected total. While the dataset listed 160 distribution rooms, 3 had station numbers that did not belong to the relevant distribution network, and 8 rooms were missing entirely. This discrepancy was manually corrected by cross-referencing with a verified list of distribution rooms. Additionally, hourly load data was incomplete. The dataset contained only 103 rooms with load profiles, of which 3 had incorrect station numbers and thus did not belong to the network—leaving 100 valid entries. As a result, load data was missing for 65 distribution rooms. These missing rooms were first added to the dataset, and then partially completed using customer-level consumption data. This required mapping EAN codes (unique customer identifiers) to their corresponding distribution rooms, which allowed for the reconstruction of load profiles for 40 distribution rooms. However, 25 distribution rooms remained without any load data. For these, an imputation method was used: the hourly average load across all available distribution rooms was calculated and assigned to the missing ones. While this introduces some generalization, it allowed for the creation of a complete and internally consistent dataset suitable for simulation.

Once missing values were addressed, the data for the year 2025 was selected as the basis for the simulation. This year was chosen because it represents the current state of the distribution network, serving as a realistic baseline for future projections. The building blocks defined in Chapter 4 were then

manually mapped to their corresponding distribution rooms. During this mapping process, it was found that three building blocks—Greenhouse 3, Industry Sector 2.3, and Industry Sector 3—were missing parts of their 2025 hourly data (i.e., fewer than 8,760 hours). Given the relatively stable, non-seasonal consumption patterns in the greenhouse and industrial sectors, the decision was made to extrapolate the missing data using the available months (January–March). This preserves the overall structure of the dataset while still providing a realistic approximation of annual load.

The finalized dataset, titled ”Building_blocks.csv”, was saved and used as the primary input for the simulation model described in the next chapter.

Finally, connection data was missing for 64 of the 165 distribution rooms. This data refers to the number of connections—such as residential homes, commercial units, or other electricity-consuming installations—served by each distribution room. While this information is useful for certain analyses, such as identifying areas with high demand density or evaluating vulnerability under congestion scenarios, it is not required for the core simulation. The model focuses primarily on aggregate demand and capacity dynamics rather than individual connection-level behavior. Therefore, the absence of this data does not materially impact the validity or outcomes of the simulation.

5.2. Exploratory Data Analysis

This section examines the structure and behaviour of the input dataset to gain insight into the operational characteristics of the distribution network. The purpose of this analysis is to identify key trends and assess the data’s suitability for simulation.

The analysis started with an overview of the distribution network’s transformer capacity. The network includes three transformers: two rated at 40 MW and one at 25 MW. According to the widely used N-1 reliability criterion—which requires the network to continue operating even if the largest transformer fails—the theoretical capacity would be 65 MW. However, the safe operational limit used in this study is 57.5 MW, based on data provided by Stedin. This lower threshold likely accounts for additional constraints such as thermal limits, system protection settings, or safety margins, even though the exact derivation of the 57.5 MW was not specified. For the purposes of this research, 57.5 MW is used as the effective upper capacity limit of the network, in line with real-world operational practice. A lower capacity threshold of -80 MW is also applied to reflect minimum system load boundaries.

Next, the overall load on the distribution network was assessed. The dataset includes hourly load projections from 2025 to 2050 based on a scenario developed by Stedin. When plotted across time, these hourly load values (Figure 5.1) reveal a consistent daily and seasonal fluctuation pattern. However, a key feature of the projection is the increasing amplitude of these fluctuations over time. This means that while the shape of demand, such as daily peaks in the evening and seasonal winter highs, remains relatively constant, the magnitude of both peak and minimum loads increases year by year. The result is a growing variation in load, with higher peaks and deeper troughs, implying that the electricity network will need to manage not only more demand overall, but also greater variability in that demand.

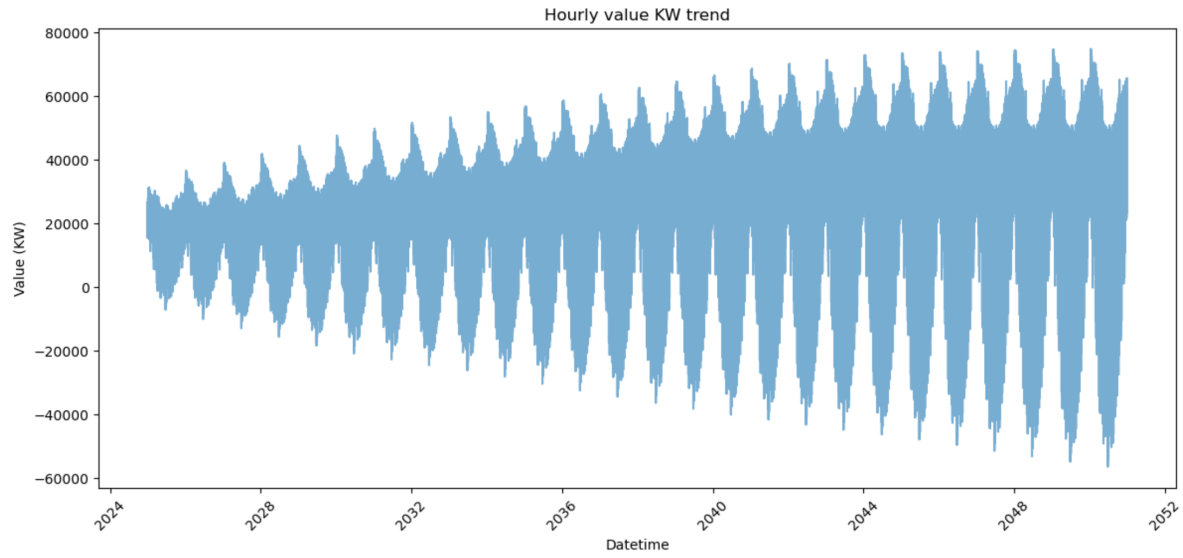

Figure 5.1: Distribution network hourly load

To further investigate potential differences within the years, the hourly load for the year 2025 was examined. As shown in Figure 5.2, power usage is significantly higher during the winter months, particularly in January and December, while the lowest levels are observed during the summer months, around June and July. This pattern reflects clear seasonal variation in energy demand, with increased consumption during colder periods likely driven by heating needs, and a relative decline in the warmer months possibly due to reduced heating demand or more efficient energy use. Additionally, during the warmer months, periods of negative load suggest net energy export to the grid, likely driven by increased solar panel generation.

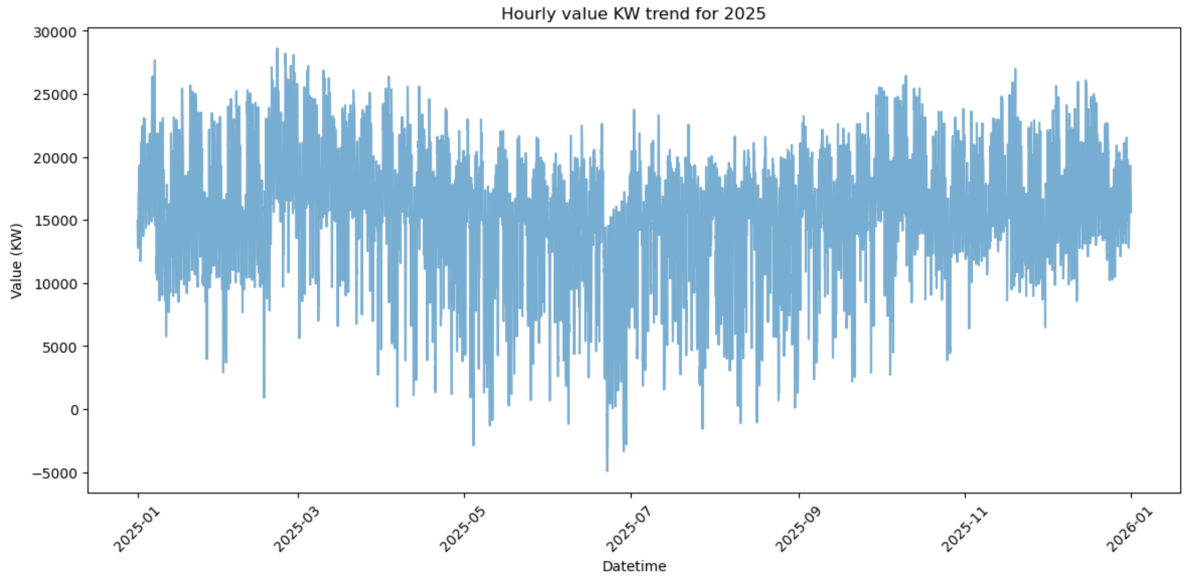

Figure 5.2: Distribution network hourly load 2025

Following the assessment of the overall distribution network, the focus shifts to the load on the distribution rooms. These rooms are grouped by building blocks to allow for a comparison of load behavior across different sectors. The analysis uses data from the year 2025, as this is the most recent year for which observed load data is available. Using the most current data helps ensure that the simulation reflects up-to-date consumption patterns and system conditions, providing a more accurate basis for evaluating the performance of future investment strategies.

As shown in Figure 5.3, Building sector 2.1 displays the highest variability in energy use, with large swings between consumption and feed-in, especially in the summer months. Greenhouse 3, by contrast, shows predominantly negative load values throughout the year, suggesting that it operates mainly as a producer feeding energy back into the grid—potentially due to extensive solar generation. In comparison, the Train network sectors exhibit exceptionally stable load patterns, with near-linear behavior across the entire year, likely reflecting tightly scheduled and predictable usage. To view the detailed hourly load profiles for each building block in 2025, please refer to the separate plots provided in Appendix F.

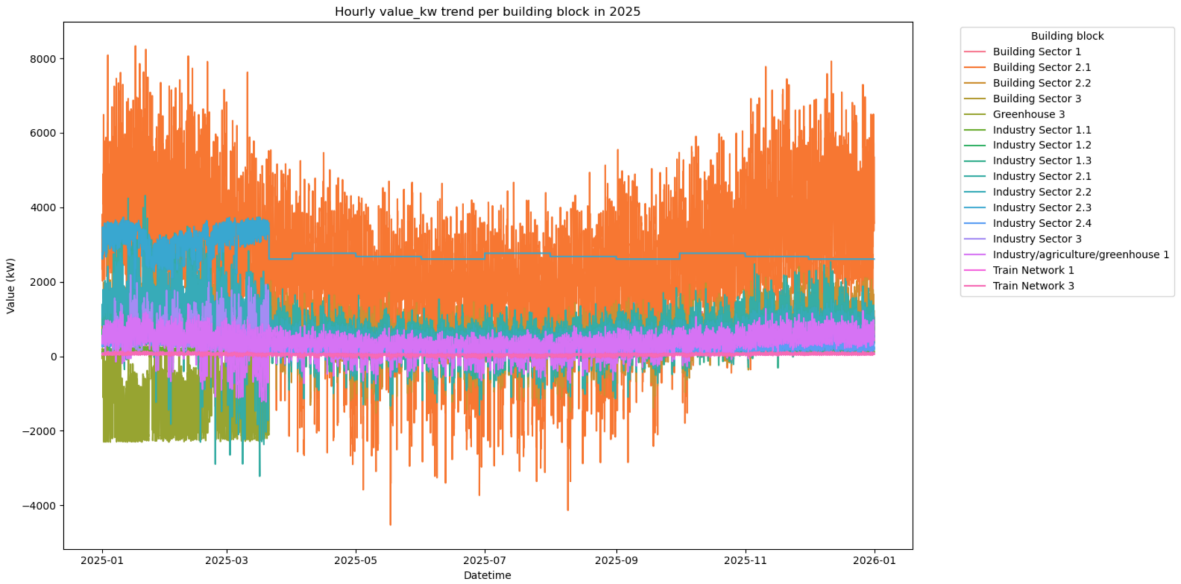

Figure 5.3: Building blocks hourly load 2025

To complement the time-series insights, Figure 5.4 presents boxplots of the hourly load values for each building block in 2025. These visual summaries highlight key differences in both the magnitude and variability of electricity demand across sectors. Industry Sector 2.3 and Building Sector 2.1 stand out with the highest median load values, indicating that they are among the most energy-intensive areas of the network. However, their patterns differ: Industry Sector 2.3 shows consistently high demand with relatively limited variation, while Industry Sector 2.1 exhibits a much wider range, reflecting significant fluctuations in hourly load. Train Network 1 and 3 again demonstrate exceptional stability, with narrow interquartile ranges and low median values. Additionally, several sectors — including Greenhouse 3 and Industry Sector 3 — show frequent negative load values, as evidenced by boxplot whiskers extending below zero. This confirms regular energy export to the grid, likely due to surplus renewable generation. These distributional characteristics reinforce earlier observations and offer a deeper understanding of sector-specific load behavior.

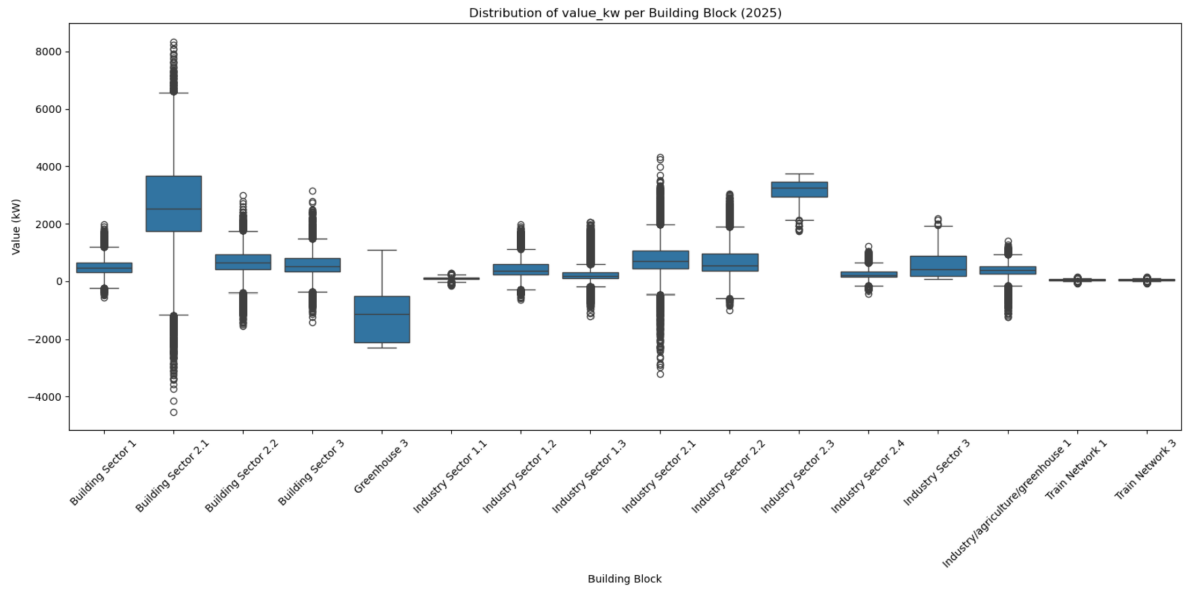

Figure 5.4: Boxplot building blocks

Shifting focus from load behavior to network structure, the analysis also assessed the number of connections per distribution room. This revealed significant variation, with the number of connections ranging from a minimum of 1 to a maximum of 620, and an average of 118 connections. This wide variation indicates uneven demand aggregation across the network, which could lead to localized capacity constraints in certain areas. However, as noted earlier, the dataset was incomplete, so definitive conclusions cannot be drawn.

Additional details on the cleaning and processing steps can be found in the ”Data_cleanen” file within the ”Results” repository on Github.

5.3. Additional data from external sources

In addition to data provided by Stedin, external sources were required to supplement the 2025 simulation input. For each defined building block, data was collected on the number of houses, cars, greenhouses, industrial facilities, solar panels, air conditioning systems, and heating types. This level of detail was not available in the original Stedin dataset but is essential for scenario development. These variables are expected to change over time and directly influence hourly electricity demand and supply—the primary focus of this study. Therefore, establishing a detailed and accurate 2025 baseline was necessary to model how different developments may impact the distribution network under various future scenarios.

To determine the number of houses per building block, data from [16] were used. By cross-referencing the map on the cited website with PowerFactory and the distribution network schematic, the residential distribution across building blocks was identified. As a result, the current number of houses in each ”Building Sector” block could be accurately determined and assigned to the simulation.

Next, heating types for these residential buildings were derived using data from the year 2022, as reported in [44]. Individual boilers and block heating systems were categorized under gas boilers, based on the assumption that block heating is gas-fueled. District heating systems without gas consumption were classified under the heat network category, while electrically heated homes without gas use were considered fully electric (i.e., powered by electric heat pumps (eHP)). Electrically heated homes with high or low gas consumption were classified as using hybrid heat pumps (HHP). The remaining 6% of homes, based on the source, were assumed to use air conditioning (airco) for heating, completing the categorization to a full 100%.

In terms of cooling, it was assumed that per building block 20% of existing households are equipped with airco’s for cooling purposes, based on the findings in [48]. For solar panel adoption, [6] indicated

that more than 35% of Dutch households have solar panels. Based on this, it was assumed that per building block 4 out of 10 (40%) existing homes in the simulation are equipped with solar panels.

Following the residential data, the surface area of greenhouses in the region was determined using [43], which reported 74,300 m^2 under glass horticulture. This area was evenly distributed between the ”Industry/Agriculture/Greenhouse 1” and ”Greenhouse 3” building blocks.

For industrial activity, data from [45] were consulted. Only economic activities classified under categories B (Mining and quarrying), C (Manufacturing), D (Energy supply), E (Water supply and waste management), F (Construction), G (Trade), H (Transport and storage), J (Information and communication), and L (Real estate activities) were included. This selection was made to ensure that only sectors likely to contribute significantly to industrial electricity demand were counted. Other categories—such as A (Agriculture, forestry and fishing), I (Hospitality), P (Education), and Q (Health care)—were excluded, as they typically represent non-industrial or low-load consumer profiles that are not central to the analysis of industrial energy use.

Finally, based on data from [52], it was determined that households in this area own, on average, one car each—resulting in a total of 13,607 cars. These cars were then evenly distributed across all building blocks, assigning an equal number of cars to each block.

Besides block-specific data, other simulation inputs were required. For solar panels, [11] reported that the peak power per panel typically ranges from 250 to 400 W; a value of 400 W was chosen for this study. Furthermore, the solar park energy yield was set at 120 kWh per m^2 per year. Finally, EV data from [Data from Stedin] indicated that 1.85% of all vehicles are electric, with peak charging hours occurring between 16:00 and 21:00 [46].

In addition to the data required for modeling energy demand and supply, key infrastructure costs were incorporated to support network upgrade assessments. These cost estimates were primarily based on [32], and further refined through expert consultation with Stedin. The construction of a new substation, for instance, was estimated at €12.5 million. Each new substation includes two large transformers, with a combined cost of approximately €200,000. When relocating building blocks from one substation (substation A) to another (substation B), it was necessary to evaluate whether the existing cables could support a voltage level of 20 kV. If not, new medium-voltage cables had to be installed, with costs estimated at €400 per meter. Additionally, all distribution room transformers associated with the relocated building blocks required replacement due to the voltage level change, with each transformer costing approximately €15,000. These numbers provide a consistent and realistic basis for evaluating the financial impact of future infrastructure adaptations.

6 Simulation

The distribution system model was implemented in Python as part of the exploratory modeling framework using EMA Workbench. The objective was to develop a modular and scalable representation of an electricity distribution system, capable of simulating various demand scenarios and identifying potential points of overload. The model adopts an object-oriented design, reflecting the hierarchical nature of a typical distribution system. The complete implementation of the code is available on GitHub under ”Simulation.py”.

6.1. Experimental setup

The experimental setup consists of a custom-built simulation model designed to project electricity demand and network stress under future uncertainties from 2025 to 2052. Developed entirely in Python, the model uses object-oriented programming to encapsulate key components—such as substations, transformers, sections, and building blocks—into modular classes. The EMA Workbench facilitates systematic scenario generation, sampling, and policy intervention management. Although the simulation runs independently, EMA serves as a wrapper for sampling and uncertainty exploration. Model uncertainty exploration is conducted by randomly sampling discrete scenario pathways (A, B, or C) across multiple uncertainties, where each pathway corresponds to fixed numerical parameter trajectories over time. This random discrete sampling enables 1,000 simulation runs to capture a broad range of future uncertainty combinations. The building blocks represent the most granular elements of the network, corresponding to various real-world entities such as residential areas, industrial zones, greenhouse clusters, and transport infrastructure. Each building block is characterized by attributes like housing numbers, solar panel adoption, electric vehicle usage, and industrial activity, all influencing local electricity demand. These attributes and their data sources are detailed in Chapter 5.3.

At the start of the simulation, the baseline year 2025 is established using hourly demand data sourced from the file ”Building_blocks.csv”. These demand profiles are mapped to individual building blocks based on their attributes and serve as the starting point for future projections. The network’s structure is initialized by defining the capacity limits of the main substation, its connected transformers, and subordinate sections. This setup allows the model to calculate aggregated demand for each part of the network and evaluate potential overloads by comparing projected demand against designed capacity constraints.

To incorporate long-term uncertainty, the Energy Model class integrates scenario-based inputs that influence key drivers of demand. These uncertainties—such as cooling demand, solar adoption, and electric vehicle growth—are encoded in dictionaries that assign values to each parameter across different scenario pathways (A, B, or C) and simulation years. When a scenario is selected, the model retrieves the corresponding values for each uncertainty and applies them to adjust the relevant building block attributes over time. All uncertainties are fixed at their 2025 baseline until 2028, after which they begin to evolve according to the assumptions embedded in the scenario trajectories. The full set of numerical values used for these uncertainties is documented in the file ”Scenario space - uncertain-

ties.xlsx", available on GitHub for reproducibility.

Time is modeled in three-year steps, from 2025 to 2052. To capture intra-annual variability, the simulation uses ten representative days that reflect typical seasonal and weather conditions—such as hot summer days or cloudy winter periods. Each representative day has an assigned weight indicating how many actual days it stands for in the three years. These weights are adjusted over time to reflect anticipated climate shifts, such as an increasing number of warm days. For each representative day, hourly profiles of heating and cooling demand as well as solar generation (both rooftop and park-scale) are generated based on realistic base patterns, with added random variation to reflect natural fluctuations. These time profiles serve as dynamic inputs in each simulation run, allowing for realistic load and generation modeling across years and scenarios.

Finally, the validity of the model's internal calculations—particularly those governing scenario-driven changes in demand—is tested and documented in Appendix D. There, the behavior and order of magnitude of the uncertainty-driven outputs are assessed to ensure they evolve correctly over time and align with the intended logic. This validation step confirms that the model provides a reliable foundation for exploring how future uncertainties may impact electricity distribution networks.

6.2. Calculations per uncertainty

This section explains how each uncertainty affects energy demand and supply, detailing their influence on hourly electricity consumption and generation. For a complete description of the underlying calculations, consult the full code on GitHub and the detailed documentation in Appendix E.

6.2.1. Solar panels existing houses

Solar panel adoption in existing residential buildings is modeled via hourly solar generation profiles, evolving from the fixed 2025 baseline. Each building block starts with a known number of houses and a defined subset already equipped with solar panels (solar_houses). Beginning in 2028, an annual adoption factor is applied to the remaining houses without panels to simulate growing uptake over time.

Each solar-equipped house is assumed to have a fixed number of panels (10 per house [6]), each with a specified peak generation power [11], which represents the theoretical maximum output under ideal conditions. To reflect variations in performance and future technological improvements, a year-specific efficiency factor is applied to this peak value. This factor starts below 1 to account for real-world losses and suboptimal conditions in earlier years, and gradually increases toward 1.0 or beyond in later years.

Hourly solar generation is derived by combining this adjusted peak output with normalized 24-hour solar production curves based on representative days. These daily curves, which peak at 1.0 under ideal midday conditions, are weighted by their annual frequency and aggregated to form full three-year hourly generation profiles for each building block.

In this setup, if the efficiency factor reaches 1.0 and the normalized generation curve is at its peak (value 1.0), then each panel will produce the full 400 W. In earlier years, lower efficiency factors like 0.85 mean that even under ideal conditions, only 340 W per panel would be generated.

The final result is a detailed hourly time series of expected solar energy generation per block and year. This generation is then subtracted from total electricity demand to calculate the net hourly demand.

6.2.2. Heat transition existing buildings

To account for the impact of the heat transition in residential buildings, the model simulates how different heating technologies evolve over time and how they influence hourly electricity consumption. This transition is only applied to building blocks categorized as part of the building sector.

For each building block, the model tracks the number of houses using each type of heating system, including gas boilers, HHP, eHP, heat networks, and airco. From 2028 onward, a portion of gas boilers is gradually phased out each year, based on a transition rate defined by a yearly heat factor.

A part of these transitioning houses adopts hybrid heat pumps, according to an annual hybrid factor. Hybrid systems are tracked over time, including their replacements after a predefined lifespan. The

remaining transitioning houses are redistributed across the other heating technologies according to a pre-defined heating mix. Importantly, for the baseline year 2025, building sectors eligible for connection to the heat network were identified. Only these sectors can receive heating network connections throughout the simulation. If a building block does not support connection to the heat network, its share in the heating mix is proportionally reallocated to the other available technologies (electric heat pumps and air conditioning).

Each heating technology is associated with a fixed energy consumption per house per hour, based on technical assumptions. These values are used to calculate total hourly heating demand per block, multiplied by normalized heating profiles from representative days. Each profile represents typical daily heating patterns and is scaled by its frequency to create a realistic year-round demand profile. The result is a full three-year hourly time series of heating energy use for each building block and year. This output serves as a key input to the final demand calculation, significantly affecting how total hourly electricity demand evolves under different heating transition scenarios.

6.2.3. Cooling transition existing buildings

To simulate the impact of increasing cooling demand in residential areas, the model incorporates a dynamic adoption process for airco technologies over time. Prior to 2028, cooling demand is assumed to originate only from existing households already equipped with larger air conditioning units (big airco). The number of such units is derived directly from the input dataset per building block.

From 2028 onward, a cooling adoption process is introduced to account for the increasing demand for cooling driven by climate change, rising comfort expectations, and potential policy changes. This process targets only a subset of households deemed eligible based on their heating configuration. Specifically, households that use airco's for heating and those connected to HHPs or heat networks are considered eligible to adopt cooling systems.

The rationale for this selection is based on technical compatibility and realistic household behavior. Airco heating users are assumed to already have an air conditioning unit installed for space heating, which can typically also function in cooling mode. Therefore, to achieve full cooling capability, these households only require a relatively modest upgrade, modeled as the addition of a smaller cooling unit (small airco). In contrast, households with HHPs or heat networks generally lack any form of air conditioning, and thus need to install a complete, larger cooling system (big airco) to meet their cooling needs. Households using eHPs are excluded from the cooling adoption model. This is because eHPs typically operate through systems such as low-temperature radiators or convectors that can provide both heating and cooling. As such, these households are assumed to already have adequate cooling capability integrated into their existing setup, eliminating the need for separate air conditioning installations. A yearly adoption factor determines what share of these eligible households installs cooling systems.

To estimate the hourly energy usage for cooling, each airco type is assigned a typical energy consumption per house per hour. However, it should be noted that the cooling demand provided by eHP systems is not explicitly accounted for in the total hourly cooling consumption, which represents a limitation of the model. Small airco units are assumed to consume 50% less energy than big airco units, reflecting their lower power ratings and cooling capacity. Cooling energy demand over the year is distributed using normalized hourly profiles derived from representative days. Each representative day contains a typical 24-hour cooling pattern and is weighted based on its occurrence frequency. These weighted profiles are combined to create a full-year hourly time series for cooling energy consumption per building block and year. The resulting output captures both the increase in cooling technology penetration and the evolving electricity demand for cooling in the residential sector, allowing for detailed comparison across years.

6.2.4. Vehicles

The model simulates the transition in vehicles for each building block, including both the growth in the total number of vehicles and the increasing share of EVs over time. This two-step process ensures that the demand for electric mobility reflects not only technological adoption but also overall trends in mobility demand.

Each building block starts with a fixed number of vehicles, defined in the base year. From 2028 onward, a yearly vehicle growth factor is applied to simulate changes in vehicle ownership. This growth factor is applied each year based on the original 2025 baseline. This approach ensures that the number

of vehicles per building block increases in a controlled and predictable manner, without compounding effects. The resulting annual vehicle counts form the basis for further modeling of EV adoption.

The share of electric vehicles within the total fleet changes over time. Before 2028, the model assumes a low EV penetration rate of 1.85%, reflecting current adoption trends [8]. From 2028 onward, a scenario-specific EV adoption factor is applied each year to the total vehicle count in each block. This factor increases over time, capturing the accelerating shift toward electrification in the transportation sector.

The total number of EVs in each building block and year is further disaggregated into four vehicle categories: cars, vans, buses, and trucks. This division is based on a predefined category mix reflecting future projections of the electric fleet. Each category is assigned an average annual driving distance (in kilometers) and an energy consumption rate (in kilowatt-hours per kilometer). Multiplying these factors yields the total annual electricity demand for EV charging per category, building block, and year.

However, understanding the total electricity demand is not sufficient on its own. To assess the implications for the power grid, the model estimates the time required for vehicles to charge and obtain the necessary electricity. This is calculated by dividing each category's electricity demand by an assumed charging power (in kilowatts), based on vehicle size. Larger vehicles such as buses and trucks are assigned higher charging power values than smaller vehicles like cars and vans. The outcome represents the total number of hours vehicles in each category must be connected to a charger each year.

Both annual driving distances and energy consumption rates are derived from assumptions reflecting typical usage patterns. Cars and vans generally cover moderate to high annual distances, while buses and trucks, due to their commercial roles, tend to travel significantly more. Similarly, energy consumption per kilometer increases with vehicle size and weight.

To simulate when charging occurs, the model incorporates behavioral variation among EV users. Users are grouped into three categories:

- Grid-aware users charge mostly during off-peak hours and adjust to grid signals.
- Grid-unaware users charge mainly during peak demand hours (17:00–19:00), potentially stressing the grid.
- Average users are between grid-aware and grid-unaware users.

The total annual charging hours are allocated among these groups using scenario-specific behavioral weights, allowing the model to assess the timing of EV electricity demand.

Once charging hours are distributed across behavior groups, the model constructs detailed hourly charging profiles. These profiles convert required charging hours into hourly power demand, taking into account each vehicle category's charging power. Charging by grid-unaware users is concentrated during the 17:00–19:00 window, while the remaining hours—primarily off-peak periods—are allocated to average and grid-aware users. Charging durations are then evenly spread across their respective time slots. This process generates a representative daily power profile for EV charging.

To construct a full-year charging profile, the daily profile is scaled and replicated based on the weights of the representative days defined earlier in the simulation. This results in an hourly EV charging demand profile for each building block, vehicle category, and year. The resulting temporal granularity enables analysis of the dynamic impact of EV charging on electricity demand across different user behaviors and infrastructure development scenarios.

Beyond demand estimation, the model also evaluates the infrastructure required to support EV adoption. A fixed ratio of charging points per EV is applied to determine the number of charging stations needed per building block and year. These are further categorized into home, company, and public chargers. Public chargers are additionally divided into decentralized and centralized types to reflect differing infrastructure layouts. While charging infrastructure does not directly influence demand in the model, it plays a critical role in the post-analysis. By identifying where chargers are needed most, the model supports planning for grid reinforcement and targeted investment in public charging facilities.

6.2.5. New buildings

The growth of new buildings over the years is an important factor for determining future electricity demand. The model assumes that all new buildings constructed will be equipped with solar panels, as mandated by European regulations starting in that year [42]. This is an important assumption since it

helps reduce the overall electricity demand from the grid, making the transition to renewable energy more feasible. The same values from panels and wattage, are used for new buildings like the calculations for existing buildings.

From 2028 onwards, the total number of buildings in each block is projected to increase annually based on a predefined growth factor relative to the 2025 baseline. The number of new buildings added in each year is computed as the difference between the total number of buildings in the current and previous year.

The energy mix for new buildings depends on the type of heating system being installed. The model assumes that new buildings can either use eHP or be connected to a heat network. The breakdown of these heating system types for new buildings is specified by the new_building_mix parameter. For instance, some new buildings may adopt eHPs, while others may connect to district heating systems.

In alignment with the cooling transition logic applied to existing buildings, the model assumes that only buildings connected to heat networks will adopt active cooling systems. The adoption rate for cooling is based on a factor that adjusts the cooling adoption depending on the year and building characteristics.

For each new building, the energy usage is calculated based on the energy profiles of heating, cooling, and solar generation. The energy profiles for each new building type are adjusted based on representative days and their corresponding weights. These profiles are then multiplied by the number of new buildings each year to calculate the total electricity demand. Specifically:

- Heating: the electricity demand for heating is derived from the energy mix of eHPs and heat networks. The heating electricity usage is determined for each representative day and scaled by the weight of the day.
- Cooling: cooling demand is assumed for buildings with heat networks. The adoption rate for cooling is determined by the new_building_cooling_factor and is multiplied by the respective cooling profiles.
- Solar Generation: solar generation is calculated using a profile based on typical solar production patterns. The total capacity is multiplied by the solar profile to obtain the hourly solar generation.

The total hourly electricity usage is calculated by summing heating and cooling demand. Solar generation is subtracted from this total to compute the net electricity demand for each hour. When net demand becomes negative, this indicates that solar production exceeds total consumption, resulting in reverse power flow to the grid.

Although the spatial distribution of new buildings—such as centralized versus decentralized developments—does not influence the energy demand calculation itself, it remains useful for post-analysis. For example, it enables the identification of areas with the highest new electricity needs or infrastructure requirements.

6.2.6. Industry

The model estimates industrial energy demand on a per-block basis, beginning in 2025. From 2028 onward, changes in industrial activity—whether expansion, stagnation, or decline—are implemented using scenario-specific growth factors. These growth trajectories reflect possible regional developments, including the expansion of industrial zones, stabilization of existing operations, or full de-industrialization due to land-use changes, policy interventions, or economic shifts.

To represent the energy transition in the industrial sector, the model incorporates a gradual phase-out of methane, which is assumed to constitute 100% of fossil-based industrial energy in 2025. This share is reduced linearly to 0% by 2049, in line with national decarbonization targets [49]. Concurrently, sustainable energy carriers—namely electrification and biogas/hydrogen—gain increasing prominence, depending on technological feasibility and policy assumptions. Additionally, a “no industry” category accounts for blocks where industrial activity ceases entirely. Each block’s industrial energy mix per year is composed of four sources:

- Methane: fossil fuel use, phased out gradually;
- Electrification: direct electric processes replacing fossil-based heating;
- Biogas/Hydrogen: applied where electrification is less feasible;

- No Industry: represents decommissioned or repurposed industrial zones.

The model uses assumed annual energy consumption values per unit of industrial activity, based on general process efficiency and fuel characteristics. These values are high-level estimates, suitable for regional energy modeling. They align with typical ranges seen in industrial decarbonization literature, though actual consumption can vary significantly by sector (e.g., steel vs. food processing). For a more granular or sector-specific model, these would ideally be adjusted based on known energy intensities by industry type.

Because industrial demand is assumed to be stable across seasons and daily cycles, annual energy demand is distributed evenly across all hours of the year. This results in an hourly energy profile for each industrial source, computed by multiplying the adjusted industrial stock in each block by the respective hourly energy consumption factor, over a simulation period of 2025 to 2028.

In some scenarios, specific building blocks may be flagged for potential industrial capacity expansion. However, the extent and timing of this expansion remain uncertain. Therefore, the model allows for manual overrides that can be activated per scenario, enabling flexibility in representing expected but undefined industrial developments.

6.2.7. Greenhouses

The modeling of greenhouse energy demand follows a structure similar to that of the industrial sector, with adjustments for the sector's distinct characteristics. The model begins by tracking the total greenhouse area per block as of 2025, with scenario-based changes applied from 2028 onward to simulate shifts in horticultural activity.

A key distinction in the greenhouse module is the accelerated methane phase-out timeline. Reflecting national climate goals, methane is reduced from 100% of fossil energy use in 2025 to 0% by 2040 [18], aligning with the sector's ambition to achieve climate neutrality by that year. As methane use declines, electrification and biogas/hydrogen are introduced as sustainable alternatives. A "no greenhouse" category accounts for blocks where horticultural activity is phased out.

As with industry, the greenhouse heat mix per block and year is divided among four categories: methane, electrification, biogas/hydrogen, and areas where greenhouse activity ceases ("no greenhouses"). Sustainable shares are adjusted dynamically to ensure realistic distribution in each year.

Unlike industry, greenhouse energy consumption is measured per square meter of greenhouse area, reflecting the nature of the initial 2025 data. Energy intensity values are based on general assumptions and are intended for regional-scale modeling. Similar to industry, energy demand is evenly distributed across the year, and hourly profiles are calculated for the full 2025–2028 simulation period by multiplying the adjusted greenhouse area in each block by the relevant hourly energy consumption factor.

6.2.8. Solar park

The model includes both general and block-specific solar park developments. Starting from a 2025 baseline, the total solar park surface area increases from 2028 onward, following scenario-specific growth factors. For each year, the total electricity production is estimated based on a reference yield of 120 kilowatt-hours per square meter per year [1], which reflects expected output under standard conditions. To account for technological improvements and performance changes over time, this base yield is adjusted using the same year-specific efficiency factor that is applied to residential solar panels. This factor starts below 1.0—representing relatively lower performance in the earlier years—and gradually increases in future years to reflect more efficient systems. As a result, the actual electricity yield per square meter grows over time. For example, if the efficiency factor is 0.85 in 2025, the effective yield is 85% of the base value; in later years, as the factor approaches or exceeds 1.0, the yield increases proportionally. The total annual electricity output from general (non-block-specific) solar parks is calculated by applying this adjusted yield to the total installed surface area for each year. This setup allows the model to represent both the physical expansion of solar park infrastructure and the improvement in energy generation efficiency over time.

In addition to this general growth, the model explicitly accounts for two specific solar park projects. The first is a large-scale installation in Building Sector 2.1, covering 400,000 square meters [Data from Stedin], which is scheduled to be build in 2040. This project is fixed and appears in all scenarios. The second project is located in Building Sector 2.2 and is modeled conditionally. Whether it is included and in which year it becomes active depends on scenario-specific settings. In some scenarios, this solar

park is activated in 2043, while in others it may be delayed until 2046 or omitted entirely. If a scenario does not enable the project, the solar park in Sector 2.2 is excluded from the calculations.

Hourly generation for both general and specific solar parks is determined using normalized 24-hour solar production curves based on representative days. These curves reflect realistic seasonal and daily variations in solar output. While electricity from general solar parks is calculated at a global level and subtracted from overall electricity demand, generation from the block-specific solar parks in Sectors 2.1 and 2.2 is modeled separately and contributes directly to the local electricity balance of their respective building blocks. This approach captures both broad, incremental solar development and the impact of major planned infrastructure projects.

6.2.9. Shore power

Shore power is included as a strategy to reduce emissions from docked ships by enabling them to use electricity instead of onboard generators. In this model, shore power is only applied to building blocks categorized as industry, since those are the only relevant locations where such infrastructure would realistically exist (e.g., at ports or industrial wharfs).

There are no shore power connections in place at the 2025 baseline. Instead, connections are introduced gradually starting from 2028, based on scenario-specific stepwise growth patterns. Each industrial block receives new connections at specific intervals depending on the scenario. These increments reflect hypothetical investments in port-side electrification infrastructure.

Shore power consumption is calculated from two distinct components. The first is a fixed “hotel load” of 30 MWh per connection, representing the basic electricity demand of docked ships over the three-year simulation window. The second component accounts for the electrification of shipping fleets. Beginning in 2028, a growing share of ships are assumed to be fully electric, based on scenario-specific adoption rates. These electric ships require significantly more electricity to charge, modeled as an additional 80 MWh per electric ship over three years. The total electricity demand for shore power in each block and year is therefore the sum of these two components: one proportional to the number of total shore power connections, and another proportional to the number of electric ships among those connections.

To capture temporal dynamics, the total electricity demand from shore power is distributed over time using a representative daily profile. This profile introduces hourly variation that reflects typical ship activity, with higher demand during daytime and early evening hours. The result is an hourly load profile for each block and year, reflecting both the quantity of shore power infrastructure in place and the evolving role of electric shipping in total energy demand.

6.2.10. Solar panels on large roofs

To model solar panel adoption on large roofs of industrial buildings, the simulation calculates hourly solar generation over a three-year period, similar to the approach for existing buildings. The key differences are that only industrial building blocks are considered, and each roof is assumed to have 20 panels, each with a 500 W peak power—values based on assumptions for existing buildings. Solar energy generation is determined using representative daily profiles, which are adjusted for efficiency improvements over time. The generated energy is then subtracted from the building’s electricity demand, reducing its net grid demand.

6.3. Investment plan

The investment plan modeled after Stedin’s strategy focuses on maintaining substation capacity limits by introducing a new substation and relocating selected building blocks. In this initial iteration, four building blocks have been selected for relocation: Building Sector 2.1, Building Sector 2.2, Industry Sector 2.4, and Industry/Agriculture/Greenhouse 1. These were chosen based on their proximity to the planned substation and their potential to relieve demand pressure on the existing substation. The goal is to offload a sufficient portion of the existing demand to ensure both substations operate within their capacity limits. The new substation is configured with a maximum capacity of 70 MW and a minimum capacity limit of -140 MW. A trigger threshold of 40 MW is used to initiate the investment: once the simulated hourly demand surpasses this value, a new substation is scheduled for construction. The construction process spans seven years, after which relocated building blocks begin transferring their load to the new substation. In every scenario, only a single new substation is built over the entire

simulation horizon.

Additionally, the simulation incorporates the extra_delays dictionary, which specifies additional delays added to the standard realization time of both the substation and the relocation of building blocks. The standard realization time for relocation is set at one year. Once a building block is relocated, the new substation begins receiving its demand. For this initial iteration, no new building blocks have yet been added to the network.

Cost assumptions are also integrated into the model. These include standard investment costs for building a new substation and installing two transformers. An analysis using PowerFactory was conducted to evaluate whether the existing cables in the relocated building blocks support a 20 kV voltage level. For each cable, it was assessed whether replacement was necessary or whether existing infrastructure could remain. In addition, all transformers located in the distribution rooms of relocated blocks must be replaced, which contributes further to the investment cost.

Assumptions

The assumed realization times for key infrastructure developments—building a new substation, relocating building blocks, and adding new building blocks—are based on estimated durations that reflect typical project timelines and practical considerations.

For the construction of a new substation, a period of seven years has been adopted. This duration is intended to cover the complete lifecycle of the project, including preliminary feasibility studies, environmental assessments, permitting procedures, detailed engineering and design, and the actual construction and commissioning of the substation. In practice, this process is highly regulated and frequently subject to unforeseen delays, often due to land acquisition challenges, alignment with broader infrastructure developments, or the need to coordinate with local authorities and stakeholders.

The relocation of a building block is assumed to take one year. This relatively short timeframe reflects the more straightforward nature of this task in comparison to constructing entirely new infrastructure. It accounts for the necessary planning, the disconnection from the original substation, any required physical rewiring or underground cabling, and the reconnection and commissioning at the new substation. The one-year estimate assumes that the relocation occurs within an already developed urban or industrial grid, where the need for new permits or extensive groundwork is minimal.

The addition of an entirely new building block, although not yet implemented in this iteration of the model, is assumed to require a period of two years. This reflects the greater complexity involved in expanding the grid into new areas. Such a process would typically include location-specific assessments, securing the necessary permits, planning new infrastructure connections, and physically constructing the components needed to support the new demand. The two-year window is considered a reasonable approximation under the assumption of moderate regulatory and logistical challenges.

6.4. Capacity risk

As defined in Chapter 3, capacity risk is the risk of insufficient grid capacity to meet future demand due to uncertainties. To calculate capacity risk, the model simulates the total electricity demand across all building blocks and compares this combined demand against the substation's capacity limits. The substation's capacity is set at 57.5 MW for maximum demand and -80 MW for the return of electricity into the grid. The capacity for a new substation is 70 MW for maximum demand and -140 MW for feed-in capacity.

Two risk thresholds are established to assess capacity risk. The first threshold identifies days when the total network demand exceeds 120% of the substation's maximum capacity or drops below 120% of its minimum capacity at any point during the day. The second threshold focuses on sustained stress: it flags days when demand exceeds 110% of maximum capacity (or falls below 110% of minimum capacity) for six or more hours within a single day.

For each simulation year, the model aggregates the hourly electricity demand of all building blocks into a single combined demand profile, covering a full three-year period (reflecting the simulation's time steps). This allows a detailed view of network demand patterns, hour by hour. The model then analyzes each day within this period by dividing the combined demand into 24-hour segments. It checks whether any hour in the day breaches the first risk threshold and counts the number of hours that breach the second threshold.

If a day exceeds either of these thresholds, it is marked as a risky day. The model tracks how many risky days occur each year, as well as how many are specifically linked to each risk threshold. This

provides a detailed picture of both extreme peak demands and prolonged periods of high stress on the network.

Figure 6.1 presents a visual overview of this evaluation process. As shown, each simulation day is assessed individually in a loop, where demand values are compared against the defined thresholds to determine whether the day is flagged as a capacity risk.

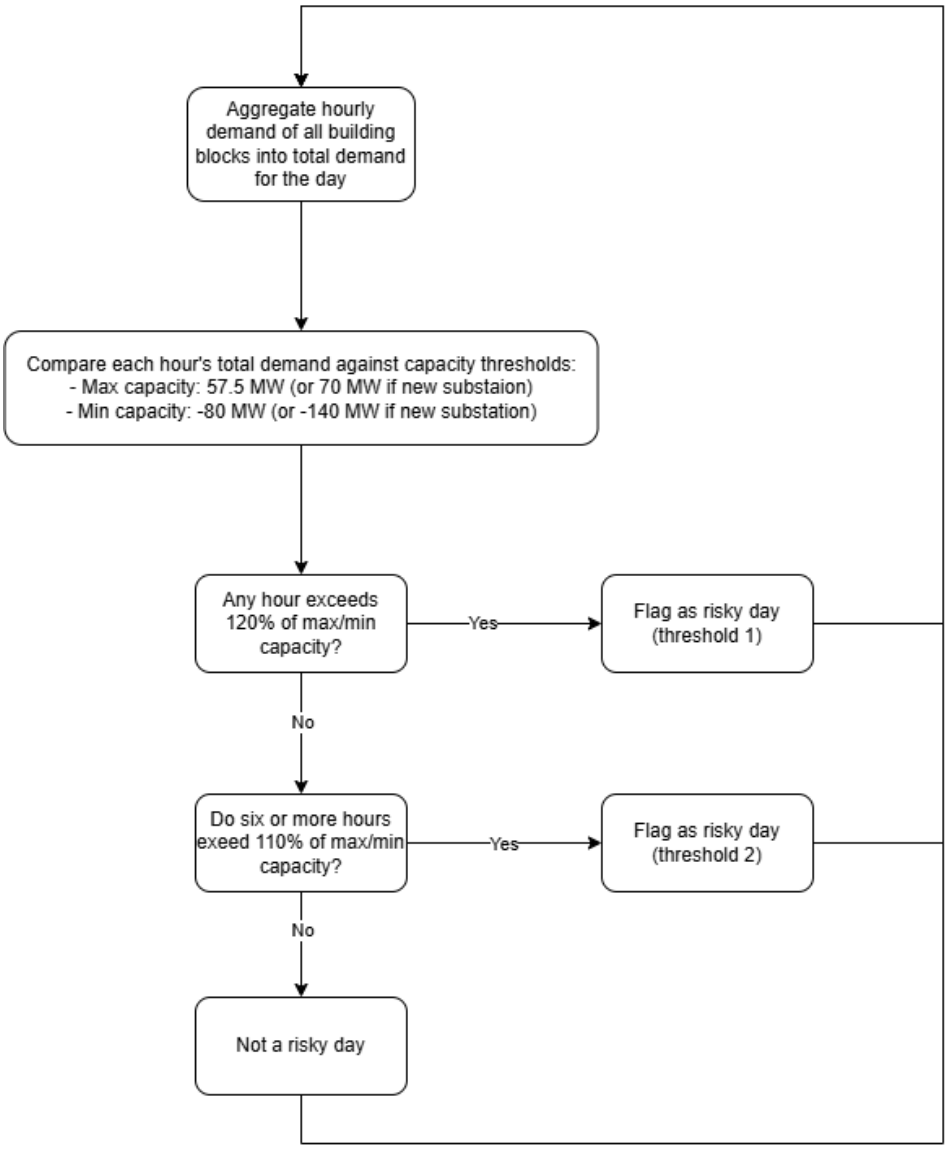

Figure 6.1: Flow chart for daily capacity risk evaluation

Assumptions

The thresholds defined for capacity risks are based on practical assumptions. These assumptions aim to strike a balance between sensitivity to grid stress and robustness against minor, non-critical fluctuations.

The first threshold is set at 120% of the substation's maximum and minimum capacity. This value is chosen because electricity networks, while engineered to handle occasional short-term spikes, typically operate with built-in safety margins to prevent overloads and maintain system reliability. Surpassing 120% represents a level of demand well beyond normal operational tolerance and can pose a serious risk of equipment strain, overheating, or activation of safety mechanisms. By flagging any instance where demand exceeds this threshold—even for just one hour—the model captures critical peaks that could realistically threaten grid reliability.

The second threshold focuses on sustained stress: 110% of maximum capacity (or below 110% of minimum capacity) sustained for six or more hours within a single day. This assumption reflects the understanding that while grids can temporarily tolerate moderate overloads, sustained high demand over several hours places significant stress on infrastructure, increases wear and tear, and heightens the risk of cascading failures. The slightly lower threshold of 110% allows the model to capture these longer-duration stress periods that might otherwise be overlooked if only extreme peaks were considered.

Applying these thresholds uniformly across all simulation years ensures consistency and comparability between different scenarios. While in reality, network upgrades and new technologies might slightly alter capacity margins over time, these thresholds provide a conservative, stable benchmark that highlights relative differences in risk between scenarios rather than attempting to predict exact failure points.

7

Results

This chapter presents the key findings from the stress-testing simulation and subsequent PRIM analysis. It identifies when and under which conditions capacity risks arise, which building sectors are most critical, and how the current and new substations perform under uncertainty. These results inform the identification of trigger conditions and future infrastructure needs.

7.1. Stress-testing results

Following the completion of the simulation, results were analyzed using the notebook ”Demand analyse.ipynb”, which is publicly available on GitHub. Multiple output files were generated during this process, with particular attention given to the file capacity_risks.csv. This file contains, for each scenario, the total number of days with capacity risks for both the current and proposed new substation. It also indicates whether a new substation was added, reports total system costs, and provides a breakdown of the number of risky days every three years for each substation separately.

Across all 1,000 simulated scenarios, a new substation was always added. Consequently, total system costs remained constant. In every scenario, the current substation experienced a non-zero number of risky days, whereas the new substation showed zero risky days in 611 scenarios.

The distribution of total risky days for the current substation (Figure 7.1) reveals a right-skewed pattern. The bulk of scenarios result in between 800 and 1,400 risky days, with a concentration of values peaking around 1,100 to 1,300 days. Given that the simulation spans 28 years (2025–2052), totaling 10,220 days, this peak implies that in these scenarios, approximately 13% (e.g., 1,300 ÷ 10,220 ≈ 13%) of all days are flagged as capacity risk days. This is not a rare edge case: about 140 out of the 1,000 simulated scenarios fall within this range. In other words, there’s a substantial likelihood that the substation will face prolonged and recurring overload issues unless mitigating action is taken. The distribution also features a long tail extending beyond 2,000 risky days, highlighting the presence of outlier scenarios with elevated risk levels. These scenarios likely reflect conditions such as accelerated electrification or delays in planned infrastructure expansions. Conversely, the rarity of scenarios with fewer than 500 risky days suggests that achieving consistently low-risk outcomes would require substantive changes to the current investment trajectory.

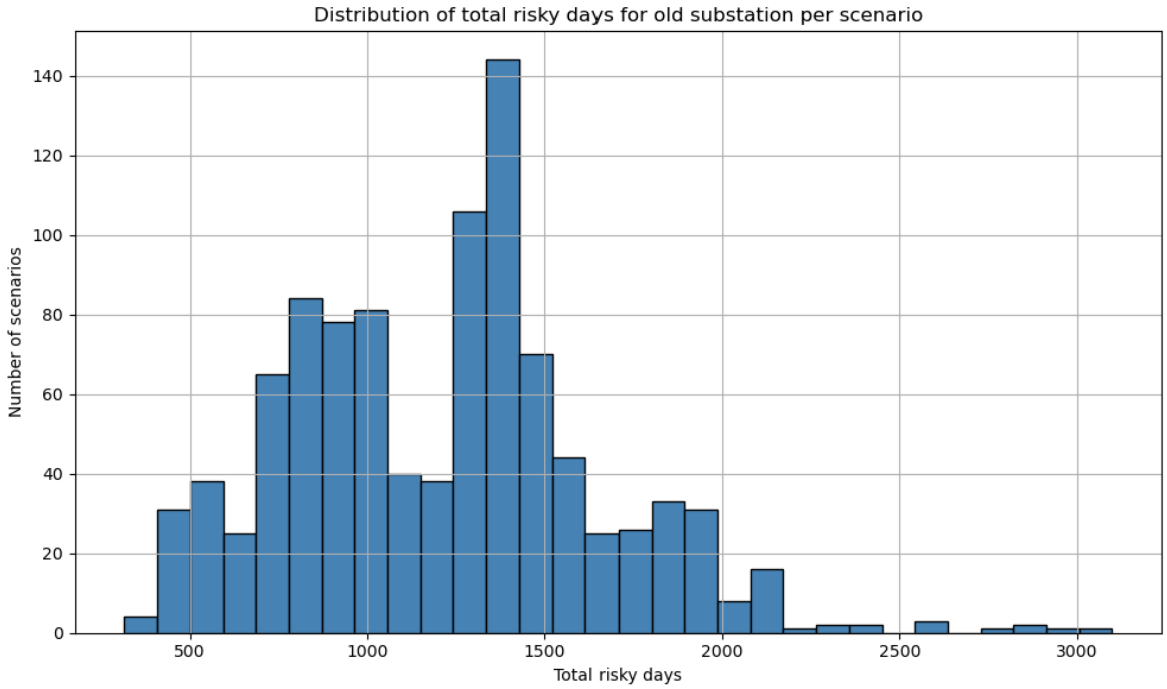

Figure 7.1: Distribution of capacity risks at the current substation across all simulated years (2025–2052)

For the new substation (Figure 7.2), the distribution of risky days also exhibits a right-skewed pattern but is structurally different. A clear majority of scenarios—over 60%—report zero risky days, indicating that the new substation performs effectively under typical or moderately adverse conditions. Nonetheless, a minority of scenarios show between 200 and 500 risky days. These cases likely correspond to instances of rapid demand escalation or elevated levels of electricity fed back into the grid from distributed generation sources, such as rooftop solar or small-scale renewables. Although the new substation is designed with higher capacity, it is not immune to these extremes.

The results underscore that the addition of the new substation substantially reduces the frequency and magnitude of capacity risk events. However, risk is not entirely eliminated. Future infrastructure planning must therefore extend beyond median expectations and incorporate provisions for tail-end risks, which—though infrequent—may carry significant operational and financial consequences.

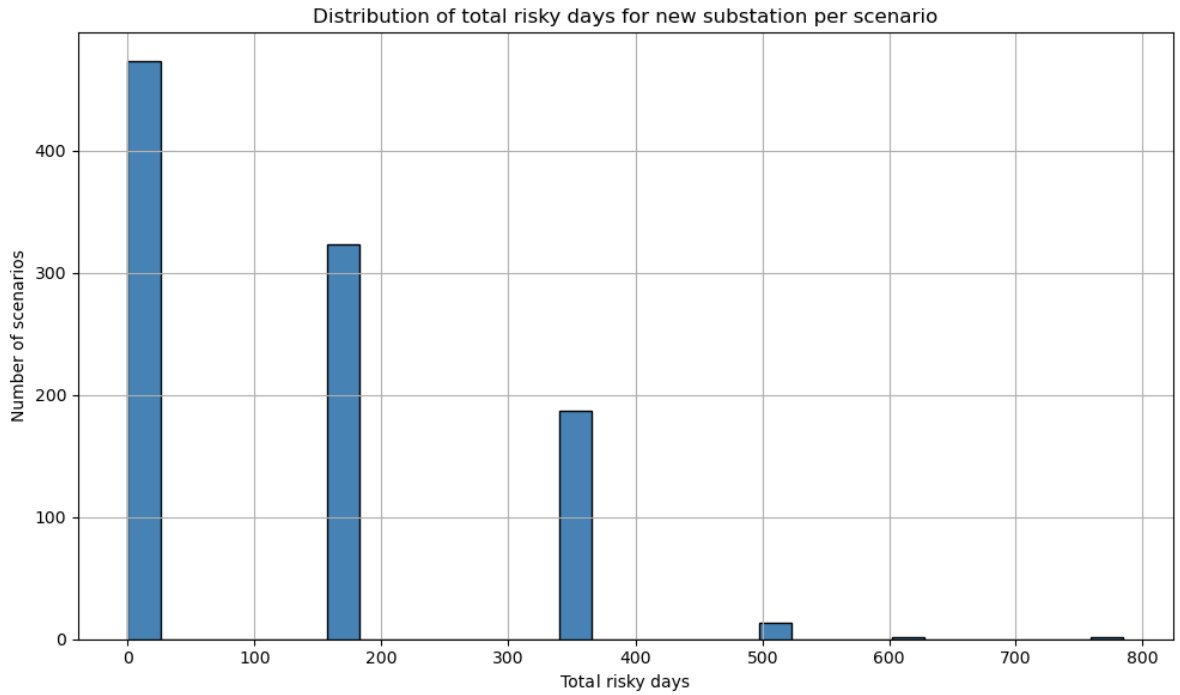

Figure 7.2: Distribution of capacity risks at the new substation across all simulated years (2025–2052)

Across 1,000 simulated scenarios, capacity risk emerges as a persistent challenge. The current substation experiences some level of capacity risk in all scenarios, while the new substation performs significantly better, eliminating capacity issues in 47.3% of cases. Even so, the majority of scenarios still exhibit capacity risks in one or both substations, demonstrating that while the new substation enhances system robustness, it does not fully resolve underlying vulnerabilities.

A year-by-year breakdown of capacity risk (Table 7.1) reveals a clear temporal pattern. The current substation operates without issue in the early years of the simulation (2025–2028). Starting in 2031, however, capacity risk begins to rise sharply, peaking in 2034 and 2037, where 82.9% and 92.0% of scenarios, respectively, show capacity risks. This spike coincides with accelerating load growth that outpaces existing capacity, during a period when neither the new substation nor the associated infrastructure upgrades—such as building block relocations—have yet been completed. The system is particularly vulnerable during this transitional phase. Once the new substation is commissioned around 2031 and gradually integrated through to 2040, capacity risk at the current substation declines significantly. By 2046, only 0.2% of scenarios report any risk. This drop reflects the relieving impact of the new infrastructure and suggests that timely implementation is critical: delays during this high-risk window could lead to widespread service disruptions.

The new substation, by contrast, shows minimal capacity risk until the final years of the simulation. Between 2025 and 2043, no scenarios report risky days, and even by 2046, only 1.5% are affected. However, beginning in 2049, signs of strain begin to appear, with 20.4% of scenarios showing risk, increasing to 52.7% by 2052. This late-stage rise indicates that demand pressures—possibly from continued electrification or decentralized generation—may again exceed system capacity in the long term. Although the new substation is effective in stabilizing the network through the 2030s and 2040s, it is not a final solution.

Together, these findings point to two major conclusions. First, the new substation is essential for resolving mid-term capacity issues and preventing widespread risk during the 2030s. Second, system expansion cannot stop there. Long-term robustness will depend on further capacity planning beyond 2045 to address new demand drivers and maintain low-risk operation across the entire system life cycle.

Table 7.1: Risky days statistics for current and new substation scenario's

Column	Non-zero scenarios	Total scenarios	% with risky days
Risky days current in 2025	0	1000	0.0%
Risky days current in 2028	0	1000	0.0%
Risky days current in 2031	134	1000	13.4%
Risky days current in 2034	829	1000	82.9%
Risky days current in 2037	920	1000	92.0%
Risky days current in 2040	582	1000	58.2%
Risky days current in 2043	82	1000	8.2%
Risky days current in 2046	2	1000	0.2%
Risky days current in 2049	74	1000	7.4%
Risky days current in 2052	341	1000	34.1%
Risky days new in 2025	0	1000	0.0%
Risky days new in 2028	0	1000	0.0%
Risky days new in 2031	0	1000	0.0%
Risky days new in 2034	0	1000	0.0%
Risky days new in 2037	0	1000	0.0%
Risky days new in 2040	0	1000	0.0%
Risky days new in 2043	0	1000	0.0%
Risky days new in 2046	15	1000	1.5%
Risky days new in 2049	204	1000	20.4%
Risky days new in 2052	527	1000	52.7%

In addition to the capacity risk metrics, analysis of 20 time-series output files revealed key patterns in substation demand and associated risks. Yearly plots of maximum and minimum demand highlighted important trends across all 1,000 scenarios.

Figure 7.3 shows annual maximum demand trajectories for the current and new substations. Although many scenario lines overlap due to their similarity, several clear patterns emerge. For the current substation (left), demand begins to exceed the trigger threshold shortly after 2028, marking the onset of capacity risks and signaling the need for new infrastructure. This finding aligns with the sharp increase in capacity risk scenarios observed from 2031 onward, confirming load growth as a critical vulnerability driver.

The right plot shows that in some scenarios, at least one ring is relocated to the new substation by 2037, while in others this occurs as late as 2046. This makes sense as a new substation can be realized after 7 years already without extra delays. As demand shifts to the new substation, the left plot shows a corresponding decrease in load at the current substation, which corresponds to the subsequent decline in risk levels after 2037. By 2052, the final year of the simulation, every scenario indicates that the new substation's maximum demand exceeds its capacity limit, underscoring the capacity risks highlighted in Table 7.1. At the same time, the current substation consistently operates above its capacity limit across all scenarios, emphasizing the persistent and critical capacity challenges it faces. Without effective load management or further infrastructure upgrades, these risks are likely to continue.

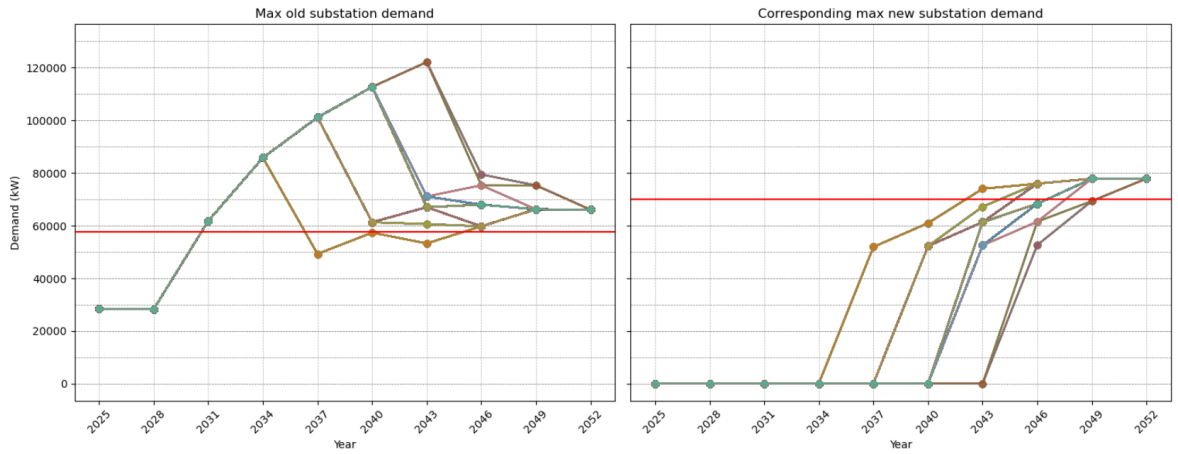

Figure 7.3: Maximum hourly demand over the years for all scenario's

Figure 7.4 shows the hourly minimum demand over time for the same scenarios, illustrating the amount of electricity fed back into the grid at both the current (left plot) and new (right plot) substations. The results remain relatively stable until around 2040 and 2043, where noticeable drops occur in the current substation's minimum demand. These drops coincide with the integration of two solar parks connected to building blocks that are eventually relocated to the new substation. The observed dips suggest that in scenarios where relocation has not yet taken place, solar generation temporarily reduces net demand at the current substation. This interpretation is supported by Figure D.9, which shows that a solar park can already contribute close to -130,000 kW of electricity being fed back into the grid during an hourly peak by 2040—closely matching the magnitude of the dips seen in Figure 7.4.

In all scenarios, the new substation's minimum demand drops below its minimum capacity limit—indicated by the red horizontal line—reflecting increased solar feed-in from rooftop panels and solar parks. After the solar parks' implementation, none of the scenarios show the current substation falling below its minimum capacity limit, indicating that minimum load challenges are more relevant for the new substation.

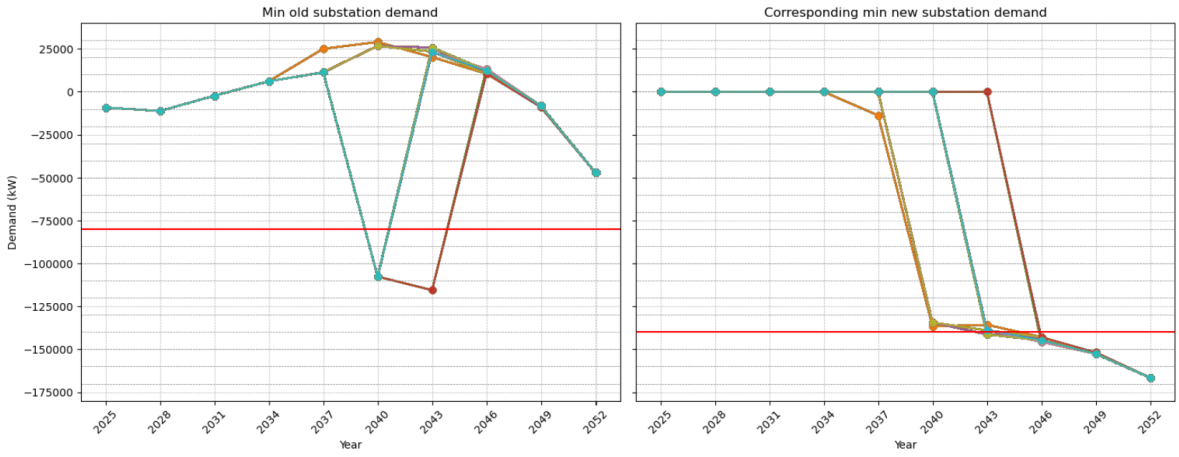

Figure 7.4: Minimum hourly demand over the years for all scenario's

Figure 7.5 presents the maximum hourly demand per building block over the years, based on all 1,000 simulated scenarios. For each year, the highest and lowest observed hourly values across all scenarios were selected to create the annual range of demand per block. Building Sector 2.1 clearly stands out with the highest demand, which rises sharply from 2025 onward and remains relatively stable from around 2037.

This trend in rising demand can be explained by the characteristics of the sector: in 2025, Building Sector 2.1 contains 83% of all residential units. These households are transitioning away from gas

boilers and adopting eHPs and HHPs. While HHPs use gas primarily for heating during the winter months—when gas is generally more efficient or cost-effective for maintaining warmth—they switch to electric operation in the summer. During this period, the heat pump runs in cooling mode. As a result, electricity consumption remains significant throughout the summer due to this cooling demand and the electric components of the HHP system. This seasonal dual operation contributes to sustained electricity demand even during warmer months. Furthermore, since the projected number of new buildings in this sector is based on the existing housing stock, additional demand increases are expected over time. These combined factors can explain why demand from this building block is significantly higher than in others. From around 2037 onward, the trend stabilizes. This leveling off occurs because by then, nearly all existing gas boilers have been replaced, and all newly built homes adopt either eHPs or district heating systems—meaning no new gas boilers are added. Households then rely exclusively on these electric or network-based heating solutions (along with HHPs and airco systems), which have relatively consistent average energy consumption profiles compared to the earlier mix with gas boilers. This contributes to a more stable overall demand level, though some day-to-day variability remains due to factors like weather and user behavior.

In the later years, an upward trend in demand is also observed in several industrial sectors. This suggests that the electrification of industry and the potential adoption of shore power technologies within these sectors will contribute to future electricity demand.

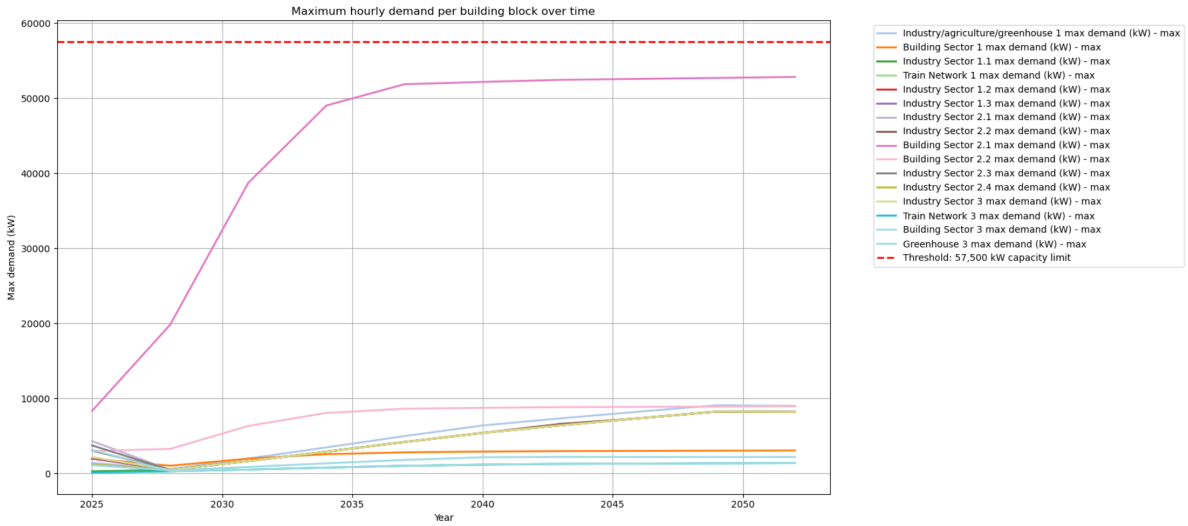

Figure 7.5: Range of maximum hourly demand per building block over the years, based on all 1,000 scenarios

Figure 7.6 illustrates the minimum hourly demand per building block over time, representing periods when electricity is fed back into the grid. Once again, Building Sector 2.1 stands out—this time for exhibiting the highest levels of feed-in. This trend is primarily driven by the planned construction of a large solar park in the sector by 2040. Additionally, because Building Sector 2.1 contains the largest number of existing residential units, it also has the highest potential for rooftop solar generation. Residential solar installations are modeled as a percentage of total housing units, further amplifying the sector's contribution to grid feed-in. As a result of the increased local generation, Building Sector 2.1's demand eventually drops below the -140,000 kW capacity limit of the new substation, which may introduce capacity risk.

Aside from these developments, the overall results remain relatively stable. Only a few industrial sectors show slight declines in demand, likely due to the installation of solar panels on the large rooftops of industrial buildings.

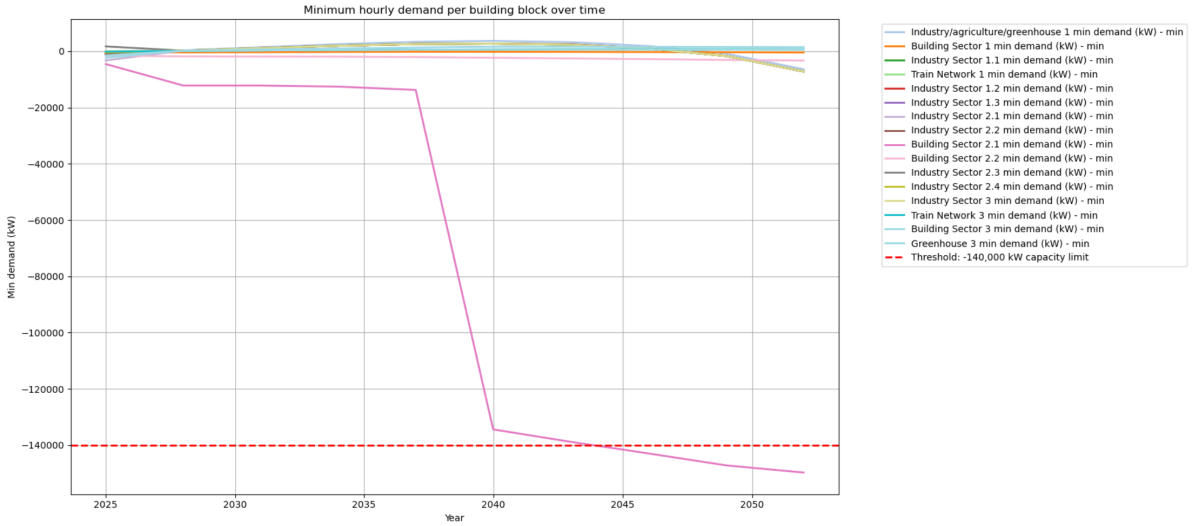

Figure 7.6: Range of minimum hourly demand per building block over the years, based on all 1,000 scenarios

7.2. PRIM

Now that the severity and timing of capacity risks per substation have been identified, the next step is to understand why these risks occur on certain days. To explore the underlying drivers for capacity risks of the current investment plan, a PRIM analysis is conducted. PRIM is a scenario discovery technique that identifies regions—or ”boxes”—in the input space where a specific outcome (in this case, capacity risk) is significantly more likely to occur [47]. These boxes are defined by ranges of uncertain input parameters and are useful for interpreting and communicating the conditions under which risk arises. PRIM is characterized by three key metrics:

- Coverage: the proportion of all risk cases that fall inside the box. High coverage indicates the box captures a large share of the total risk space.
- Density: the proportion of cases inside the box that result in risk. High density implies the box is concentrated with high-risk scenarios.
- Restricted dimensions: the specific uncertainties (input variables) that define the box boundaries. These are the key drivers most strongly associated with the occurrence of capacity risk.

In other words, PRIM helps identify which combinations of uncertainties lead to high probability of capacity risk, and how concentrated or widespread those risks are within the uncertainty space. Ideally, boxes with high density and high coverage are sought while keeping the number of restricted dimensions to a minimum. This balance is important because a simpler box with fewer restrictions is easier to interpret and more actionable. In this study, however, when a trade-off is necessary, high density is prioritized over high coverage, ensuring that the identified region predominantly contains risky scenarios. This makes the insights more reliable for targeted decision-making.

To enhance the analysis, a modified iterative PRIM procedure was applied rather than stopping after identifying a single box. After each run of PRIM, the cases falling within the identified box were temporarily reclassified as non-risk (by setting their binary outcome to 0), allowing the algorithm to search for additional, distinct high-density boxes in subsequent iterations. This process continued until no further boxes above the predefined density threshold could be found. Such an approach—based on the method proposed by Guivarch et al.—avoids overlapping regions and helps uncover multiple independent scenario ”drivers” that can each lead to capacity risk. It improves the diversity of discovered patterns and strengthens the explanatory power of the results.

To support this analysis, data was extracted from the 20 time-series output files, which together comprise the full set of 1,000 scenarios. These files included daily maximum and minimum substation demands, flags for capacity risk occurrence, and uncertainty factor classifications (A, B, or C). For

PRIM to work correctly, the outcome variable must be binary—indicating whether a capacity risk occurred (1) or did not (0)—while the input variables (i.e., uncertainties) must be numerical or ordinal. Data preprocessing was required to meet these criteria and included formatting and encoding steps. The full preprocessing workflow is documented in the GitHub repository under the notebook “Prim analyse.ipynb.”.

To generate meaningful insights, the PRIM analysis was performed separately for each substation and each year, allowing a detailed examination of the conditions that lead to risk over time. For the new substation, the years 2049 and 2052 were analyzed, as these are when capacity risks begin to emerge. For the current substation, PRIM was applied to the years 2031, 2034, 2037, 2040, 2043, 2049, and 2052—corresponding to periods of increasing and declining risk as identified earlier. This targeted approach allows for a deeper understanding of the temporal and spatial drivers behind capacity risk across different system configurations.

A density threshold of 0.8 was used for every analysis, aligning with common practice in exploratory modeling and scenario discovery. This value strikes a practical balance between selecting boxes with sufficiently pure concentration of risk cases while still maintaining broad enough coverage to capture meaningful patterns—ensuring the results remain interpretable and actionable. For example, the EMA Workbench documentation adopts a similar density threshold in its standard PRIM implementation [22].

Using a lower density threshold (e.g., 0.6) would allow boxes with lower purity, potentially including more non-risk cases and thus making it harder to identify clear drivers of risk. Conversely, a higher density threshold (e.g., 0.9 or above) would select boxes with very high purity but might exclude many risk cases, resulting in very small or overly specific boxes that miss broader patterns. Therefore, a density threshold of 0.8 is used as a balanced compromise.

7.2.1. Current substation

2031

The first year of analysis for the current substation is 2031. Box 6 was selected for the first iteration, with a density of 0.845 and a coverage of 0.366. In other words, this box captures 36% of all risky scenarios, and more than 8 out of 10 scenarios inside the box are indeed risky. However, the relatively low coverage indicates that nearly two-thirds (64%) of risky scenarios lie outside this identified cluster. This highlights that while Box 6 describes a significant and concentrated subset of risk drivers, capacity risk is not confined to a single, clearly defined combination of uncertainties. Instead, the risk is distributed across a broader and more diverse range of conditions. As a result, managing capacity risk effectively will require strategies that address multiple pathways and scenarios, rather than focusing solely on the dominant cluster identified here.

Five key drivers are associated with this box: the progress of the heat transition (i.e., moving away from gas boilers), the uptake of air conditioning, the adoption of eHP’s, moderate changes in industrial activity (−5% or +10%), and a low share of ”no industry” (10–15%) in the industrial mix. The first three are straightforward—electrification of heating and increased cooling demand both raise household electricity use, which aligns with Figures 7.5 and 7.6 where residential buildings in Building Sector 2.1 dominate demand in 2031.

Industrial activity plays a more nuanced role in capacity risk. Interestingly, both a moderate increase (+10%) and a slight decrease (−5%) in industrial activity are associated with elevated risk in this analysis. The increase is relatively straightforward: as new industrial sectors grow, they tend to be more electrified by design, driving up electricity demand. The decrease, while initially surprising, also makes sense in the context of the model. A 5% reduction in industry reflects the decline of methane-based processes. As these are phased out, the remaining industrial activity can look more dominated by electrified processes. This shift can raise the overall electricity load, even if total industrial output falls.

The ”no industry” variable adds further complexity. While ”no industry” implies zero industrial electricity demand, a low share of ”no industry” (10–15%) in the mix implies that the remaining industrial composition is dominated by sectors with high electrification potential. In the model, this means electrification rates in the remaining industry can reach up to 60%, significantly increasing electricity consumption. Thus, a low share of ”no industry” acts as a proxy for highly electrified industrial scenarios, amplifying system-wide load—particularly when combined with rising residential electrification.

After reclassifying the cases in box 6 as non-risk (i.e., setting their outcome to 0) for the second PRIM iteration, no additional boxes met the density threshold of 0.8. This suggests that, although Box 6 captures only part of the risky scenarios, it represents the most concentrated and clearly defined cluster of capacity risk drivers in 2031. The absence of other high-density boxes indicates that the remaining risky scenarios are more dispersed and do not form distinct, easily identifiable patterns at this density level. Consequently, while Box 6 highlights a key risk profile, the broader risk landscape remains diffuse and may require more nuanced or multi-faceted approaches to fully understand and manage.

2034

For the year 2034, box 1 was selected in the first PRIM iteration, with a density of 0.993 and a coverage of 0.800. This means the box encompasses 80% of all scenarios involving capacity risk, with nearly all the included cases being high-risk—suggesting a highly representative and reliable result.

Only one key driver is associated with this box: the heat transition. As in 2031, this is a straightforward finding. Replacing gas boilers with electric alternatives increases household electricity consumption, reinforcing the importance of the heat transition in shaping early system vulnerability. This result again aligns with Figures 7.5 and 7.6, where residential buildings dominate demand patterns.

In the second iteration, additional structure was found. Box 4 was selected, with a density of 0.88 and a coverage of 0.68. Three key drivers characterize this box: the heat transition, moderate changes in industrial activity (−7% or +20%), and a low share of ”no industry” (10–15%). These factors mirror those seen in 2031, suggesting consistent mechanisms behind capacity risks during this early period.

A third iteration was performed, but no additional boxes met the density threshold of 0.8. This suggests that the most relevant combinations of drivers for 2034 were already captured in the first two iterations.

While Box 1 clearly represents the dominant risk profile due to its high coverage and density, Box 4 highlights that a substantial portion of capacity risk is also influenced by industrial activity and the composition of the industrial mix. Thus, although the heat transition emerges as the primary driver of risk in 2034, industrial factors remain an important secondary consideration. Together, these two boxes capture the main distinct patterns of capacity risk, indicating that effective risk management should address both household electrification and evolving industrial dynamics.

2037

In 2037, the analysis identified a single box in the first iteration with a perfect density of 1.0 and a coverage of 0.729. This indicates that every scenario within the box exhibits capacity risk, and that the box captures approximately 73% of all risky scenarios for this year.

The key driver here is the delay in constructing the new substation, which is intuitive. As shown in Figure 7.3, scenarios where the new substation is already operational see demand drop to within capacity limits. Conversely, scenarios without the new substation by this year—and where building blocks are still allocated to the current substation—experience rising demand, with some projections reaching 120,000 kW by 2040 (see Figure 7.3). This delay prevents demand from being split between two substations, leading to almost always significant capacity risks at the current substation.

In the second iteration, box 3 was identified, again with a perfect density of 1.0 and a coverage of 0.38. This box is defined by two key drivers: the continued delay in constructing the new substation and the ongoing transition away from gas boilers. The latter reflects the growing shift toward electrified heating technologies such as HHPs, eHPs, heat networks, and air conditioning systems—changes that increase electricity demand and exacerbate capacity constraints.

The third iteration also yielded a valid box—box 5—with a density of 1.0 and an increased coverage of 0.51. This box shares the same two drivers as the previous iteration (substation delay and gas boiler phase-out) and introduces a third: the widespread adoption of HHPs. This addition is consistent with model behavior, as HHPs consume significant electricity during peak periods, thereby contributing directly to elevated system load and increasing the likelihood of capacity risk.

Interestingly, the pattern of coverage across iterations—initially decreasing and then increasing—provides

insight into the structure of the scenario space. The initial drop in coverage (from 0.729 to 0.38) reflects the fact that the most dominant and clear-cut cluster of high-risk scenarios was captured in the first box. Subsequent boxes, by design, must explore less dominant or more specific regions of the input space. However, because previously covered cases were only temporarily reclassified as non-risk (i.e., not removed from the dataset), scenarios included in earlier boxes remained available in later iterations. As a result, the increase in coverage during the third iteration (to 0.51) may reflect some re-capturing of scenarios from the first box rather than the discovery of a fully distinct cluster. This suggests that box 5 intersected a larger portion of the high-risk scenario space, possibly overlapping with earlier iterations rather than uniquely expanding on them.

This fluctuation highlights two important interpretive points. First, capacity risks in 2037 are not confined to a single set of conditions—while substation delay remains the consistent root cause, its interaction with different demand-side factors (e.g., electrification technologies) creates multiple, overlapping risk archetypes. Second, the increase in coverage at a later stage does not necessarily indicate a newly uncovered structure but rather reinforces the explanatory strength of already-identified conditions. It also underscores the value of iterative PRIM in revisiting the full dataset to reveal persistent patterns across overlapping clusters.

No further boxes meeting the density threshold were identified in the fourth iteration, indicating that the most salient risk-driving patterns in the 2037 scenario space had been successfully captured.

2040

In 2040, box 1 was identified in the first iteration with a density of 0.838 and a remarkably high coverage of 0.966. This indicates that the box captures nearly all scenarios in which capacity risk occurs, while maintaining a strong concentration of true risk cases. Such a result points to a highly dominant risk pattern in the scenario ensemble for this year. The sole driver associated with this box is the delay in constructing the new substation.

No additional boxes met the density threshold in the second iteration.

2043

No boxes were identified at the 0.8 density threshold in 2043. This indicates that no single, well-defined region of the scenario space captures a sufficiently large and concentrated portion of capacity risk cases. In other words, capacity risks for the current substation in this year are more diffuse and do not cluster strongly around specific combinations of input uncertainties. This suggests that the risk drivers are more varied or that capacity issues may be less pronounced or more evenly spread across scenarios, making it harder to isolate dominant risk patterns for targeted intervention.

2049

In 2049, box 5 was selected with a density of 0.861 and a coverage of 0.838, indicating that it captures nearly 84% of all risky scenarios. The three key drivers within this box are suitable roofs for large solar panels, the actual installation of these large solar panels, and the efficiency of these solar panels. Notably, the combination of these three key drivers has a substantial impact on capacity risk. While suitable roofs for large solar panels and their installation are primarily tied to the industrial sector—since these large panels are mostly installed on industrial rooftops—solar panel efficiency influences all installations, including residential buildings and solar parks. Together, these factors contribute to capacity risks in 2049, with the industrial sector playing a central role due to the extensive deployment of rooftop solar and increasing electrification.

This shift is reflected in Figure 7.6, which shows a decrease in minimum hourly demand within industrial building blocks. Earlier in the planning horizon, capacity risks were mainly driven by larger building sectors, but load relocation through the new substation has largely mitigated those pressures. As a result, the focus of capacity risk has moved toward the industrial sector, where the interplay of solar panel deployment and efficiency improvements creates new challenges for the system.

No additional boxes meeting the 0.8 density threshold were identified during the second PRIM iteration.

2052

In 2052, box 2 was selected in the first iteration, with a density of 0.906 and a coverage of 0.848. The sole driver identified is the suitability of industrial roofs for large-scale solar panel installation. This result

highlights a shift in the nature of capacity risk by this point in time—away from demand-side drivers and toward risks associated with decentralized energy feed-in from industrial-scale solar generation.

In the second iteration, box 6 was selected, exhibiting a perfect coverage of 1.0 and a density of 0.81. Four key drivers define this box: suitability of roofs for large solar panels, the actual construction of the solar panels, solar panel efficiency and moderate changes in industry activity (-25% or +20%). Since this box captures all remaining risk cases, no further iterations were conducted.

Taken together, these findings reveal a temporal progression in the drivers of capacity risk at the current substation: early-stage risks are predominantly linked to residential electrification, mid-term risks are shaped by infrastructure delays and heating transitions, and long-term risks are increasingly driven by high levels of industrial solar feed-in. This evolution reflects the shifting balance between consumption and generation in the grid, emphasizing the need for adaptive planning over time.

7.2.2. New substation

2049

For the new substation in 2049, box 4 was identified with a density of 0.899 and a coverage of 0.608. The key drivers associated with this box are: suitability of roofs for large solar panels, actual construction of large-scale solar installations, and solar panel efficiency (both on residential rooftops and solar parks). These drivers reflect the same risk mechanisms previously observed in the current substation. Specifically, they indicate high levels of solar energy generation and corresponding grid feed-in. This aligns with earlier observations in Figure 7.4, where the new substation exceeds its minimum capacity threshold in several scenarios—pointing to issues related to reverse power flow caused by excessive distributed generation.

The second PRIM iteration did not identify any additional boxes that met the density threshold of 0.8, suggesting that the primary risk structure had already been captured in the first box.

2052

In 2052, box 2 was selected with a high density of 0.875 and a coverage of 0.732. Two key drivers reappear: suitability of roofs for large solar installations and solar panel efficiency. These are consistent with the 2049 results and reinforce the role of solar-related variables in shaping risk. Their impact is again evident in Figure 7.4, where the minimum demand at the new substation drops below the operational threshold in several scenarios. This reflects a system imbalance in which high feed-in, rather than high consumption, drives the capacity constraint. As with 2049, the second iteration did not yield any boxes exceeding the density threshold, further indicating that risk in this period is concentrated in a well-defined subset of scenarios.

Overall, these results highlight a key distinction in the nature of capacity risk at the new substation. Unlike the current substation—where risk is initially driven by increasing demand and delayed infrastructure—the new substation faces challenges primarily related to reverse flows from excessive solar generation. As solar deployment expands, particularly on industrial rooftops and in solar parks, managing energy feed-in becomes a central issue for long-term system stability and planning.

7.2.3. Summary of findings

To synthesize the PRIM findings for each year and substation, Table 7.2 below summarizes the primary drivers of capacity risk across time. This table captures the year-by-year evolution of capacity constraints, the substation affected, and the key drivers responsible for high-risk scenarios. It provides a compact overview of how capacity risk shifts from demand-driven pressures (e.g. heating electrification) in earlier years to generation-driven issues (e.g. excess solar feed-in) in later years—particularly.

Table 7.2: Summary of capacity risk drivers per substation and year first iteration

Year	Substation	Key drivers of capacity risk
2031	Current	Gas boiler phase-out, uptake of air conditioning for cooling, adoption of eHP's, moderate industry changes (−5% or +10%), low share of "no industry" (10–15%)
2034	Current	Gas boiler phase-out, moderate industry changes (−7% or +20%), low share of "no industry" (10–15%)
2037	Current	Delay in new substation construction, gas boiler phase-out, adoption of HHPs
2040	Current	Delay in new substation construction
2049	Current	Industrial rooftop suitability for solar, installation rates, solar panel efficiency
2052	Current	Suitability of roofs for large solar panels, construction of the solar panels, solar panel efficiency, moderate industry changes (−25% or +20%)
2049	New	Industrial rooftop suitability for solar, installation rates, solar panel efficiency
2052	New	Suitability of roofs for large solar installations and solar panel efficiency

This summary confirms that early-stage risks (2031–2040) at the current substation are largely driven by growing residential demand—especially from heating and cooling electrification—compounded by delays in infrastructure deployment. In contrast, longer-term risks (2049–2052) at both substations are shaped by high levels of decentralized solar generation, especially from industrial-scale rooftop installations. These risks point to the emergence of reverse power flow and the growing importance of managing distributed generation as part of future grid planning.

7.3. Second iteration

7.3.1. Trigger conditions

Based on the assessment of maximum and minimum demand trends for both substations over the years, along with insights from the PRIM analysis, two adjustments to the investment plan are proposed (see Table 7.3).

Table 7.3: Comparison of simulation assumptions: first vs. second iteration

Parameter	First iteration	Second iteration
Substation construction trigger	Triggered by demand exceeding threshold	Construction begins in 2025 regardless of demand
Solar park connection	May connect to current or new substation depending on timing	Always connects to new substation due to early completion
Code version	`Simulation.py`	`Simulation second iteration.py`

First, the demand is projected to rise sharply after 2028, reaching nearly 120,000 kW by 2040 for some scenarios (see Figure 7.3). Notably, the years 2034 and 2037 show capacity risks across almost all scenarios (see Table 7.1). This trend indicates that the current trigger threshold of 40,000 kW for building a new substation is insufficiently responsive. Therefore, it is recommended to initiate construction of the new substation in 2025, irrespective of whether demand has yet reached the original trigger level.

Proactive investment in 2025 is expected to significantly reduce the occurrence of capacity risks in 2034, 2037, and 2040 across most, if not all, scenarios. While residual risks may still occur—particularly in scenarios involving construction delays—this revised timing should address the bulk of the system stress during these critical years.

In addition, Figures 7.4 and 7.6 highlight that the large solar park planned for 2040 introduces significant reverse power flow into the grid. This solar park is located in a building block that is intended to be relocated to the new substation. However, in some scenarios, this relocation has not occurred by 2040, resulting in capacity risks for the current substation.

To address this, the solar park should be connected exclusively to the new substation. Given its higher capacity, the new substation is better equipped to manage the additional feed-in without exceeding capacity limits. This measure will reduce the likelihood of capacity risks at the current substation and support long-term system reliability under increased electrification.

To operationalize these adjustments, two modifications were made to the code. First, the trigger condition based on demand thresholds was removed from the policy. Second, the apply_policy function was modified to ensure that construction of all new substations begins in 2025, independent of projected demand levels. The code used to run the second iteration can be found on GitHub under ”Simulation second iteration.py”.

As a result of these changes, the solar park will automatically be connected to the new substation rather than the current one. This is due to the timeline of substation realization: with a construction time of seven years and a maximum possible delay of three years, the new substation will be operational by 2035 at the latest. Since the building block containing the solar park is always scheduled first for relocation, it will be transferred to the new substation and fully realized by 2039—even in the worst-case delay scenario. Because of this, there is no need to add an additional building block to absorb the solar feed-in, avoiding unnecessary complexity and additional costs.

7.3.2. Results

In the second iteration, the same analysis approach was applied as in the first. The full set of results can be reviewed in the corresponding Jupyter Notebook titled ”Demand analyse second iteration.ipynb”, available on GitHub.

Capacity risk

One key change in this iteration is that construction of the new substation begins in 2025 across all scenarios. So again, the investment costs are identical in every case. The adjustment has had a noticeable impact on the distribution of risky days at the current substation. Compared to the first iteration, where the distribution was broader and more varied, two distinct peaks now emerge: one between 0–100 risky days and another between 300–400 days. This indicates that, in many scenarios, the current substation experiences either minimal or moderate operational stress. However, a long right tail remains, with some scenarios accumulating over 1500 risky days—highlighting a subset of cases with prolonged capacity risk. Compared to Figure 7.1 from the first iteration, these peaks have shifted to a lower number of total risky days, suggesting that beginning construction in 2025 effectively reduces the overall number of risky days. The distribution of risky days at the new substation remains largely unchanged, which aligns with expectations since no structural changes were made that directly influence this component.

An examination of risky days per substation per year shows a marked improvement compared to the first iteration. Looking across all 1,000 scenarios, the current substation now operates without capacity risk in 23.4% of scenarios, a significant improvement from the 0% risk-free scenarios in the first iteration. The new substation remains largely robust, with 46.6% of scenarios showing no capacity risk, a result consistent with earlier findings. These results suggest that initiating substation construction earlier has meaningfully improved overall system robustness.

From 2025 to 2028, no capacity risks are present at either substation (see Table 7.4). In 2031, risk levels begin to rise again at the current substation, peaking in 2034, when 60.1% of scenarios show capacity risk. This is substantially lower than the 82.9% observed in the first iteration. These residual risks in 2034 likely stem from the fact that not all building blocks have yet been relocated due to delays. From 2037 through 2046, no capacity risk is observed at the current substation in any scenario, demonstrating the effectiveness of having the new substation fully realized and populated by that time. Despite the improved infrastructure, capacity risks begin to reappear in 2049 and 2052 in a portion of the scenarios. This suggests that long-term growth in demand and supply may again begin to challenge system capacity, even with the presence of the new substation.

At the new substation, results are nearly identical to the first iteration, as expected. Notably, the assumption that the new substation could accommodate the solar park planned for 2040 proves valid—no capacity risk occurs in any scenario for that year.

To better understand where and when capacity challenges are most acute, a filtered analysis was

conducted excluding the problematic years 2049 and 2052. Under this condition, the current substation's share of risk-free scenarios increases to 36.5%, while the new substation's share rises dramatically to 97.4%. This clearly identifies 2049 and 2052 as the main contributors to risk at the new substation, whereas for the current substation, the key risk years remain 2031 and especially 2034.

Overall, although initiating substation construction earlier has significantly reduced the total number of risky days, further analysis is needed to understand the re-emergence of capacity risks in the later years of the simulation period—and to see whether different uncertainties are driving these outcomes compared to the first iteration.

Table 7.4: Risky days statistics for current and new substation scenario's second iteration

Column	Non-zero scenarios	Total scenarios	% with risky days
Risky days current in 2025	0	1000	0.0%
Risky days current in 2028	0	1000	0.0%
Risky days current in 2031	128	1000	12.8%
Risky days current in 2034	601	1000	60.1%
Risky days current in 2037	0	1000	0.0%
Risky days current in 2040	0	1000	0.0%
Risky days current in 2043	0	1000	0.0%
Risky days current in 2046	0	1000	0.0%
Risky days current in 2049	90	1000	9.0%
Risky days current in 2052	377	1000	37.7%
Risky days new in 2025	0	1000	0.0%
Risky days new in 2028	0	1000	0.0%
Risky days new in 2031	0	1000	0.0%
Risky days new in 2034	0	1000	0.0%
Risky days new in 2037	0	1000	0.0%
Risky days new in 2040	0	1000	0.0%
Risky days new in 2043	1	1000	0.1%
Risky days new in 2046	26	1000	2.6%
Risky days new in 2049	227	1000	22.7%
Risky days new in 2052	534	1000	53.4%

Demand analysis

To investigate the continued occurrence of capacity risks in the later years, the next step involves examining the maximum hourly demand over time. Figure 7.7 supports the findings in Table 7.4. For the current substation (left plot), demand exceeds the capacity limit in 2031 and 2034 in several scenarios, which can be attributed to delays in relocating the building blocks. Once the new substation becomes operational, demand at the current substation drops below the capacity threshold and remains stable through 2046. However, from 2049 until 2052, the maximum demand slightly goes up again, which aligns with the reappearance of capacity risks in those years.

For the new substation (right plot), demand increases steadily after construction and begins to go towards the capacity limit around 2040. It remains below the threshold in subsequent years across all scenarios. So, the capacity risks identified in Table 7.4—particularly from 2043 onward—are likely not driven by peak demand, but rather by reverse power flows back into the grid during periods of low demand and high solar generation.

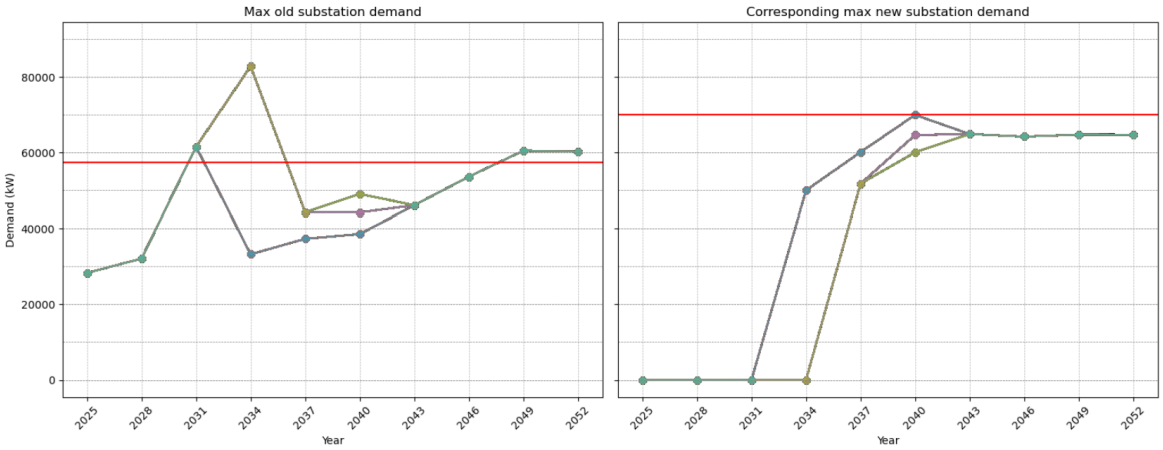

Figure 7.7: Maximum hourly demand over the years second iteration

Figure 7.8 illustrates the minimum hourly demand for both substations across all scenarios. Compared to the first iteration, the current substation no longer experiences minimum demand falling below the lower capacity limit until 2052. In contrast, the first iteration showed that in 2040 and 2043, a few scenarios resulted in demand dropping below this threshold. This change can be attributed to the revised assumption that new solar parks are always connected to the new substation, which prevents the excessive negative demand that previously appeared at the current substation.

For the new substation, a sharp decline in minimum demand is observed starting in 2040, clearly indicating the impact of the solar park's integration. Following this, the trend continues to decrease steadily, eventually surpassing the lower capacity limit in 2046, 2049 and 2052. This drop explains the occurrence of capacity risks in these years, as reflected in Table 7.4.

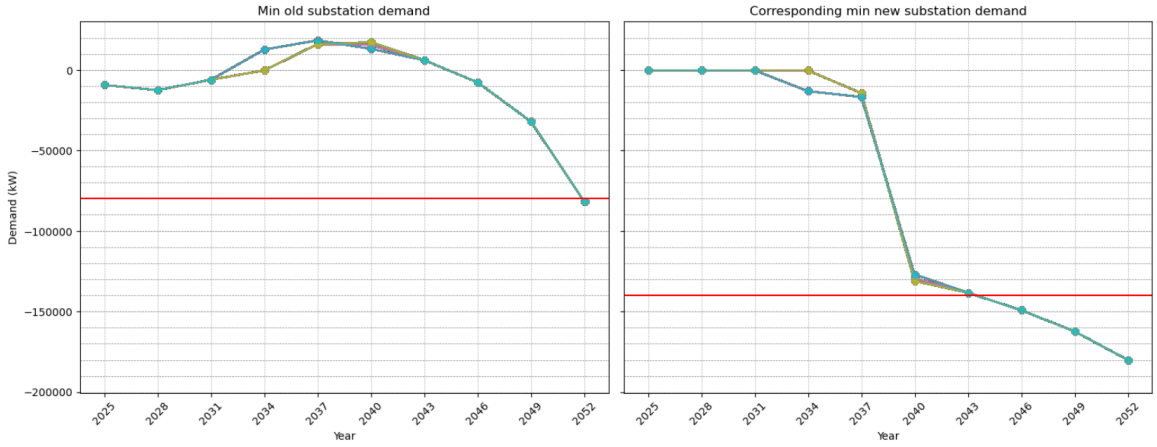

Figure 7.8: Minimum hourly demand over the years second iteration

In summary, advancing the construction timeline of the new substation has significantly mitigated short- and mid-term capacity risks. The early years of the simulation (2025–2028) show no issues, and even the high-risk period around 2034 has seen substantial improvement compared to the first iteration. The current substation operates well within capacity after the investment is realized, and the revised assumption regarding solar park connections has effectively resolved issues related to minimum demand. However, capacity risks re-emerge from 2049 onwards at both substations—despite the expanded infrastructure. This suggests that long-term demand dynamics or other interacting factors may be pushing the system toward new stress points.

To understand what is driving these later-year risks—whether it's specific patterns in electrification, solar expansion, relocation delays, or other uncertainties—a more detailed diagnostic is needed. To

uncover which combinations of uncertain parameters are most associated with capacity risk during this later period, a PRIM analysis is needed.

PRIM

Based on the capacity risk results, a PRIM analysis was performed for the current substation in the years 2031, 2034, 2049, and 2052. For the new substation, analysis focused on 2049 and 2052, as these were the only years showing notable capacity risk. The complete code and results can be found in the notebook titled ”Prim analyse second iteration.ipynb”, available on GitHub.

In 2031 no box was identified at the 0.8 density threshold. Capacity risks for the current substation in this year are more diffuse and do not cluster strongly around specific combinations of input uncertainties.

In 2034, box 1 was selected with a very high density of 0.857 and full coverage (1.0), meaning all risky scenarios fall within this box. Interestingly, only one key driver is found here: a substation delay of 1 to 2 years. This is a notable shift from the first iteration, where the heat transition played a dominant role. The fact that the new substation is already constructed in more scenarios reduces the influence of the heat transition; now, the length of the delay in substation delivery is the critical factor. This highlights the increasing importance of timely infrastructure delivery to avoid risk.

Because box 1 already includes all risky scenarios, a second iteration cannot technically proceed using it—it leaves no residual high-risk cases. To explore additional structure in the data, another box with slightly lower coverage was used instead. Box 2, with a coverage of 0.769 and a very high density of 0.987, was selected for this purpose. It reveals a slightly different risk cluster, where substation delay is again central, but now interacts with the heat transition. This suggests that while delay remains the dominant factor, electrification of heating still contributes meaningfully to elevated risk in a subset of scenarios.

By setting box 2 to 0 (i.e., removing its scenarios from the dataset), a second PRIM iteration was conducted. This resulted in the selection of box 5, which had a coverage of 0.734 and a density of 0.85. In this box, four key drivers emerged: delay of the substation and heat transition again, but also a moderate change in industry activity (-7% or +20%) and a low share of ”no industry” (10–15%). Interestingly, these drivers match those identified in the first iteration of the 2034 investment plan for the current substation, indicating a consistent pattern of risk factors across analyses.

A third iteration was attempted but did not yield any additional boxes, suggesting that most significant high-risk patterns had already been captured in the earlier steps.

This outcome reinforces the strength and representativeness of box 1 in the first iteration. The fact that no additional boxes could extend coverage further confirms that substation delay alone is a sufficient condition for risk in this year. Nevertheless, the additional boxes offer valuable insights into how other drivers modulate or compound this risk. The re-emergence of the heat transition, along with industrial variables in box 5, suggests that while they are not essential for risk to occur, they do intensify the system’s vulnerability when combined with infrastructure delays. Together, these findings underline that although substation delay is the primary bottleneck in 2034, managing demand-side developments—particularly heating and industrial transitions—remains important for reducing cumulative system stress under more complex or delayed infrastructure pathways.

In 2049, results closely mirror those from the first iteration. Box 5 shows a coverage of 0.767 of risky scenarios with a density of 0.896. The same three key drivers are identified here as in the first iteration: the suitability of industrial rooftops for solar PV, the actual realization of large-scale solar rooftop installations and the efficiency of the solar panels. Here again, the second PRIM iteration did not identify any additional boxes.

2052 presents results that are almost identical to the first iteration. Box characteristics and the key driver remain unchanged, reinforcing the persistence and predictability of risk factors in this later stage. Furthermore, the second PRIM iteration did not identify any additional boxes, suggesting that the dominant risk patterns were already fully captured in the initial analysis.

Together, these findings indicate that early and mid-term capacity risks have been significantly mitigated through infrastructure planning and adjusted assumptions. However, long-term risks persist and

have evolved in nature. While demand-side factors—such as industrial growth—were critical in the first iteration, they are no longer key drivers in this iteration. Instead, infrastructure timing (e.g., substation delays) and decentralized generation deployment (e.g., rooftop solar) have emerged as the dominant risk factors. This transition suggests that the effectiveness of long-term capacity planning will increasingly depend on addressing uncertainties in infrastructure delivery and local energy production, rather than purely managing demand growth.

For the new substation in 2049, box 4 was selected with a high density of 0.899 and a moderate coverage of 0.67. This box includes three key drivers, all of which are consistent with those identified in the first iteration—indicating stable risk factors across analyses. Notably, the second PRIM iteration did not reveal any additional boxes, suggesting that the primary sources of risk were already effectively captured.

In 2052, box 2 was selected with a density of 0.87 and a coverage of 0.742. The same two key drivers are identified as in the first iteration. The second iteration did again not reveal any additional boxes.

7.3.3. Summary of findings second iteration

Table 7.5 summarizes the primary drivers of capacity risk across time, by capturing the year-by-year evolution of capacity constraints, the substation affected, and the key drivers responsible for high-risk scenarios.

Table 7.5: Summary of capacity risk drivers per substation and year second iteration

Year	Substation	Key drivers of capacity risk
2034	Current	Transition away from gas boilers, delay in constructing the new substation, moderate industry changes (−7% or +20%), low share of ”no industry” (10–15%)
2049	Current	Suitability of industrial rooftops for solar PV, realization of large-scale solar rooftop installations, the efficiency of the solar panels
2052	Current	Suitability of industrial roofs for large-scale solar panel installation
2049	New	Industrial rooftop suitability for solar, installation rates, solar panel efficiency
2052	New	Industrial rooftop suitability for solar, solar panel efficiency

This summary confirms that early-stage risks in 2034 at the current substation are largely driven by growing residential demand—especially from heating electrification—compounded by delays in infrastructure deployment. In contrast, longer-term risks (2049–2052) at both substations are again shaped by high levels of decentralized solar generation, especially from industrial-scale rooftop installations. These risks point to the emergence of reverse power flow and the growing importance of managing distributed generation as part of future grid planning.

8

Actionable advice for the investment plan

8.1. MoSCoW

The comprehensive analysis and modeling results presented throughout this report culminate in a set of actionable advice designed to mitigate the identified capacity risks within Stedin's distribution network, thereby directly addressing sub-question 3. To effectively prioritize these actions, the MoSCoW method has been employed. This prioritization framework classifies interventions based on their criticality, feasibility, and expected impact, ensuring that resources are allocated optimally in addressing both immediate and long-term challenges.

As a brief refresher, the MoSCoW method categorizes recommendations as follows: Must have's denote critical actions that are essential for preventing capacity risks and possess a high certainty of positive impact; Should have's are important measures that significantly enhance system robustness but may face greater implementation complexity or reduced urgency; Could have's represent desirable improvements that contribute to system robustness and flexibility, though they are non-essential and can be considered as supplementary; finally, Won't have's are those interventions deemed inappropriate or ineffective at present due to factors such as low impact, high uncertainty, or lack of actionable levers.

To provide a clear overview of the recommended responses to the capacity risks identified in this report, Table 8.1 summarizes all proposed mitigation actions. These interventions are based on the findings of the first and second iteration—particularly the PRIM analysis and scenario-based capacity risk assessments—and are subsequently categorized using the MoSCoW method.

ID	Intervention	Description
1	Substation construction (2025)	Begin new substation construction without waiting for the 40 MW threshold
2	Manage distributed rooftop PV	Apply spatial zoning policies and co-located storage to limit rooftop solar's impact on substation capacity
3	Mitigate substation delays	Improve project management and stakeholder coordination to avoid 1–2 year delays
4	Long-term capacity planning	Explore options for a third substation or major upgrades to existing infrastructure beyond 2046
5	Operational flexibility (future)	Investigate flexible operational schemes such as dynamic load sharing to manage local oversupply
6	Influence AC/heating rollout	Attempt to moderate growth in air conditioning and heating demand (low feasibility and low leverage)

Table 8.1: Overview of Recommended Capacity Risk Mitigation Measures

The foremost **must-have** recommendation is the initiation of construction for the new substation in 2025, independent of the previously applied demand threshold trigger of 40,000 kW. The second iteration's scenario analyses revealed that the original threshold proved insufficiently responsive to anticipated sharp demand increases after 2028 and capacity risks peaking in 2034 and 2037. By commencing construction proactively in 2025, the grid infrastructure will better accommodate rising demand, significantly reducing the incidence and severity of risky days at the current substation through the early 2030s. Although residual capacity risk remains in 2034—largely attributable to potential delays in relocating building blocks—this strategic shift in timing marks a substantial improvement compared to the first iteration, mitigating almost 25 percent of risk scenarios at critical years. This adjustment directly addresses the most urgent vulnerability identified in the mid-term horizon and is therefore imperative.

Complementary to the substation construction timing, the management of large-scale distributed solar PV generation emerges as another critical **must-have** action. The PRIM analyses for 2049 and 2052 clearly identify the proliferation of rooftop solar installations on industrial buildings as a dominant driver of capacity risks at both the current and new substations. This is further corroborated by the observed minimum hourly demand profiles in these years, where demand falls below the lower capacity limits, indicating substantial reverse power flows that strain substation capabilities.

Unlike the singular large solar park addressed in the revised infrastructure plan—which is connected exclusively to the new substation and thus mitigates risk in the mid-term—these distributed rooftop installations represent a widespread and evolving challenge. Their impact is less centralized and more difficult to manage through conventional infrastructure upgrades alone. As such, targeted operational and planning interventions are required. Firstly, implementing detailed grid-impact studies before approving new rooftop solar projects on industrial buildings will enable identification of locations where generation might exceed local substation capacity. This can inform spatial zoning policies that limit the concentration of large-scale rooftop PV in vulnerable network areas. Lastly, deploying battery energy storage systems co-located with rooftop solar can absorb excess generation, flattening demand profiles and reducing stress on substations.

Collectively, these interventions will be crucial to managing distributed solar PV expansion within the network's physical limits, maintaining substation reliability, and supporting the ongoing electrification trajectory. Failure to implement such measures risks recurring capacity risks, potentially undermining system's robustness despite infrastructure investments.

While these two measures form the core of the must-have category, attention must also be paid to minimizing delays in the construction and commissioning of the new substation. The second iteration's PRIM analysis indicates that even a one- to two-year delay significantly increases the likelihood of capacity risk in 2031 and 2034, underscoring the critical role of timely project delivery. These delays prolong reliance on the current substation, which is increasingly stressed as demand grows. Consequently, robust project management, contingency planning, and stakeholder coordination are strongly recommended to reduce uncertainty around infrastructure deployment schedules. These operational controls constitute **should-have** measures—essential for safeguarding investment effectiveness and ensuring that anticipated benefits are realized in practice.

In the longer term, capacity risks re-emerge from 2049 onward at both substations, despite the new infrastructure's presence. The PRIM results demonstrate a notable shift in the dominant drivers of these late-stage risks compared to earlier years. Unlike the first iteration, where demand growth and heat transition dynamics played prominent roles, the second iteration identifies infrastructure timing (particularly delays) and decentralized generation factors—specifically, the suitability and actual deployment of industrial rooftop solar PV—as principal risk contributors. This evolution reflects the system's transition from demand-driven to supply-side and infrastructure delivery constraints as primary challenges. Accordingly, **could-have** recommendations include advancing strategic planning for additional capacity expansions or flexible operational schemes beyond 2046. This may entail preparatory feasibility assessments for a third substation or upgrades to existing facilities, as well as exploring operational flexibility mechanisms such as dynamic load sharing to manage localized oversupply from distributed generation. These initiatives offer valuable risk mitigation potential but are less urgent than must-have actions and should be pursued as part of long-term robust planning.

Finally, certain measures fall into the **won't-have** category due to limited leverage or impact from Stedin's perspective. These include attempts to influence demand-side factors such as the rate of air conditioning adoption or the pace of the heat transition rollout. While these elements contribute to early capacity stress, they are largely exogenous and less amenable to direct intervention by the grid operator.

In conclusion, the second iteration's insights validate the critical importance of early infrastructure investment, particularly the 2025 substation construction commencement, coupled with strategic management of large-scale distributed solar connections. Addressing infrastructure delivery delays is vital for realizing these benefits fully. Long-term system robustness depends increasingly on accommodating decentralized generation growth and planning for additional capacity enhancements. By aligning its investment and operational decisions with this advice, Stedin can proactively manage capacity risks and maintain a reliable, adaptable grid in a rapidly evolving energy landscape.

9

Discussion

The simulation results demonstrate that initiating the new substation's construction in 2025—decoupled from the original demand-based trigger—significantly improves system performance by reducing capacity risks throughout the mid-term period, particularly in critical years such as 2034 and 2037. This proactive infrastructure strategy emerged effective across all modeled scenarios. While this early action mitigates the majority of mid-term vulnerabilities, capacity risks resurface in 2049 and 2052 at both the current and new substations. These late-stage risks are primarily driven by reverse power flows from widespread rooftop solar PV installations on industrial buildings, as identified in the PRIM analysis. These findings highlight not only the value of early infrastructure development but also the importance of strategic coordination with decentralized generation.

While these results offer valuable insights into mitigating mid- and long-term capacity risks, it is important to acknowledge several limitations that frame the interpretation and applicability of the findings.

First, the simulation incorporated a carefully selected set of uncertainties, chosen through a combination of literature review and a dedicated focus group session with Stedin. This process ensured that the most relevant and commonly acknowledged drivers of future electricity demand were included, lending credibility and alignment with current scenario practices at Stedin. The inclusion of a focus group further grounded the analysis in the operational realities and decision-making practices of distribution system operators. However, the risk remains that both this research and Stedin's internal analyses may have overlooked certain factors that could influence future demand, particularly as societal, technological, or policy dynamics evolve. While the current selection provides a solid foundation, it does not eliminate the possibility that unmodeled uncertainties—whether emerging or simply underappreciated—could significantly alter demand trajectories in the long run.

Second, the adoption factors assigned to each uncertainty scenario (A, B or C) are all assumptions. Though care was taken to span a plausible range of outcomes, these values are not empirically validated forecasts. Interestingly, the demand projections in this research result in substantially higher values than those used in Stedin's own scenario planning, despite alignment on the underlying uncertainties. This raises a critical point: if the divergence is not caused by different sets of uncertainties, then the differences in adoption factors could explain the gap. The results prompt a useful area for further research—comparing the most influential uncertainties and their assigned adoption levels between modeling efforts to uncover any significant discrepancies in assumptions about the future. This kind of cross-validation would strengthen both the robustness and mutual understanding of scenario outcomes.

In this context, a notable and somewhat unexpected outcome was the absence of EV charging as a critical driver of capacity risk in the PRIM analysis. It was initially expected that EVs—particularly in scenarios involving grid-unaware charging behavior—would surface as a significant contributor to peak load stress. However, this did not occur. A likely explanation lies in the adopted assumptions: in the uncertainty scenarios, the maximum share of grid-unaware EVs in 2025 was limited to 30%, and this grid-unaware share declines over time. Given the low penetration of EVs in the early simulation years (1.85%), and the relatively modest proportion of uncontrolled charging, the overall impact on peak demand remains limited. Moreover, the grid-aware and average charging profiles are more temporally

distributed, reducing peak load effects. As such, EV charging did not emerge as a dominant factor. This finding highlights a useful path for future exploration: revisiting the assumptions around grid-unaware charging—particularly increasing its share or extending its relevance to later years—may reveal that EV charging becomes a more prominent source of capacity stress under different conditions.

Third, another area of modeling assumption involves the use of representative days for solar generation. The number of representative days included in the simulation, how often each occurs over the three-year period, and the shape of their hourly generation profiles are all based on simplified assumptions. These factors directly influence both the total electricity generated and the distribution of that generation across hours and seasons. As with adoption factors, alternative choices here could yield different results. Future sensitivity testing could help clarify how variations in these assumptions affect outcomes and support a more robust modeling framework.

Building on this need for sensitivity testing, another limitation is the absence of a Sobol sensitivity analysis. Unlike PRIM, which highlights conditions linked to extreme outcomes, Sobol analysis quantifies how much each uncertainty contributes to overall output variance. This would offer a clearer ranking of influential factors and help validate or complement the PRIM results. Including it in future work could strengthen the robustness of the findings and guide where investments are needed.

A fifth limitation concerns the input data used for hourly load profiles across the distribution network. The original dataset included 100 usable distribution rooms with existing load data, while 65 others lacked such information. To address this, customer-level consumption data was mapped to distribution rooms wherever possible, reconstructing profiles for 40 additional rooms. The remaining 25 rooms were imputed using average load patterns from the available data. While this approach enabled a complete and internally consistent simulation input set, it inevitably introduced some generalization that may have smoothed over local variations in actual demand. Nonetheless, it is unlikely that this imputation meaningfully changed the overall magnitude or spatial distribution of the main capacity risks identified.

An additional limitation concerns the treatment of eHPs: this study did not account for the electricity consumption of air conditioning (cooling mode) by eHPs, either for existing or new houses. As a result, the overall electricity demand—particularly during summer months—may have been underestimated. Inclusion of air conditioning consumption would likely have led to somewhat higher peak loads in the warmer periods, which could influence the assessment of capacity risks.

Finally, the simulation scope was constrained to 1,000 iterations rather than the preferred 10,000, as was used in the Gridmaster project [57], due to computational and storage limitations. With 30 total uncertainties—13 of which were independent and each assigned three adoption levels—the scenario space was large. Running more iterations would have enabled a more exhaustive exploration of this uncertainty landscape. However, the 1,000 runs still provide a representative sample from which robust conclusions about relative system performance can be drawn. While the uncertainty bands around point estimates would likely tighten with more runs, the core patterns and risk dynamics observed—particularly the timing and drivers of capacity stress—are expected to remain stable. This expectation was further supported by a re-run of both simulation iterations after removing an unused uncertainty variable (demand variability) from the code. Although this change slightly altered some scenario outcomes, especially within the PRIM analysis where a few key drivers shifted, the overall patterns remained intact and logically consistent. These observations reinforce the reliability of the simulation results despite the limited iteration count.

Taken together, these limitations do not undermine the validity of the findings, but they do underscore the importance of interpreting results as directional and scenario-based rather than predictive forecasts. The model serves as a tool for stress testing future conditions under plausible uncertainty rather than as a definitive outlook.

This research makes a meaningful contribution to the broader body of literature on energy infrastructure expansion planning under deep uncertainty. While many existing approaches still rely on deterministic or narrowly bounded scenario analyses [26], this study applies the RDM methodology to the distribution network level using real-world data. In doing so, it demonstrates how infrastructure investment decisions—such as the timing of a new substation—are robust not for a single expected future, but for a wide range of plausible, deeply uncertain futures. This represents a step forward in the operationalization of robust planning approaches for distribution networks.

That said, while the investment strategy proposed here is robust, it is not yet adaptive in the sense

that decisions do not change in response to how uncertainties unfold over time. The improved outcomes in the second iteration were based on a revised investment plan tested across many scenarios, but this strategy remains static regardless of real-world developments. In other words, the PRIM analysis was used retrospectively to understand key drivers of risk, but not prospectively to design adaptive triggers or contingent pathways. Future research could extend this work by using the PRIM insights—particularly the strong influence of rooftop solar PV on capacity risks in 2049 and 2052—to develop adaptive strategies. For instance, a trigger condition could be formulated such that if industrial rooftop solar adoption exceeds a critical threshold by a certain year, a targeted investment or operational intervention is activated. This kind of dynamic strategy design would complete the full vision of uncertainty-aware planning introduced in this study.

Directly comparing these results to other studies is difficult, as no other work has yet applied RDM in this way at the distribution network level. The only partially comparable effort is the Gridmaster HIC Rotterdam project [57], which applied RDM principles to transmission-level infrastructure planning. However, it focused on different system scales and types of uncertainty, involving cross-vector infrastructure and regional coordination. Because of these fundamental differences, the results of this study cannot be directly compared to those of Gridmaster. Notably, Gridmaster also did not implement adaptive triggers in investment decisions, highlighting a broader gap in the literature around truly adaptive planning.

In summary, this research helps close an important part of the literature gap by demonstrating how robust investment strategies for distribution expansion planning can be developed under deep uncertainty using RDM. It also lays the groundwork for future research to explore adaptive mechanisms that not only enhance the robustness of infrastructure decisions but also make them responsive to how uncertainty unfolds over time—thereby helping to close a critical gap in the current literature.

Building on these insights, future research should also consider how the methodology developed in this study could be scaled or generalized to larger segments of the energy system. While the current model focuses on a single distribution network, its object-oriented architecture—built around modular classes—allows for relatively straightforward expansion to include multiple substations and additional network elements. This opens the door to applying similar robust planning principles across broader regions or even the entire Dutch distribution grid. However, generalizing the model in this way will require careful contextual adaptation. Each distribution network is unique in its topology, operational constraints, and exposure to uncertainties, meaning that some assumptions or scenario elements used here may not transfer directly. Consequently, localized adjustments to uncertainties, adoption ranges, or input data structures will remain essential.

Moreover, extending the approach to the high-voltage transmission level introduces a different set of challenges. Some of the demand-side uncertainties—such as the impact of rooftop solar PV—could be less relevant for transmission operators, who deal with aggregated flows rather than local generation and load imbalances. In addition, uncertainties at the transmission level may relate more to inter-regional electricity trade, centralized generation expansion, or geopolitical factors affecting supply chains and grid stability. Future research should therefore investigate how the model structure and scenario design would need to evolve to suit these different system layers, and whether links can be created between models at different voltage levels. This multi-layered approach could ultimately support more integrated, uncertainty-aware infrastructure planning across the entire energy system.

Future research should also explore how alternative building block configurations—such as shifting different rings to the new substation—might reduce implementation costs while maintaining similar capacity benefits. These spatial optimizations could lead to more cost-effective network layouts, particularly if certain connections provide a better balance of load relief and construction complexity. To properly assess such alternatives, a more detailed financial analysis would be needed, including explicit net present value (NPV) calculations. While this study assumed equal total investment costs for both strategies, the timing of those costs differs: in the baseline plan, substation construction is triggered adaptively once aggregate demand exceeds the 40 MW threshold, whereas the forward strategy brings these costs forward to 2025. Because future expenditures are discounted more heavily, early investments carry a higher NPV burden, potentially making the forward strategy less attractive financially despite its operational robustness. Evaluating these trade-offs—both spatial and temporal—would allow future work to refine investment decisions that are not only robust under uncertainty but also economically optimized over time.

To maximize the practical value of these extensions, future research should also focus on developing interactive decision-support tools that actively engage decision-makers. Involving planners and operators directly in generating and stress-testing solutions can help ensure that investment plans remain flexible, locally relevant, and aligned with operational realities. Such participatory frameworks would make robust planning methods like RDM more accessible and actionable for distribution network operators facing deep uncertainty and rapid change.

For Stedin, these insights provide a valuable decision-support framework for navigating future grid investments under uncertainty. By applying and further developing this type of analysis, Stedin can not only improve the robustness of infrastructure decisions but also build toward a more adaptive, scalable planning approach that aligns with both local realities and national energy transition goals.

10

Conclusion

This research sets out to answer the central question: **How robust is Stedin's investment plan for distribution network expansion under deep uncertainty?**

To address this, the study examined three sub-questions:

1. What are the key characteristics of long-term uncertainty in distribution network expansion planning?
2. What is the design of a simulation model that can effectively stress-test a distribution network expansion plan across multiple scenarios?
3. What actionable advice can stress-testing provide for Stedin's investment decisions?

Starting with the first sub-question, the research identified several defining features of long-term uncertainty in distribution network expansion. A particularly significant source of uncertainty lies in the proliferation of PV systems—ranging from residential rooftop panels and installations on industrial buildings to large-scale solar parks. Each of these forms contributes differently to grid dynamics and capacity challenges. In parallel, the accelerating electrification of sectors such as transport, heating, industry, and greenhouses introduces additional complexity. The adoption of EVs, the shift from gas-based to electric heating systems, the growing use of air conditioning, and the transformation of industrial and greenhouse processes all contribute to rising and less predictable electricity demand patterns.

Furthermore, anticipated residential development will increase the number of grid connections and the need for timely infrastructure upgrades. Additional uncertainties emerged from stakeholder input, such as the potential role of shore power for port operations and the risk of delays in infrastructure delivery due to permitting or labor shortages. These uncertainties affect both the magnitude and timing of future capacity needs, and often interact in non-linear and compounding ways. Together, these factors create a dynamic and uncertain landscape for electricity demand, requiring careful consideration in distribution network expansion planning.

To answer the second sub-question, a scenario-based simulation model was constructed using principles from the RDM framework. The model simulates hourly electricity flows across substations and network components from 2025 to 2052, assessing capacity stress under a wide range of future developments. Uncertainty is introduced through 30 parameters, each adopting one of three predefined pathways (A, B, or C). Each pathway corresponds to fixed numerical parameter trajectories over time. By randomly sampling combinations of these discrete pathways across multiple uncertainties, 1,000 diverse scenarios were generated, reflecting plausible yet deeply uncertain futures. The model's modular architecture is implemented in Python, with classes representing key network infrastructure elements. Scenario design and experiment coordination are facilitated by the EMA Workbench, linking uncertainty sampling with model execution. To manage data storage while retaining critical insights, only the daily maximum and minimum values are recorded in the output files, preserving essential information on peak load conditions and reverse power flow risks.

The model accounts for both centralized and decentralized developments, such as rooftop solar, and simulates capacity risks on a daily basis. This setup allows for a thorough stress test of investment decisions, evaluating how well they hold up across a wide array of demand and supply trajectories. The result is a transparent and scalable simulation tool that enables strategic decision making by revealing how infrastructure plans perform across a wide spectrum of deeply uncertain futures, highlighting vulnerabilities, trade-offs, and opportunities for timely intervention.

For the third sub-question, the stress-testing framework produced several valuable and actionable insights for Stedin. Most notably, it revealed that the original, threshold-based substation construction plan was insufficiently robust. Initiating substation development in 2025—regardless of whether demand has reached a specific threshold—substantially reduced capacity risk, particularly in mid-term years like 2034 and 2037. This recommendation was supported by PRIM, which clarified how clusters of uncertainties (such as rooftop PV adoption and infrastructure delays) created high-risk conditions. The analysis also highlighted the importance of operational contingencies: even minor delays in substation construction could sharply increase exposure to capacity risk. Moreover, long-term challenges such as reverse power flow due to decentralized generation were found to require non-infrastructure solutions, including spatial zoning and storage. Importantly, the stress-testing approach also helped differentiate between uncertainties that Stedin can act on and those that are largely exogenous, allowing for more focused and strategic resource allocation.

Bringing these insights together, the central research question can be answered. The stress-testing results indicate that the original, threshold-based investment plan is not robust under deep uncertainty. Under this plan, the current substation experiences capacity risk in 100% of simulated scenarios, with no scenario achieving zero risky days over the full simulation period. Even the addition of the new substation under this original plan shows limited effectiveness, achieving zero capacity risk in only 47.3% of scenarios. A year-by-year breakdown reveals more about when these vulnerabilities are most pronounced. For the current substation, nearly all scenarios show capacity risk in 2034 and 2037, highlighting these as critical years of mid-term exposure. Moreover, in the later years—2049 and 2052—capacity risk re-emerges, indicating that long-term challenges are not sufficiently addressed by the initial plan. These patterns make clear that relying on demand thresholds to trigger substation construction is inadequate for managing both mid- and long-term risks.

In contrast, the second iteration of the investment plan, which initiates construction of the new substation in 2025 regardless of demand thresholds, shows marked improvement. Under this updated approach, the current substation achieves zero capacity risk in 23.4% of scenarios, and the new substation achieves this in 46.6% of scenarios. This represents a meaningful step forward.

Still, capacity risks persist in the majority of futures, indicating that even the updated plan is not fully robust. Temporal analysis again reveals critical vulnerabilities. For the current substation, capacity risks are concentrated in 2031 and 2034, then decline to minimal levels until re-emerging in 2049 and 2052. The new substation, in contrast, shows most capacity risk in the later years, particularly 2049 and 2052. Excluding those two years from the evaluation significantly increases the robustness of the new substation, with 97.4% of scenarios showing no capacity risk. However, under the same condition, the current substation still only avoids risk in 36.5% of scenarios, indicating deeper structural vulnerability in the mid-term.

These patterns align with the insights derived from the stress-testing framework. Addressing capacity risks at the current substation requires minimizing delays in infrastructure delivery, particularly in the mid-term years 2031 and 2034. For the new substation, long-term risks—primarily driven by high levels of decentralized generation such as rooftop solar PV—are less likely to be resolved by infrastructure investment alone. Instead, a combination of spatial, operational, and infrastructure-oriented measures will likely be required to manage these risks effectively. For example, conducting local grid impact assessments prior to rooftop PV deployment, applying spatial zoning to prevent generation clustering in vulnerable areas, and co-locating battery storage systems are operational and planning tools that can reduce pressure on substations. While these measures are often implemented at the distribution level, their aggregated impact can extend beyond local nodes, potentially affecting upstream transmission infrastructure as well.

In summary, both the first and second iterations of the investment plan remain insufficiently robust to confidently withstand a wide range of uncertain futures. Reducing short- to mid-term capacity risks—

particularly at the current substation—requires timely implementation of the proposed infrastructure package. For long-term robustness, especially under futures with high levels of solar PV adoption, a combination of measures will be needed: construction of the new substation, controlled spatial distribution of rooftop PV through zoning and permitting, and operational strategies such as co-located storage to limit local congestion impacts. Together, these targeted infrastructure, spatial planning, and operational measures form a more robust and adaptable approach to distribution network expansion under deep uncertainty.

Bibliography

[1] 123zonnepanelenvergelijken. Vermogen zonnepanelen per m2 [solar panel capacity per m2], n.d. URL https://123zonnepanelenvergelijken.nl/algemeen/vermogen-zonnepanelen-per-m2/#:~:text=Om%20u%20toch%20een%20gemiddelde,120%20kWh%20aan%20stroom%20oplevert.

[2] Alliander. Electricity network in residential areas is approaching maximum capacity, 2023. URL https://www.alliander.com/en/financial-news/electricity-network-in-residential-areas-is-approaching-maximum-capacity/.

[3] M. Armendáriz, K. Paridari, E. Walling, and L. Nordström. Comparative study of optimal controller placement considering uncertainty in pv growth and distribution grid expansion. *Electric Power Systems Research*, 155:48–57, 2018. doi: 10.1016/j.epsr.2017.10.001. URL https://www.sciencedirect.com/science/article/abs/pii/S0378779617303991?via%3Dihub.

[4] H. Bakker, F. Dunke, and S. Nickel. A structuring review on multi-stage optimization under uncertainty: Aligning concepts from theory and practice. *Omega*, 96, 2020. doi: 10.1016/j.omega.2019.06.006. URL https://www.sciencedirect.com/science/article/abs/pii/S0305048318314002.

[5] Michael Blonsky, Adarsh Nagarajan, Shibani Ghosh, Killian McKenna, Santosh Veda, and Benjamin Kroposki. Potential impacts of transportation and building electrification on the grid: A review of electrification projections and their effects on grid infrastructure, operation, and planning. *Current Sustainable/Renewable Energy Reports*, 6, 2019. doi: 10.1007/s40518-019-00140-5. URL https://link.springer.com/article/10.1007/s40518-019-00140-5#citeas.

[6] Coolblue. Hoeveel zonnepanelen heb je nodig? [how many solar panels do you need?], n.d. URL https://www.coolblue.nl/zonnepanelen/advies/hoeveel-zonnepanelen-heb-je-nodig.

[7] Polina Danilova. Permitting procedures for renewable energy projects in the european union. Master's thesis, Technische Universität Wien; Diplomatische Akademie Wien, ETIA 16, 2024. URL https://doi.org/10.34726/hss.2024.123054. Available on reposiTUm.

[8] Data from Stedin.

[9] J. Dyszynski, T. Downing, and T. Takama. Robust decision making: Xlrm framework, 2011. URL https://weadapt.org/knowledge-base/adaptation-decision-making/xlrm-framework/.

[10] G.S. Eskeland and T.K. Mideksa. Electricity demand in a changing climate. *Mitigation and Adaptation Strategies for Global Change*, 15:877–897, 2010. doi: 10.1007/s11027-010-9246-x. URL https://link.springer.com/article/10.1007/s11027-010-9246-x#citeas.

[11] Essent. Hoeveel kwh levert een zonnepaneel op? [how many kwh does a solar panel produce?], n.d. URL https://www.essent.nl/kennisbank/zonnepanelen/wat-zijn-zonnepanelen/hoeveel-kwh-zonnepanelen.

[12] Sabine Fuss, Daniel J. A. Johansson, Jana Szolgayova, and Michael Obersteiner. Impact of climate policy uncertainty on the adoption of electricity generating technologies. *Energy Policy*, 37, 2009. doi: 10.1016/j.enpol.2008.10.022. URL https://www.sciencedirect.com/science/article/pii/S0301421508005818.

[13] C. Guivarch, J. Rozenberg, and V. Schweizer. The diversity of socio-economic pathways and co2 emissions scenarios: Insights from the investigation of a scenarios database. *Environmental Modelling Software*, 80, 2016. doi: 10.1016/j.envsoft.2016.03.006. URL https://www.sciencedirect.com/science/article/pii/S1364815216300706.

[14] Roman J. Hennig, Laurens J. de Vries, and Simon H. Tindemans. Congestion management in electricity distribution networks: Smart tariffs, local markets and direct control. *Utilities Policy*, 85, 2023. doi: 10.1016/j.jup.2023.101660. URL https://www.sciencedirect.com/science/article/pii/S0957178723001728?via%3Dihub.

[15] Team IO+. Dutch electricity grid 'unprepared' for the green transition, 2024. URL https://ioplus.nl/en/posts/dutch-electricity-grid-unprepared-for-the-green-transition.

[16] KadastraleKaart. Gemeenten in nederland [municipality in the netherlands], n.d. URL https://kadastralekaart.com/gemeenten.

[17] X. Kan, L. Reichenberg, and F. Hedenus. The impacts of the electricity demand pattern on electricity system cost and the electricity supply mix: A comprehensive modeling analysis for europe. *Energy*, 235, 2021. doi: 10.1016/j.energy.2021.121329. URL https://www.sciencedirect.com/science/article/pii/S0360544221015772.

[18] Redactie Groen Kennisnet. Klimaatneutrale glastuinbouw in 2040 [climate-neutral greenhouse horticulture in 2040], 2020. URL https://groenkennisnet.nl/nieuwsitem/klimaatneutrale-glastuinbouw-in-2040-1.

[19] S. Klyapovskiy, S. You, H. Cai, and H.W. Bindner. Incorporate flexibility in distribution grid planning through a framework solution. *International Journal of Electrical Power Energy Systems*, 111, 2019. doi: 10.1016/j.ijepes.2019.03.069. URL https://www.sciencedirect.com/science/article/pii/S0142061518325079.

[20] G. Koreneff, M. Ruska, J. Kiviluoma, J. Shemeikka, B. Lemström, R. Alanen, and T. Koljonen. Future development trends in electricity demand, 2009. URL https://www.researchgate.net/publication/297092492_Future_development_trends_in_electricity_demand.

[21] Jan H. Kwakkel. The exploratory modeling workbench: An open source toolkit for exploratory modeling, scenario discovery, and (multi-objective) robust decision making. *Environmental Modelling & Software*, 96:239–250, 2017. doi: 10.1016/j.envsoft.2017.06.054. URL https://www.sciencedirect.com/science/article/pii/S1364815217301251?via%3Dihub.

[22] J.H. Kwakkel. Scenario discovery in python, 2015. URL https://waterprogramming.wordpress.com/2015/08/05/scenario-discovery-in-python/.

[23] J.H. Kwakkel and M. Haasnoot. Supporting dmdu: A taxonomy of approaches and tools. *Decision Making under Deep Uncertainty*, 306:355–374, 2019. doi: 10.1007/978-3-030-05252-2_15. URL https://link.springer.com/chapter/10.1007/978-3-030-05252-2_15.

[24] S. La Fleur, M. Rijken, J. Nutma, and M. Konsman. Afschakelen van zonnepanelen niet gelijk verdeeld hoe verdelen we de lasten op een rechtvaardige manier? [disconnecting solar panels not evenly distributed how do we distribute the burden in a fair way?], 2023. URL https://energy.nl/publications/afschakelen-zonnepanelen/.

[25] Vincent A. W. J. Marchau, Warren E. Walker, Pieter J. T. M. Bloemen, and Steven W. Popper. *Decision Making under Deep Uncertainty: From theory to Practice*. Springer Nature, 2019. doi: 10.1007/978-3-030-05252-2.

[26] A. Moreira, M. Heleno, A. Valenzuela, J.H. Eto, J. Ortega, and C. Botero. A scalable approach to large scale risk-averse distribution grid expansion planning. In *IEEE Transactions on Power Systems*, volume 39, pages 2115–2128. IEEE, 2023. doi: 10.1109/TPWRS.2023.3273195. URL https://ieeexplore.ieee.org/abstract/document/10115468.

[27] G. Muñoz-Delgado, J. Contreras, and J.M. Arroyo. Multistage generation and network expansion planning in distribution systems considering uncertainty and reliability. In *IEEE Transactions on Power Systems*, volume 31, pages 3715–3728. IEEE, 2015. doi: 10.1109/TPWRS.2015.2503604. URL https://ieeexplore.ieee.org/abstract/document/7353222.

[28] G. Muñoz-Delgado, J. Contreras, J.M. Arroyo, A. Sanchez de la Nieta, and M. Gibescu. Integrated transmission and distribution system expansion planning under uncertainty. In *IEEE Transactions on Smart Grid*, volume 12, pages 4113–4125. IEEE, 2021. doi: 10.1109/TSG.2021.3071385. URL https://ieeexplore.ieee.org/abstract/document/9395702.

[29] Energie Nederland. Position electricity infrastructure, . URL https://www.energie-nederland.nl/en/topics/infrastructure/positions/. n.d.

[30] Netbeheer Nederland. Landelijk actieplan netcongestie [national action plan for grid congestion], . URL https://www.netbeheernederland.nl/netcapaciteit-en-flexibiliteit/landelijk-actieplan-netcongestie. n.d.

[31] Netbeheer Nederland. Nationaal plan energiesysteem. [national energy system plan], . URL https://www.netbeheernederland.nl/veranderend-energiesysteem/nationaal-plan-energiesysteem. n.d.

[32] Netbeheer Nederland. Basisdocument over energie-infrastructuur (oktober 2019) [basic document on energy infrastructure (october 2019)], 2019. URL https://www.netbeheernederland.nl/publication/basisdocument-over-energie-infrastructuur-oktober-2019.

[33] Netbeheer Nederland. Scenario's investeringsplannen 2024 [scenarios investment plans 2024]. Technical report, Netbeheer Nederland, 2023. URL https://www.netbeheernederland.nl/publicatie/ip2024-scenario-rapportage.

[34] C.P. Ohanu, S.A. Rufai, and U.C. Oluchi. A comprehensive review of recent developments in smart grid through renewable energy resources integration. *Heliyon*, 10, 2024. doi: 10.1016/j.heliyon.2024.e25705. URL https://www.sciencedirect.com/science/article/pii/S2405844024017365.

[35] J. Pigden. Grid overload: The impact of the electricity grid on the dutch energy transition, 2024. URL https://auroraer.com/insight/grid-overload-dutch-energy-transition/.

[36] Rijksoverheid. Overheid en netbeheerders nemen maatregelen tegen vol stroomnet [government and grid operators take measures against full power grid], 2023. URL https://www.rijksoverheid.nl/actueel/nieuws/2023/10/18/overheid-en-netbeheerders-nemen-maatregelen-tegen-vol-stroomnet.

[37] Mahyar Kamali Saraji and Dalia Streimikiene. Challenges to the low carbon energy transition: A systematic literature review and research agenda. *Energy Strategy Reviews*, 49, 2023. doi: 10.1016/j.esr.2023.101163. URL https://www.sciencedirect.com/science/article/pii/S2211467X2300113X.

[38] B. Shavazipour, J.H. Kwakkel, and K. Miettinen. Multi-scenario multi-objective robust optimization under deep uncertainty: A posteriori approach. *Environmentall Modelling Software*, 144, 2021. doi: 10.1016/j.envsoft.2021.105134. URL https://www.sciencedirect.com/science/article/pii/S1364815221001778.

[39] B. Shavazipour, J.H. Kwakkel, and K. Miettinen. Let decision-makers direct the search for robust solutions: An interactive framework for multiobjective robust optimization under deep uncertainty. *Environmental Modelling Software*, 183, 2025. doi: 10.1016/j.envsoft.2024.106233. URL https://www.sciencedirect.com/science/article/pii/S1364815224002949.

[40] M. Shen, Z. Shahidehpour, S. Zhu, Y. Han, and J. Zheng. Multi-stage planning of active distribution networks considering the co-optimization of operation strategies. In *IEEE Transactions on Smart Grid*, volume 9, pages 1425–1433. IEEE, 2016. doi: 10.1109/TSG.2016.2591586. URL https://ieeexplore.ieee.org/abstract/document/7513444.

[41] Sustainable ships. What is the average shore power demand of a container ship?, n.d. URL https://www.sustainable-ships.org/stories/2024/average-shore-power-demand-containership#:~:text=The%20average%20shore%20power%20demand%20for%20all%20containerships%20combined%20is,kW%20to%20over%203%2C800%20kW.

[42] Soly. Europees akkoord: vanaf 2027 verplicht zonnepanelen op daken [european agreement: mandatory solar panels on roofs from 2027], n.d. URL https://soly.nl/kennisbank/europees-akkoord-vanaf-2027-verplicht-zonnepanelen-op-daken/.

[43] StatLine. Landbouw; gewassen, dieren en grondgebruik naar gemeente [agriculture; crops, animals and land use by municipality], n.d.. URL https://opendata.cbs.nl/statline/#/CBS/nl/dataset/80781ned/table?dl=66D5A.

[44] StatLine. Woningen; hoofdverwarmingsinstallaties, regio 2017-2022 [homes; main heating systems, region 2017-2022], n.d.. URL https://opendata.cbs.nl/#/CBS/nl/dataset/84948NED/table.

[45] StatLine. Vestigingen van bedrijven; bedrijfstak, gemeente [establishments of companies; industry, municipality], n.d.. URL https://opendata.cbs.nl/#/CBS/nl/dataset/81575NED/table?dl=A4ED6.

[46] Stedin. Netbewust laden van elektrische voertuigen [grid-aware charging of electric vehicles], n.d. URL https://www.stedin.net/zakelijk/energietransitie/beschikbare-netcapaciteit/congestie/netbewust-laden.

[47] TMIP-EMAT. Prim, n.d. URL https://tmip-emat.github.io/source/emat.analysis/prim.html.

[48] TNO. Tno voorziet forse groei energiegebruik van airco's [tno predicts significant growth in energy consumption of air conditioners], 2024. URL https://www.tno.nl/nl/newsroom/2024/10/groei-energiegebruik-airco/#:~:text=Steeds%20meer%20airco%27s&text=Eerder%20bleek%20al%20dat%20in,circa%206%2C3%20miljoen%20uitkomt.

[49] Ministerie van Buitenlandse Zaken. Gaswetgeving van de eu hervormd [eu gas legislation reformed], 2024. URL https://ecer.minbuza.nl/-/gaswetgeving-van-de-eu-hervormd.

[50] A. Van der Maarel and M. Seghir. Tackling grid congestion and how companies can handle energy transition within the european union, 2024. URL https://www.rsm.global/netherlands/en/insights/tackling-grid-congestion-and-how-companies-can-handle-energy-transition-within-european-union.

[51] Vattenfall. Hoe het nederlandse elektriciteitsnetwerk in elkaar zit [how the dutch electricity network is structured]. URL https://www.vattenfall.nl/grootzakelijk/energiemarkt/nederlandse-elektriciteitsnetwerk/. n.d.

[52] Centraal Bureau voor de Statistiek. Autobezit per huishouden, 1 januari 2023 [car ownership per household, january 1, 2023], 2024. URL https://www.cbs.nl/nl-nl/maatwerk/2024/08/autobezit-per-huishouden-1-januari-2023.

[53] Rijksdienst voor Ondernemend Nederland. Wat is netcongestie en wat betekent dit voor uw bedrijf? [what is grid congestion and what does it mean for your business?], 2024. URL https://www.rvo.nl/onderwerpen/netcongestie/wat-netcongestie.

[54] W.E. Walker, V.A.W.J. Marchau, and D. Swanson. Addressing deep uncertainty using adaptive policies: Introduction to section 2. *Technological Forecasting and Social Change*, 77:917–923, 2010. doi: 10.1016/j.techfore.2010.04.004. URL https://www.sciencedirect.com/science/article/pii/S0040162510000715.

[55] T. Witt, M. Dumeier, and J. Geldermann. Combining scenario planning, energy system analysis, and multi-criteria analysis to develop and evaluate energy scenarios. *Journal of Cleaner Production*, 242, 2020. doi: 10.1016/j.jclepro.2019.118414. URL https://www.sciencedirect.com/science/article/abs/pii/S0959652619332846?via%3Dihub.

[56] H.A.M. Wurth, J.N.G. van Dinther, J.H. Kwakkel, I. Nikolic, J.J. Steringa, R. Calon, W. Zappa, A.M. van Voorden, C.J.H. Kruip, and M.G. Valies. The gridmaster-toolbox, a step towards a new infrastructure investment paradigm. In *Accepted 2022 CIGRE-paper, C1, PS3*, 2022. ID 10555.

[57] Ton Wurth. Gridmaster hic rotterdam, 2022. URL https://gridmaster.nl/wp-content/uploads/2022/11/20221124-report-GridmasterHICRdam_public_final.pdf.

[58] Y. Xiang, P. Xue, Y. Wang, L. Xu, W. Ma, and M. Shafie-khah. Robust expansion planning of electric vehicle charging system and distribution networks. In *CSEE Journal of Power and Energy Systems*, volume 10, pages 2457–2469. IEEE, 2023. doi: 10.17775/CSEEJPES.2021.08540. URL https://ieeexplore.ieee.org/abstract/document/10026223.

[59] Enrico Zio and Terje Aven. Uncertainties in smart grids behavior and modeling: What are the risks and vulnerabilities? how to analyze them? *Energy Policy*, 39, 2011. doi: 10.1016/j.enpol.2011.07.030. URL https://www.sciencedirect.com/science/article/pii/S0301421511005544#s0020.

A

Focus group

A.0.1. Summary key findings

The focus group consisted of five participants with different specializations within Stedin. Two of them worked in grid capacity management, each responsible for specific regions. Their job is to forecast capacity demand using projections and to come up with technical solutions for bottlenecks. In addition, an electricity strategist took part in the discussion, bringing expertise in security issues and short-term calculations. There was also an expert in asset management and a strategist specializing in energy systems and developments. The latter had extensive knowledge of scenario development and handling uncertainties in investment planning.

Before discussing the specific uncertainties, the group first reviewed the method used to calculate scenarios. It quickly became clear that there was a strong need to analyze not just a single scenario, but multiple scenarios. Currently, investment plans rely too heavily on a single reference scenario, whereas a broader analysis of uncertainties and variables would lead to more well-founded decision-making.

During the session, the predefined uncertainties were critically analyzed. Participants gave feedback on the defined uncertainties and their values and suggested potential missing factors. One of the key topics was the heat transition in existing buildings. It was noted that district heating networks are typically not installed per individual house but rather for an entire area or cluster of homes. This means that implementing district heating is not a gradual process, but a binary decision: either an area is connected, or it isn't. Therefore, it was recommended not to define district heating coverage as a percentage within an uncertainty, but rather as a separate variable.

In addition to the heat transition, solar energy was discussed in depth. The group emphasized the importance of assessing the current situation accurately. For instance, if 20% of homes already have solar panels and an additional 20% growth is projected, this could be an unrealistic assumption. It was recommended to clearly define whether the forecast refers to absolute growth or to the total share of homes with solar panels. There was also discussion about whether peak solar production should be smoothed out, for example by eventually shifting toward centralized generation instead of panels on individual roofs.

Another point of discussion was the impact of building age. Older houses may be demolished and replaced with new construction sooner, which affects energy demand and investment planning. Currently, only existing buildings are considered, but if redevelopment is a realistic factor, it would make sense to include building age as a separate uncertainty. For example, neighborhoods with homes from the 1960s are more likely to undergo large-scale redevelopment than those with 1990s houses.

The discussion then shifted to electric mobility. Currently, the focus is mainly on the growth of electric vehicles without taking into account the total number of cars. This is a significant oversight, as the total number of vehicles could decrease in the future due to increased use of car-sharing and public transport. The uncertainty about the total number of vehicles may be just as important as the uncertainty about the share of electric vehicles. Charging infrastructure was also discussed extensively. The distribution of charging points strongly depends on the type of housing in an area. In high-density housing areas, public charging stations will be more needed, while residents of detached or semi-detached homes are more likely to have a private charger on their driveway. It was also mentioned that charging infrastructure for public transport is often developed all at once—such as at a station—rather

than gradually expanded. This means that the charging demand for electric buses increases in steps rather than growing linearly.

After discussing electric mobility, attention turned to the industrial sector and renewable energy generation. It was concluded that greenhouse horticulture is unlikely to have a major impact on grid investments in this region. There is one customer with a large connection, but other greenhouse businesses have relatively low energy demand. Regarding renewable energy generation, it was noted that a new solar park is planned in the area, as it has been designated a solar energy exploration zone. Additionally, the potential for placing solar panels on the large roofs of industrial halls was highlighted. Current scenarios only consider houses and solar parks, even though commercial rooftops are a realistic and logical location for PV installations. Moreover, the government discourages the use of agricultural land for solar parks, making it more likely that future PV installations will focus on industrial rooftops.

Finally, the topic of shore power was discussed. Currently, there are no shore power facilities in the area, and there are no concrete plans to implement them in the short term. In theory, shore power could play a role in the future since the area includes a small harbor. If it does happen, the power supply will likely be connected to existing grid connections, which would limit the impact on grid capacity.

A final comment addressed the complexity of the analytical method used. Adding multiple uncertainties and variables makes the model more detailed and realistic. At the same time, it was emphasized that it is crucial to present the results in a visually clear way. If the method and results are not communicated in an understandable manner, it could lead to low acceptance among decision-makers. However, the major advantage of this method is that it allows identification of which uncertainties have a significant impact and which do not. This provides valuable insights for future scenario development and investment decisions, as less relevant uncertainties can potentially be left out in future studies.

A.0.2. Protocol

Hello everyone, Before we begin the focus group, I'd like to start with a brief round of introductions. Please introduce yourself, mention the department you work in, and your current role.

My name is Maryvonne Marang, and as you know, I am researching the robustness of an investment plan by Stedin under deep uncertainty, specifically regarding the expansion of the electricity network from 13 kV to 21 kV. The focus is on area X and the new substations Y. Currently, there is a distribution station in the south and one in the east. Power flows from station Z into Y, and from there, it is transmitted to area X. According to the master plan, two new substations are planned: one in the north and one in the west.

The goal of today's focus group is to identify, validate, and refine the key uncertainties surrounding the expansion of the distribution network. This will help make the investment plan more robust and ensure we are better prepared for future developments.

All opinions and ideas are welcome in this discussion—there are no right or wrong answers. I will be taking notes during the session, and we will also be recording the meeting to make sure no important details are lost. A summary of the findings will be shared with you afterward, giving you the opportunity to review, suggest additions, or make corrections.

The focus group will last about one hour. We'll spend around 40 minutes discussing the uncertainties, and reserve the final 10 minutes for reflection and wrapping up.

To test how robust the plan is over time, it's important to map out the uncertainties associated with expanding the distribution network. I've already prepared an initial draft of uncertainties. In this session, I'd like to go through each of them with you, and hear your thoughts—especially regarding the values assigned to them. The order in which we go through them is random and does not reflect any prioritization. Let's get started.

[Go through all the uncertainties]

Now that we've reviewed all the uncertainties, do you think any important ones are missing? Are there other uncertainties you've encountered in your experience with distribution network expansion?

And finally, are there any other comments or suggestions you'd like to share regarding the uncertainties we've discussed?

Thank you very much for your participation. As mentioned, a summary of the key findings will be sent to you first. This gives you the chance to make any corrections or additions before the results are incorporated into the research.

A.0.3. Informed Consent

You are being invited to participate in a research study titled *Robust investment strategies for electricity distribution network expansion: applying a Robust Decision Making method and EMA to address grid congestion in the Netherlands*. This study is conducted by Maryvonne Marang from TU Delft, in collaboration with Arjan van Voorden from Stedin, and a research team from TU Delft including Igor Nikolic, Jan Kwakkel, and Ton Wurth.

The purpose of this research is to model whether an investment plan of Stedin is robust under (extreme) uncertain conditions. The focus group will be held in person at Stedin and will take approximately one hour to complete. The data collected will be used to identify uncertainties in distribution network expansion planning and will serve as input for a simulation model. You will be asked to list the uncertainties identified in the Stedin network, specify their values, and describe their impact on investment decisions.

As with any online activity, there is a small risk of data breach. Although data will be anonymized wherever possible, due to the small size of the focus group, it may still be possible to reidentify individual participants. To ensure accuracy and protect participants, a summary of key points will be shared with you prior to publication. This allows you to verify that the summary accurately reflects your input and does not include any harmful or misleading content.

The session will be audio recorded, and key points will be summarized in a written document. This summary will be sent to you, and you are welcome to suggest additions or changes. One week after the summary is sent, it will be shared with the TU Delft research team and Arjan van Voorden. The data collected will support scientific publication. Only anonymous quotes and aggregated results will be used in any publication.

All personal data collected will be retained for up to two years following the completion of the master thesis.

Your participation in this study is entirely voluntary, and you may withdraw at any time. You are free to omit any questions. If you have any questions about the processing of your data, please contact one of the researchers listed below.

Consent Statement:

I have read and understood the information above. I consent to participate in the study and to the processing of the personal data described above.

I agree that my responses, views, or other input can be quoted anonymously in research outputs:
Yes [ ] No [ ]

Name of participant (printed)	Signature	Date

TU Delft research team contact details for further information:
Maryvonne Marang
Igor Nikolic
Jan Kwakkel
Ton Wurth

Stedin contact details for further information:
Arjan van Voorden

B

List of uncertainties

Below is a list of all identified uncertainties. There are 13 categories in total, encompassing 30 uncertainties that have been programmed into the simulation. Each uncertainty can take one of three possible values, labeled A, B, or C. For the detailed numerical values corresponding to these options, please refer to the file ”Scenario space - uncertainties.xlsx” available on the GitHub repository.

Category	Uncertainty	A	B	C
1	a. Adoption new heating systems	Fast	Medium	Slow
	b. Adoption hybrid heat pumps	High adoption	Medium adoption	Low adoption
	c. Mix eHP, heat network, airco (heat)	20/40/40	40/40/20	20/60/20
	d. Life span of hybrid heat pump	10 years	15 years	20 years
2	a. Airco (cooling)	Fast adoption	Medium adoption	Slow adoption
3	a. Adoption system (PV)	Fast adoption	Medium adoption	Slow adoption
4	a. Growth of total vehicles	Fast	Medium	Low
	b. Growth of E-vehicles	Fast adoption	Medium adoption	Slow adoption
	c. Mix cars/vans/buses/trucks	70/20/5/5	60/25/10/5	50/30/15/5
5	a. Growth of charging points	Fast adoption	Medium adoption	Slow adoption
	b. Mix home/company/public	60/30/10	50/30/20	40/30/30
	c. Public decentralized/centralized	70/30	50/50	30/70
6	a. Grid aware/average/grid unaware (% of e-vehicles)	Fast	Medium	Slow
7	a. Growth of new buildings	High	Medium	Low
	b. Mix eHP, heat network	60/40	50/50	40/60
	c. Airco (cooling)	High	Medium	Low
	d. Expansion/infill	60/40	50/50	40/60
8	a. Growth of new industry	Increase	Stay the same	Decrease

Category	Uncertainty	A	B	C
	b. Mix electrification, biogas/hydrogen, no industry	60/30/10	40/40/20	30/60/10
9	a. Growth of new greenhouse horticulture	Increase	Stay the same	Decrease
	b. Mix electrification, biogas/hydrogen/geothermal, no greenhouses	50/40/10	30/40/30	30/60/10
10	a. Growth of solar park capacity	High	Medium	Low
	b. Production (% of max)	High efficiency	Average efficiency	Low efficiency
11	a. Delay new substation	High	Medium	Low
	b. Delay relocation ring	High	Medium	Low
	c. Delay add new ring	High	Medium	Low
12	a. Growth of shore power connections	Fast adoption	Medium adoption	Slow adoption
	b. Electric ships	Fast adoption	Medium adoption	Slow adoption
13	a. Growth of suitable roofs (industry only)	Fast	Medium	Slow
	b. Construction	High	Medium	Low

C

XLRM framework

This appendix provides a detailed narrative of the relationships depicted in the XLRM framework (Figure C.1). The focus is on tracing how the uncertainties affect two key system outcomes: M1: capacity risk and M2: investment costs, and how infrastructure levers are used to manage these effects.

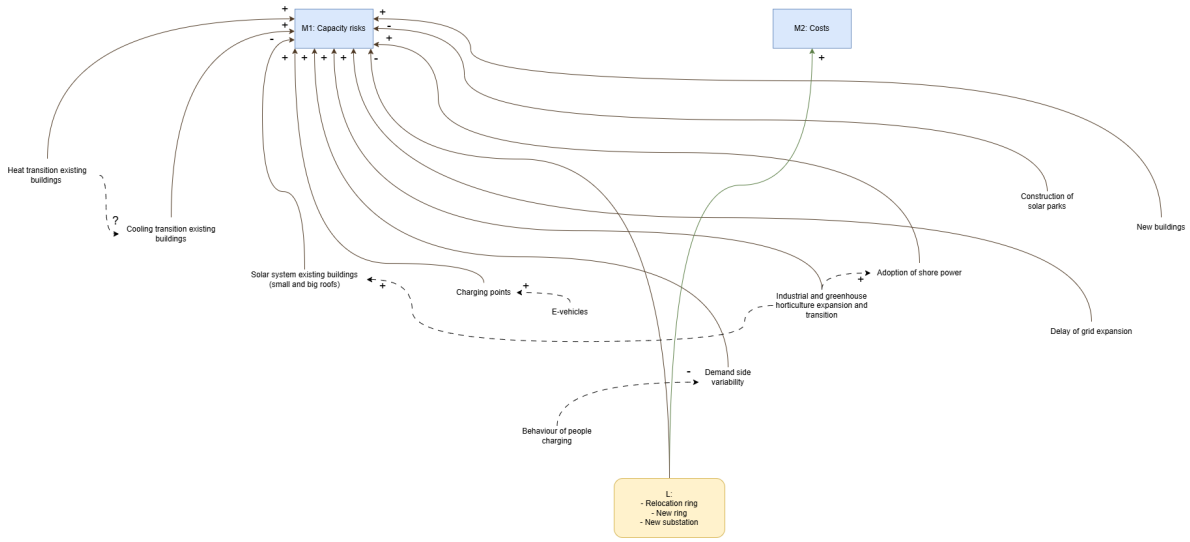

Figure C.1: XLRM framework

Beginning at the top left of the framework, the heat transition in existing buildings refers to the shift away from natural gas boilers, which are currently the dominant form of heating. As homes switch to electric alternatives such as heat pumps, district heating systems, or air conditioning units with heating functionality, electricity demand increases. This heightened demand places additional stress on the distribution network, thereby increasing capacity risk.

Adjacent to this is the cooling transition in existing buildings, representing increased adoption of air conditioning systems due to climate change or comfort expectations. Like the heating transition, this also drives up electricity consumption and, as a result, capacity risk. There is an interdependent relationship between heating and cooling transitions. For instance, certain electric heating solutions like electric heat pumps may also serve as cooling devices, potentially eliminating the need for separate installations. In contrast, other systems may still require standalone cooling units. Thus, whether additional cooling demand arises depends heavily on the type of heating system adopted.

Next, the rise in EVs contributes to increased capacity risk through two channels: the number of charging points and user charging behavior. As EV adoption grows, more charging points are installed, each adding a localized load on the network. Furthermore, if user behavior is ”grid-unaware”—that is,

not aligned with off-peak times or dynamic pricing—it introduces greater variability in demand. This behavioral uncertainty amplifies demand-side variability, which in turn increases capacity risk.

The electrification of industrial areas and greenhouse horticulture also significantly affects capacity risk. Currently, these sectors are predominantly powered by methane. However, future scenarios include transitions to electricity, biogas, hydrogen, or even a reduction in industrial or greenhouse activity. Regardless of the specific pathway, electrification leads to increased electricity consumption, thus elevating capacity risk.

There is also an interdependent relationship between industrial expansion and solar systems on large roofs. The potential for deploying solar PV at scale depends on the availability of suitable roof space, typically found on industrial buildings. Therefore, more industrial expansion could enable greater deployment of solar energy, which has mitigating effects on capacity risk.

In addition, shore power adoption—which allows ships to plug into the electricity grid while docked instead of using onboard diesel generators—can only occur in port and industrial areas. Shore power significantly increases local electricity demand and contributes to capacity risk.

New buildings further increase electricity demand, as they are required to be gas-free and typically include electric heat pumps, cooling, and rooftop solar PV. These technologies increase overall consumption, especially during peak times, contributing to higher capacity risks.

Delays in grid expansion represent another source of increased risk. When planned upgrades (e.g., new substations or ring relocation) are postponed, existing infrastructure must continue to support growing demand. As substations become increasingly overloaded, the risk of grid congestion or failure rises, increasing capacity risk.

On the other hand, solar systems on existing buildings and solar parks tend to reduce capacity risk by feeding electricity back into the local grid. This is based on the assumption that generation does not exceed system limits or trigger curtailment. Within this framework, it is assumed that solar generation helps to relieve some of the stress on the distribution network by offsetting local demand.

To manage these rising risks, the model includes three key infrastructure levers:

- Relocation of Ring – reorganizing the topology of the distribution network to better match current and forecasted demand. This can help reduce congestion and improve system efficiency in areas where demand has shifted geographically.
- New Ring – addding new cable loops into the grid to increase redundancy and load-balancing capacity. This lever is often used to address increased demand from new developments or heavily loaded zones.
- New Substation – building substations to add transformation capacity at critical locations. This is the most capital-intensive lever but is essential when existing substations reach their operational limits.

While these levers are effective at reducing M1 – capacity risk, they also significantly influence M2 – costs, as each intervention involves substantial capital expenditure. The strategic deployment of these levers is thus a balancing act between ensuring grid reliability and managing financial feasibility.

D

Behaviour uncertainties

This appendix explores how uncertainties are handled within the simulation model. The goal is twofold: first, to verify that each uncertainty is correctly implemented and computed by the model; second, to assess whether the resulting curve behaviors are plausible. Each uncertainty was tested using a single scenario. While the specific scenario may vary between plots, the focus here is not on comparing across scenarios but rather on confirming that the magnitude and pattern of each uncertainty's effect are reasonable.

D.0.1. Solar panels on existing houses

In the year 2025, the simulation assumes that 5,443 houses are equipped with solar panels. Each of these houses is modeled to have 10 panels, with each panel producing 0.4 kW of power. Multiplying these values gives a total installed capacity of 21,772 kW. To estimate the actual power output, an efficiency factor is applied. Since the analysis focuses on peak hourly production, the maximum projected efficiency by 2028—0.87—is used. Applying this factor gives 18,941 kW. This value represents the expected peak production, indicated as -18,941 kW in the simulation output (the negative sign denoting energy being fed into the grid). The value shown in Figure D.1 is slightly lower, which is consistent with the possibility of a lower efficiency being used in that specific scenario. This suggests that the starting value in the simulation is reasonable and falls within the expected range. To verify the end value, the scenario assumes that a maximum of 80% of all existing houses adopt solar panels. With a total of 13,607 houses, this results in 42,236 kW.This estimate aligns closely with the final value shown in the graph for the year 2052, confirming that the simulation accurately reflects the expected order of magnitude.

The behavior of the graph shows a nearly linear increase in solar panel production over time. This pattern is consistent with the model's assumptions, where both the number of households adopting solar panels and the efficiency of the panels increase steadily each year. Because adoption grows at a relatively constant rate and the efficiency improvement progresses gradually—peaking at 0.87 by 2028—the result is a smooth, linear rise in total installed capacity. After the efficiency factor stabilizes, the continued growth is driven solely by additional installations, which are evenly distributed across the years. This avoids exponential or sudden shifts in output. The resulting linear trend in the graph is therefore a logical outcome of the model inputs and reflects a realistic development trajectory for solar adoption on existing houses.

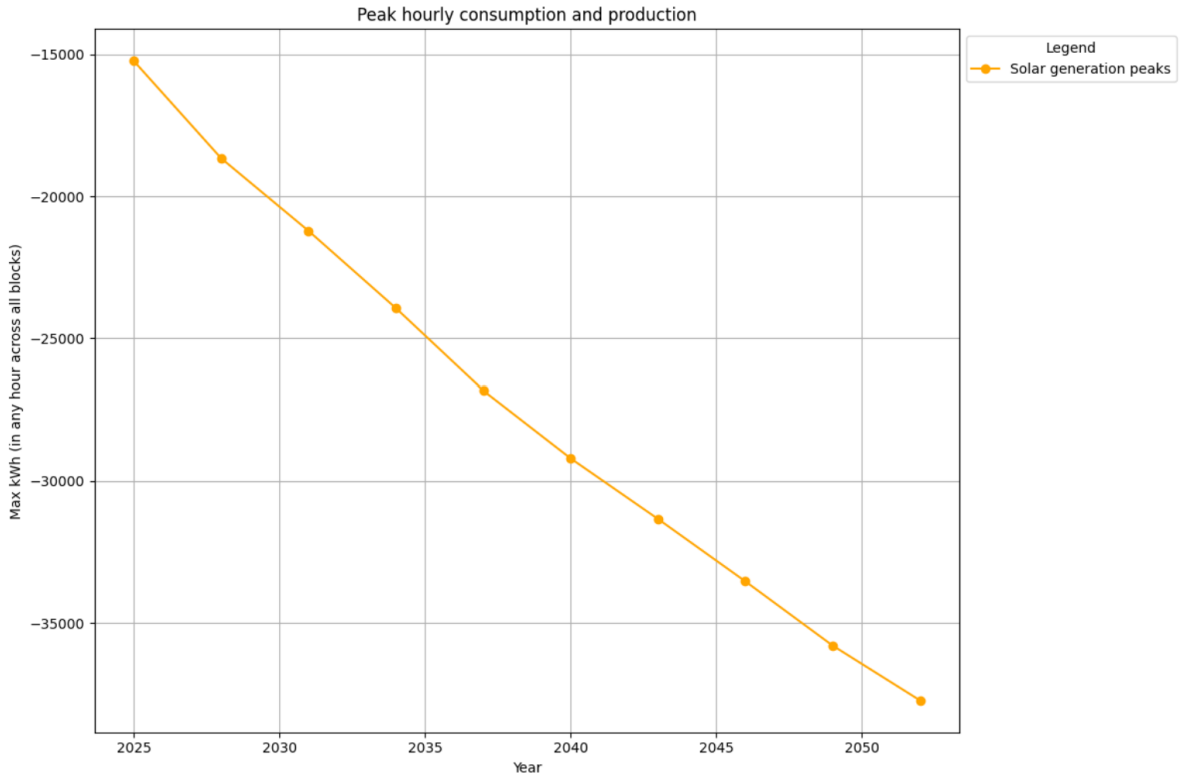

Figure D.1: Peak hourly production solar panels on existing houses

D.0.2. Heat transition in existing houses

In 2025, 97.8% of heating installations in existing houses are still gas boilers. This explains why the peak gas consumption starts off very high, while the electricity consumption peak—which includes heating networks, eHPs, HHPs, and air conditioners—starts near zero. In the model, gas boilers are assumed to consume the most energy, with a demand of 8 kW per house per hour. Given that 13,307 existing houses are equipped with gas boilers, the total peak load from gas heating can be calculated as 13,307 × 8 kW = 106,461 kW. Since peak values reflect winter conditions—where it is assumed that 100% of heating demand can be active simultaneously—this aligns well with the peak shown in Figure D.2. Due to the planned heat transition, gas boilers are gradually phased out, with full removal expected by 2034, 2037, or 2040 depending on the scenario. This is clearly reflected in the graph, where gas consumption drops to zero around 2037. At the same time, electricity-based heating becomes dominant, causing the electricity peak to rise and then level off.

While one might expect the electricity peak to decline over time—since HHPs (which use 6 kW) are eventually replaced by more efficient eHPs (4 kW)—this effect is not yet visible within the timeframe of the graph. This is likely because many HHPs remain in use until the end of their lifespan, especially in slower-transition scenarios such as C. With HHP lifespans of up to 20 years, units installed in the late 2030s may still contribute significantly to peak demand into the late 2050s. Additionally, since the graph reflects the maximum hourly load across all blocks, a few high-load areas can dominate the peak, masking any broader efficiency improvements. Therefore, although a gradual decline is expected, it may only become apparent beyond the simulated period.

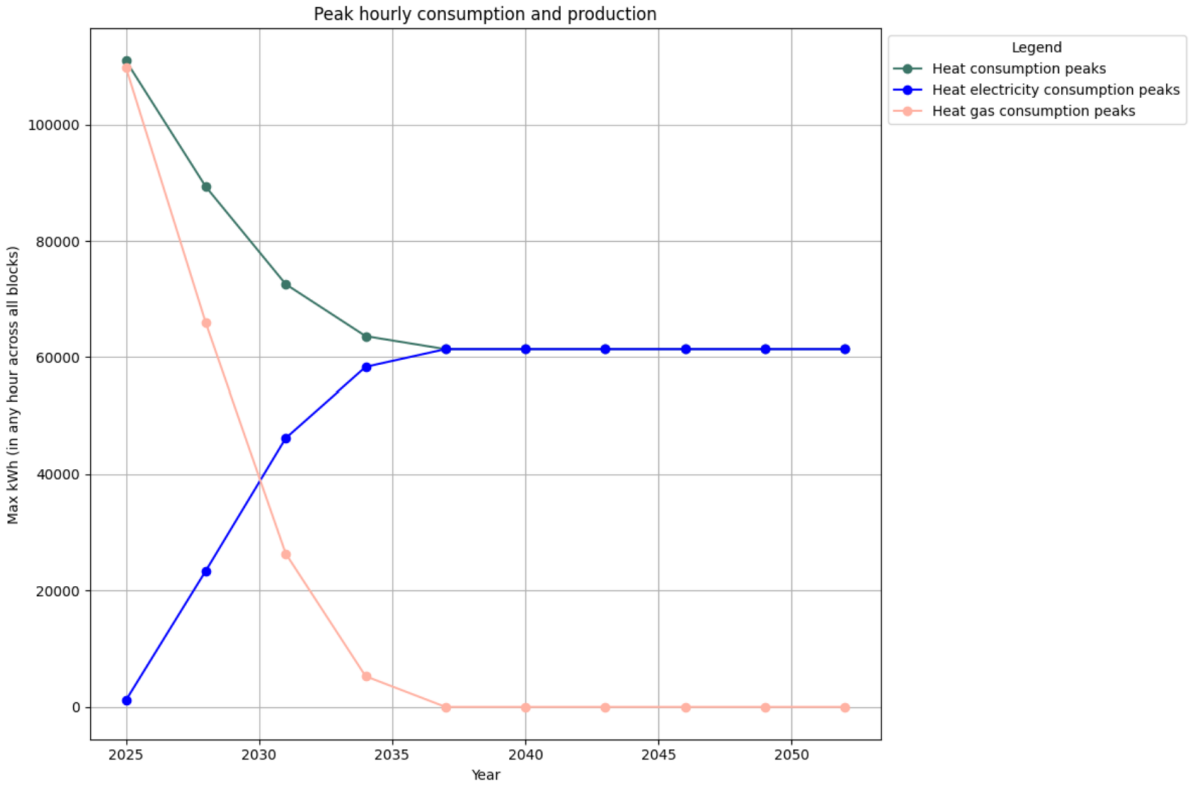

Figure D.2: Peak hourly heat consumption in existing houses

D.0.3. Cooling transition in existing houses

In 2025, 20% of existing houses are equipped with air conditioning, corresponding to 2,721 installations. At this point in time, only large air conditioning units are considered, each consuming 2 kW. This results in a total peak load of 2,721 × 2 kW = 5,442 kW, which aligns with the value shown in Figure D.3 for the year 2025. By 2052, up to 95% of existing houses are projected to have adopted air conditioning for scenario type A, equating to approximately 12,926 installations. In later years, both large and small air conditioning units are present, with smaller units consuming only 1 kW. Assuming a mixed adoption with an average load of 1.5 kW per unit, the total peak load would be around 12,926 × 1.5 kW = 19,389 kW. This is consistent with the order of magnitude seen in Figure D.3 for 2052. The trend in the graph shows a steady, linear increase over time. This behaviour is expected, as the adoption of cooling systems progresses gradually throughout the existing housing stock in the model.

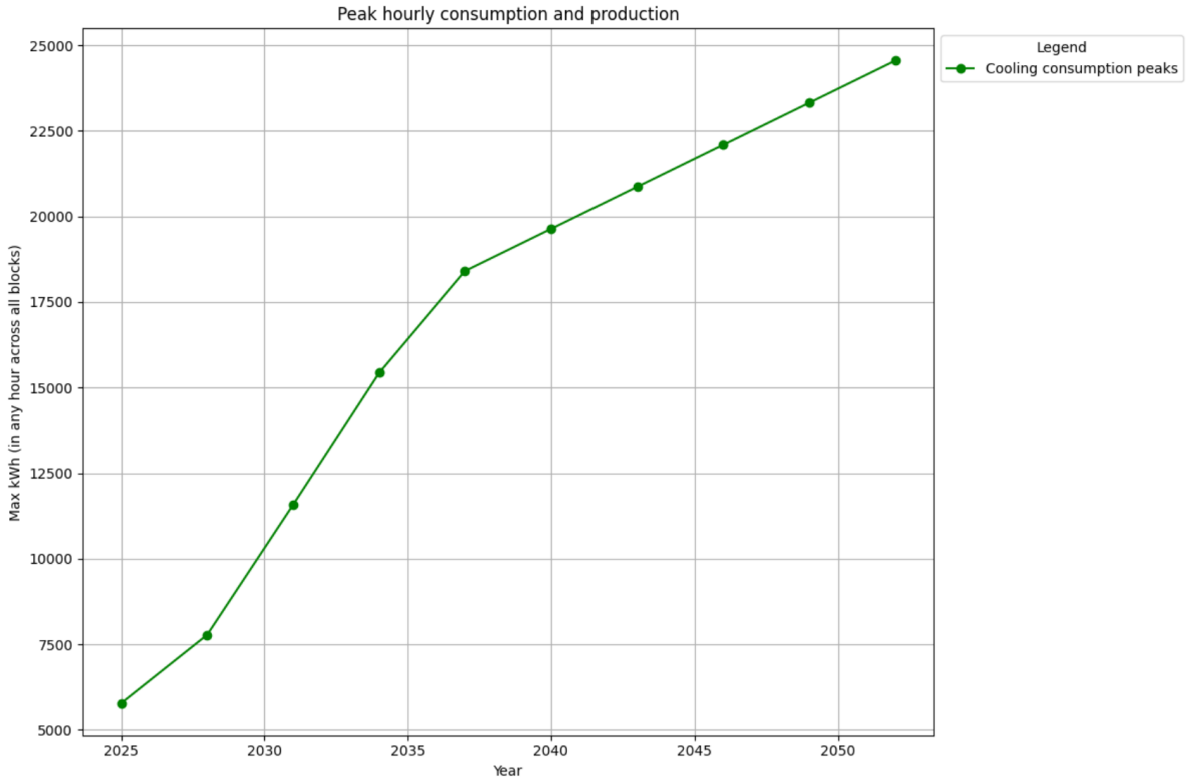

Figure D.3: Peak hourly cooling consumption in existing houses

D.0.4. Charging e-vehicles

In 2025, there are a total of 13,607 vehicles in the area, but only 1.85% of them are EVs. This results in a very small number of EVs, which explains why the electricity consumption due to EV charging in Figure D.4 starts near zero. By 2052, the total number of vehicles is allowed to grow by 80%, reaching 24,492 vehicles. The model assumes that by this year, 100% of the fleet consists of EVs. Each vehicle type has a defined average driving distance every three years—for example, passenger cars are assumed to drive 45,000 km in that period. With an energy intensity of 0.15 kWh/km, this results in a total of 6,750 kWh per car over three years, or approximately 2,250 kWh per year.

To estimate the hourly electricity demand, the model considers charging power. It is assumed that cars charge at a power rate of 11 kW, so each vehicle that is charging draws 11 kW during that time. However, not all EVs charge simultaneously; their charging behavior is influenced by their load profile, which falls into one of three categories:

1. Grid-unaware: these vehicles begin charging immediately when arriving home, typically between 17:00 and 19:00, and continue until fully charged. This creates sharp evening peaks in demand.

2. Grid-aware: charging is spread more evenly over low-demand periods, typically avoiding peak hours. This results in a flatter, more grid-friendly demand curve.

3. Average: charging is distributed uniformly across all hours of the day, serving as a neutral reference profile.

These profiles are implemented as percentages of the total EV fleet in the simulation. The presence of a significant portion of grid-unaware chargers strongly contributes to the peak demand visible in the figure. The figure shows the peak hourly load, not the average usage. If a substantial fraction of EVs—particularly those with grid-unaware behavior—are charging simultaneously during the early evening, the aggregate load can spike. For example, if around 1,800 vehicles are charging concurrently at 11 kW each it will lead to 20,000 kW. This explains the peak shown in 2052. The graph reflects not just the scale of electrification but also behavioral charging patterns, which play a crucial role in shaping demand peaks.

The behavior of the curve over time is also logical, as it reflects two compounding trends: the gradual increase in the total number of vehicles and the steady rise in EV adoption. Early on, EVs make up only a small share of the fleet, so the charging demand is negligible. As both the vehicle fleet expands and the share of EVs grows—eventually reaching 100% by 2052—the electricity demand from EV charging increases accordingly. This gradual growth pattern results in the steadily rising trend observed in Figure D.4.

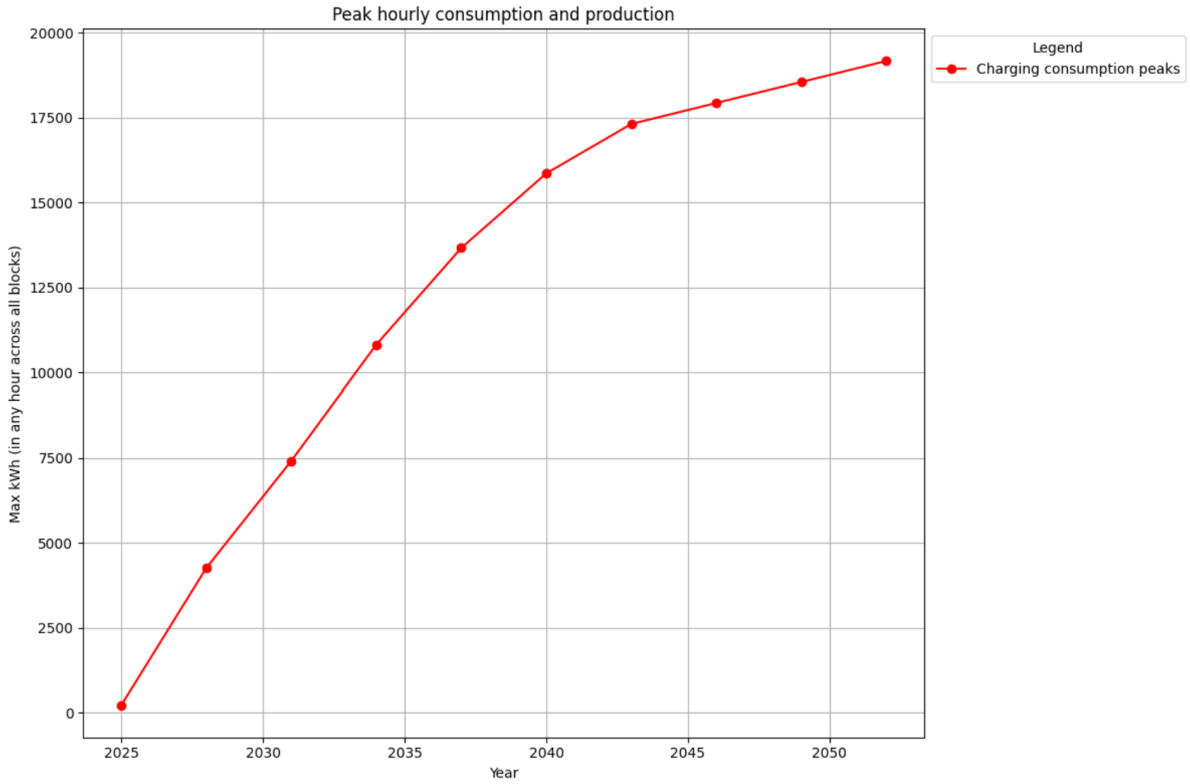

Figure D.4: Peak hourly charging consumption

D.0.5. New buildings

In 2025, there are no newly constructed buildings yet, which is why all curves in Figure D.5 start at zero. By 2052, up to 20% of all buildings are newly built, corresponding to approximately 2,721 houses. Each of these houses is assumed to have 10 rooftop solar panels, each producing 0.4 kW. This results in a total potential production capacity of 10,884 kW, which aligns well with the solar production peak observed at the end of the graph. However, an efficiency factor must also be applied to account for system losses. Assuming an efficiency of 0.97 in 2052, the effective production would be approximately 10,557 kW, which also matches with the observed production peak in Figure D.5.

Regarding energy consumption, new houses are assigned either an eHP or a connection to a heating network. Importantly, only houses connected to a heating network are assumed to also install large air conditioners. Assuming that 50% of the new buildings are assigned to the heating network, this results in approximately 1,360 houses. Of these, 80% are expected to adopt air conditioning by 2052, giving a total of around 1,088 units. Each airco uses 2 kW, resulting in a peak potential cooling demand of approximately 2,176 kW. This aligns closely with the observed value in Figure D.5 for 2052. Therefore, the graph most likely represents a summer peak day, where cooling demand is fully utilized and heating is zero. If it were a winter day with maximum heating demand the peak would be significantly higher.

Finally, it can be observed that the total consumption peak closely matches the net consumption peak in Figure D.5. While this might seem counterintuitive for a summer day—when solar production is expected to be high—the key is that the graph likely shows maximum values per component across the year, rather than values from the same representative day. In other words, the total consumption peak likely occurs during a hot summer afternoon with full air conditioning demand, while the solar production

peak might occur at a different hour (e.g., midday) or even on another day entirely. As a result, solar production contributes little or nothing during the specific hour of maximum cooling demand, explaining why the consumption peak is nearly equal to the total peak.

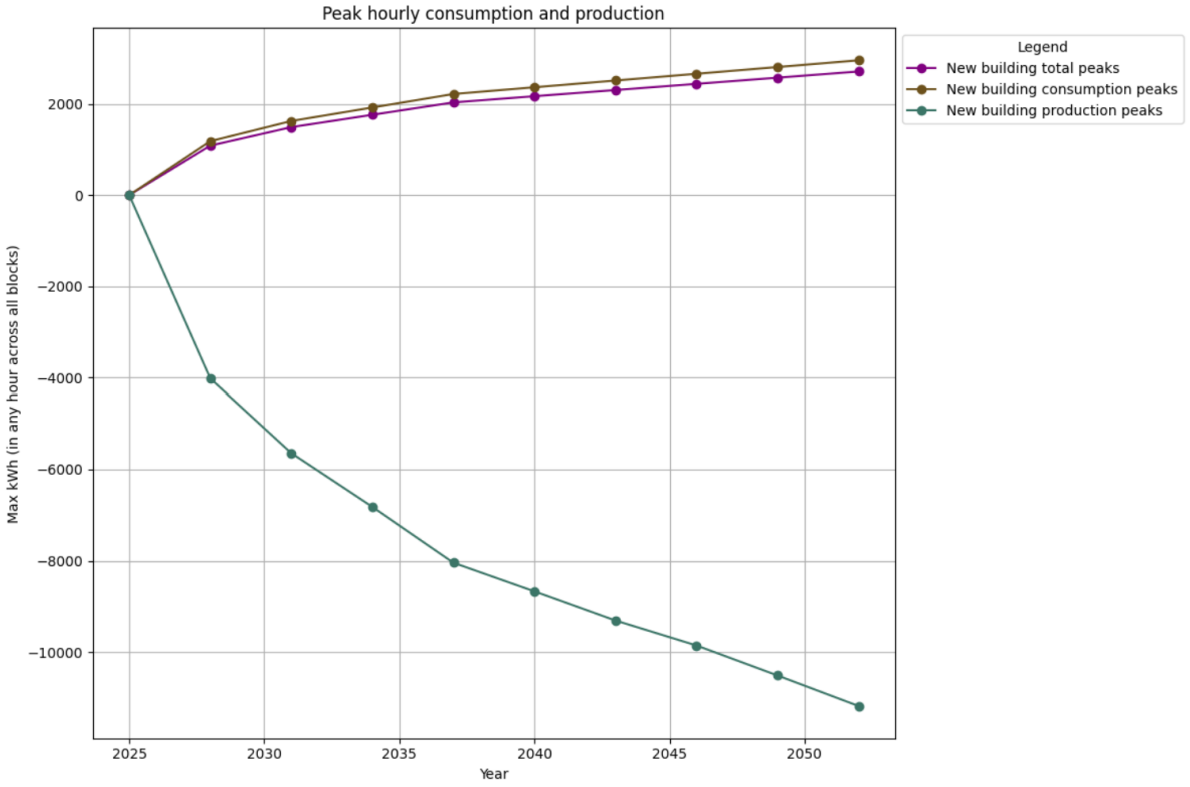

Figure D.5: Peak hourly consumption and production of new buildings

D.0.6. Industry

In 2025, all 2,520 industries are still operating using methane for their energy needs. Each industry consumes 850,000 kWh over a modeled period of three years. When this is averaged over the total number of hours in three years (26,280 hours), the result is approximately 32 kWh per hour per industry. Multiplying this by the total number of industries yields a peak hourly consumption of 81,506 kWh — which matches the value shown in the Figure D.6 for methane consumption in 2025. Following this point, methane use is gradually phased out, reaching 0% by 2049. As methane consumption declines, it is progressively replaced by other energy carriers — primarily electrification and biogas/hydrogen. This transition begins to reflect in the increasing peak hourly consumption values for these two categories.

Despite the complete transition away from methane and the growing reliance on alternative energy sources, the total peak hourly consumption remains relatively stable throughout the modeled period. Starting at just over 70,000 kWh in 2025, it slowly declines to approximately 64,000 kWh by 2050. This slight decrease suggests that the total energy demand during peak hours remains relatively stable, likely because the higher energy intensity of electrification is offset by the lower consumption associated with biogas and hydrogen technologies.

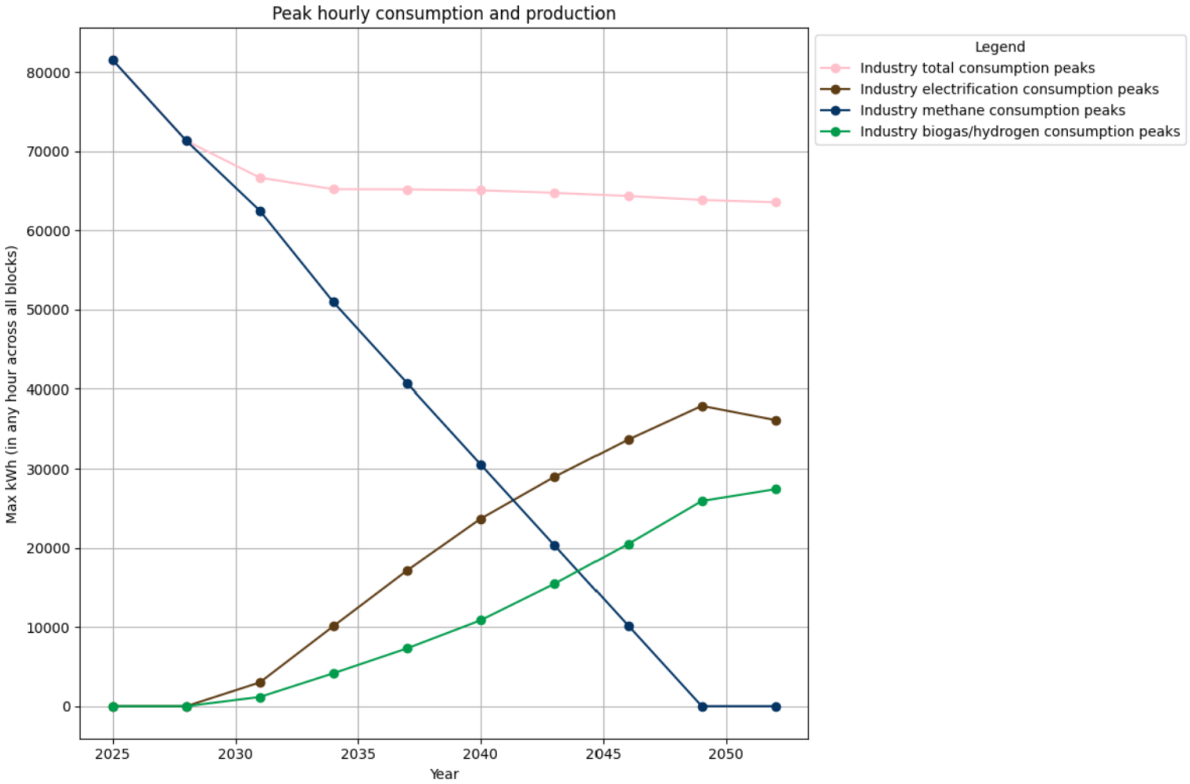

Figure D.6: Peak hourly consumption of industry

D.0.7. Greenhouses

In 2025, the total greenhouse area amounts to 74,300 m², with all energy consumption still based on methane. The modeled methane consumption is 1,350 kWh per m² over a three-year period, which translates to approximately 0.05 kWh per hour per m². Multiplying this hourly value by the total area results in a peak hourly consumption of 3,715 kWh, which aligns with the starting point for methane consumption in Figure D.7. A complete phase-out of methane in greenhouses is assumed by 2040. As with industry, this reduction is offset by the increasing adoption of electrification and biogas/hydrogen systems to meet energy needs.

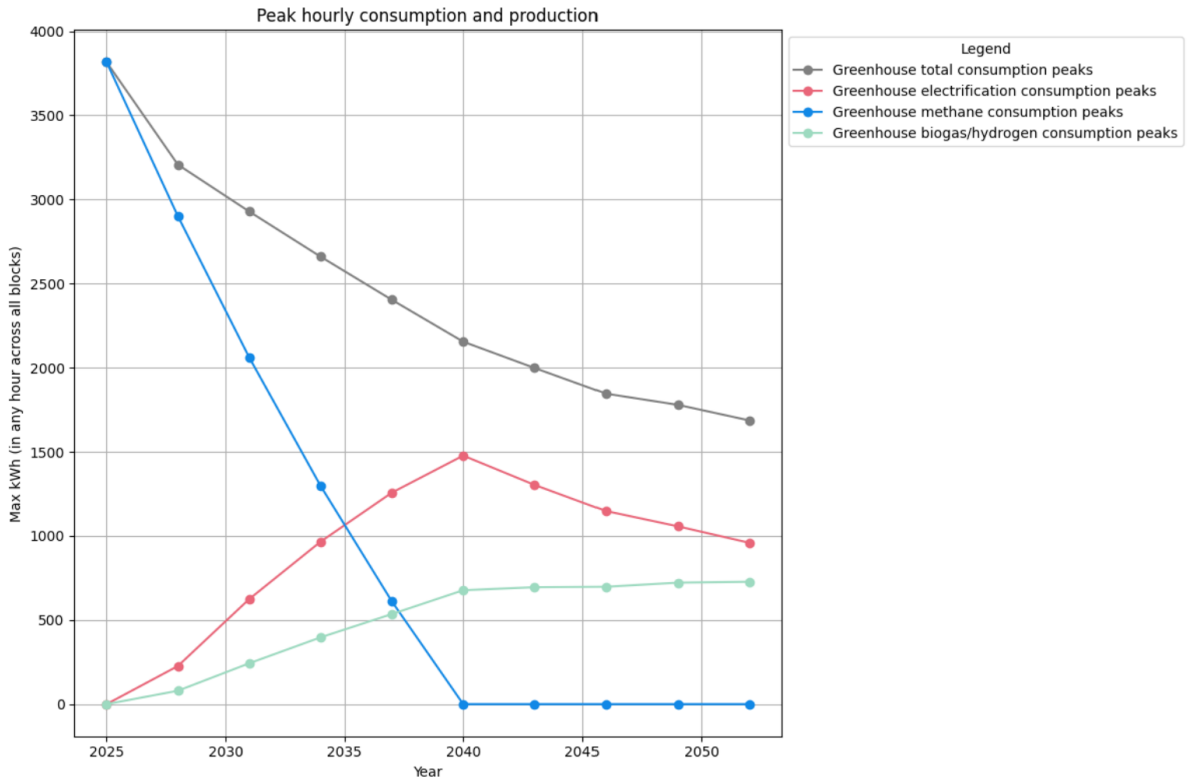

Figure D.7: Peak hourly consumption of greenhouses

D.0.8. Shore power

In 2025, no shore power connections are planned yet. From 2028 onward, connections are introduced gradually and increase in discrete steps every few years for each industrial area (labeled A, B, and C). Each new connection contributes a fixed amount of ”hotel load” energy—non-propulsion power used while a ship is docked. This load is calculated as the number of connections multiplied by a fixed energy requirement of 30 MWh per ship per 3 years. In parallel, a growing share of these ships is assumed to be electric. For these electric ships, an additional charging energy is included, calculated by multiplying the number of shore power connections by the electric ship share (which increases over time) and then by a fixed charging requirement of 80 MWh per ship per 3 years. These two components—hotel load and charging load—are added together to yield the total shore power energy demand over each 3-year period, per industrial block and per year. To represent peak hourly demand (as shown in the figure), this 3-year energy total is distributed across all hours using a standardized daily usage profile. The maximum value from this hourly distribution becomes the peak hourly shore power consumption shown on the graph.

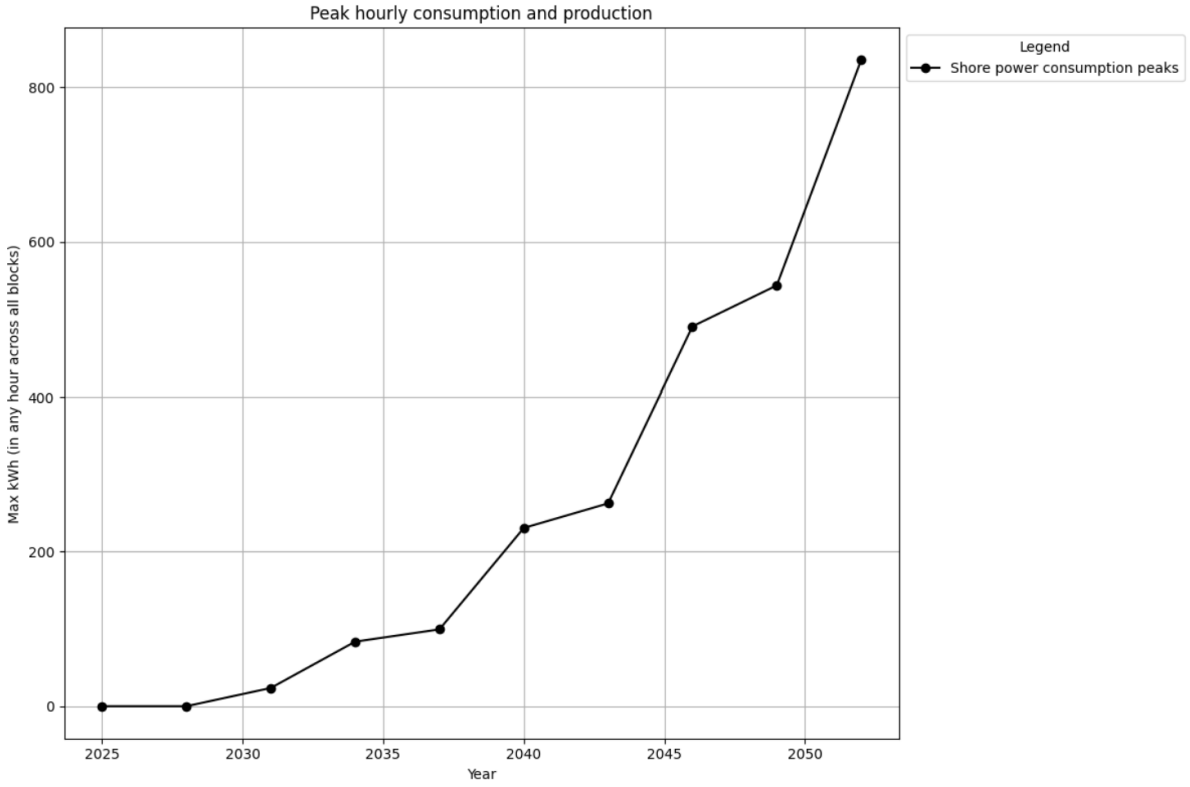

Figure D.8: Peak hourly consumption of shore power

D.0.9. Solar parks

In 2025, there are no solar parks constructed yet, and although a small amount of solar capacity may begin to grow in the years that follow, this early growth is too minor to be visible in Figure D.9. The first noticeable impact occurs in 2040, when a large solar park with a total surface area of 400,000 square meters is added. This park significantly increases solar energy production. Given that each square meter of solar park area generates 360 kilowatt-hours of electricity over a three-year period, the total energy produced by this installation equals 144 million kilowatt-hours (400,000 m^2 × 360 kWh/m^2). When this total is distributed evenly across the 1,095 days that make up three years, the average daily output amounts to approximately 131,506 kilowatt-hours. This value closely matches the sharp increase observed in the graph at the year 2040, after system efficiency losses are accounted for. Following the introduction of this solar park, no additional large parks are added in later years, which explains why the graph plateaus again after 2040, similar to the flat trend seen before that year.

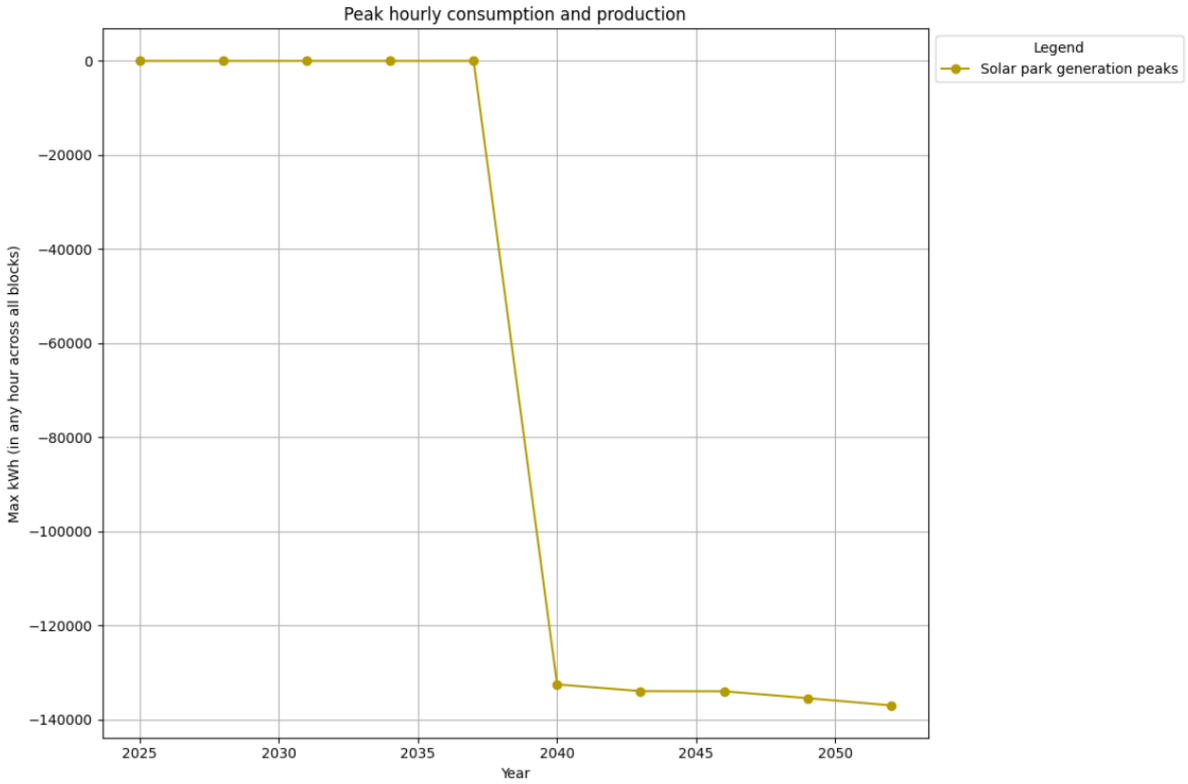

Figure D.9: Peak hourly production of solar parks

D.0.10. Solar panels on large roofs

Only industrial buildings are eligible for large rooftop solar panels in this model. In 2025, no panels are installed yet, but over time, a growing portion of these industries will be deemed suitable for solar installations. By design, not every industry becomes suitable at once—each year sees a gradual increase, based on a predefined growth rate. Then, from the pool of suitable rooftops, only a fraction actually get solar panels constructed, governed by a separate construction rate.

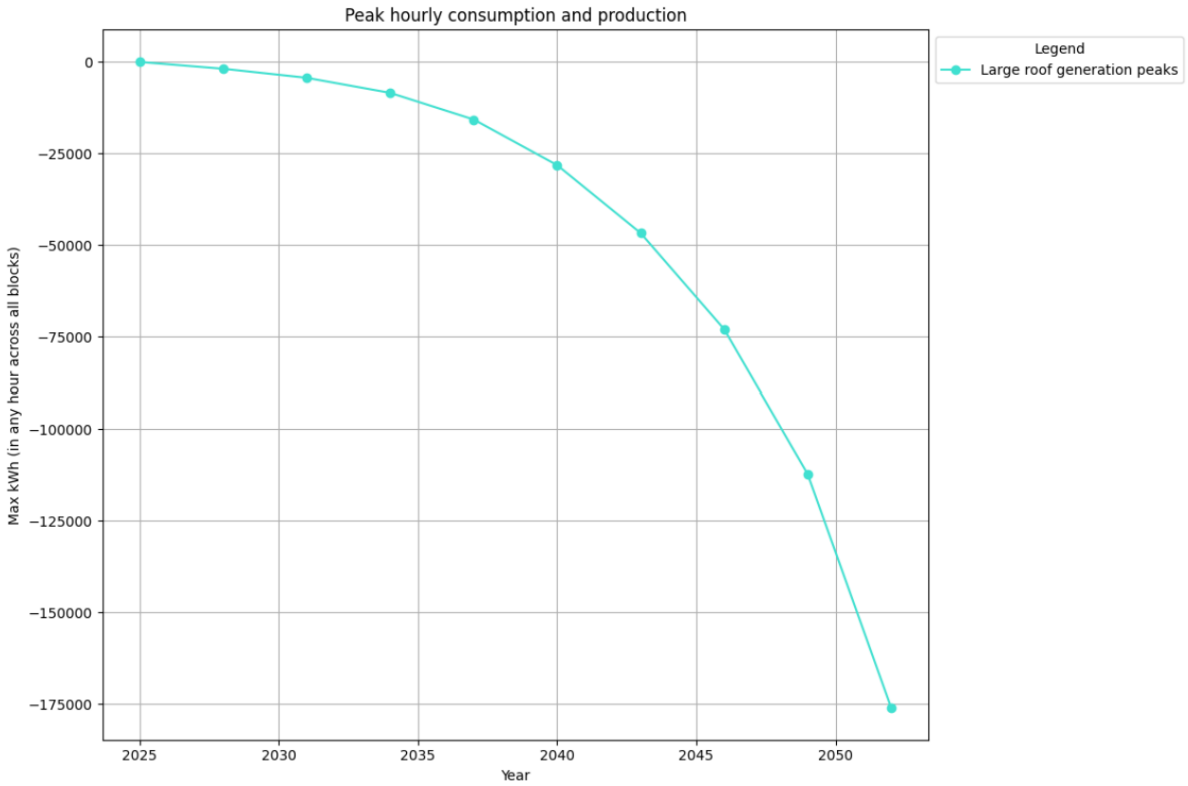

Figure D.10: Peak hourly production of solar panels on large roofs

D.0.11. All uncertainties together

The scenario below combines all uncertainties. It clearly shows that the solar park contributes the lowest minimum demand by a wide margin, making it a significant factor in potential capacity risks.

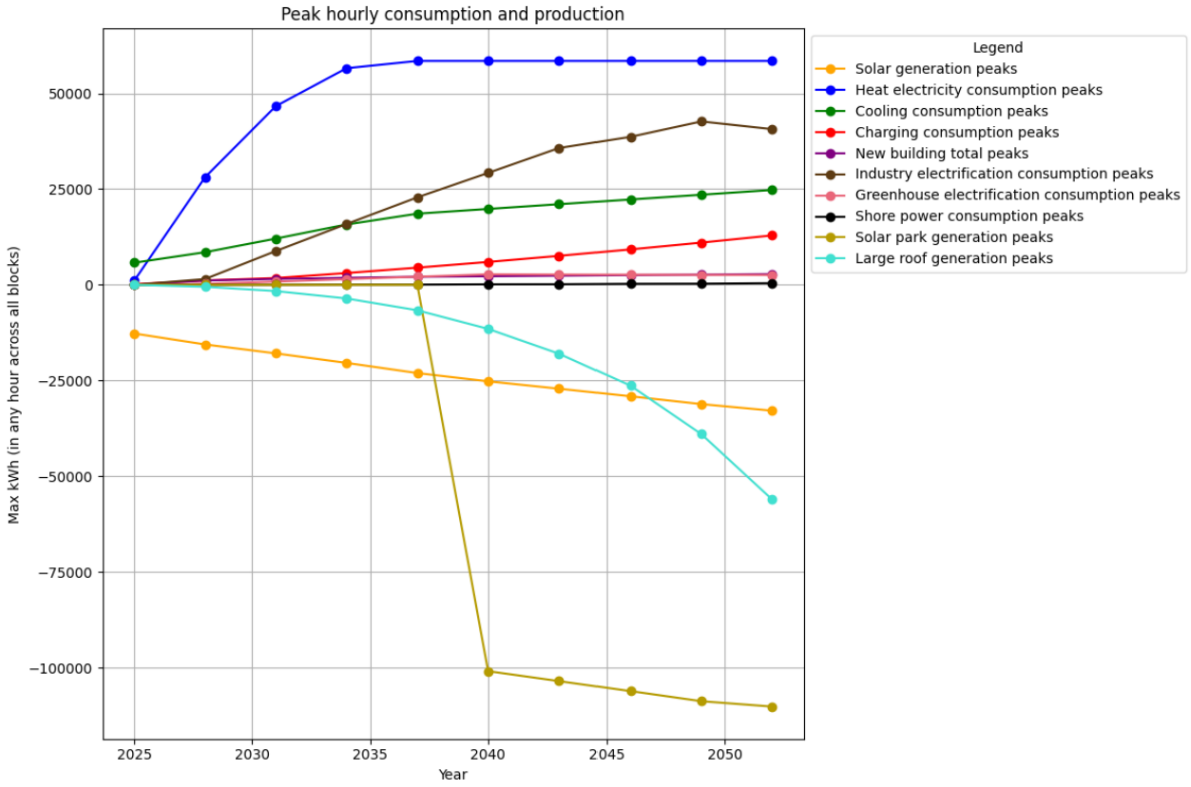

Figure D.11: Peak hourly consumption and production of all uncertainties

E

Calculation uncertainties

This appendix explains how electricity use is calculated for each of the uncertainties.

E.0.1. Solar adoption existing houses

This section describes the simulation of hourly solar electricity generation for existing houses, disaggregated by building block and simulated across multiple years. The generation depends on several factors: the number of panels per house, panel capacity, and efficiency (all static), as well as dynamic inputs such as the number of houses adopting solar each year and the expected solar production on representative days.

The installed solar capacity per building block per year is computed using the following formula:

$$\text{Installed capacity (kW)} = N_{\text{solar houses}} \times N_{\text{panels per house}} \times P_{\text{panel}}$$

Where:
$N_{\text{solar houses}}$ = Number of houses with solar panels in that year
$N_{\text{panels per house}} = 10$
$P_{\text{panel}} = 0.4$ kW

To obtain hourly solar generation, this installed capacity is multiplied by a normalized hourly solar profile and an efficiency factor:

$$\text{Hourly Generation} = \text{Installed Capacity} \times \text{Profile}_{\text{hour}} \times \eta_{\text{efficiency}}$$

Where: $\eta_{\text{efficiency}}$ = Year-specific efficiency factor from `solar_park_efficiency`

The hourly solar profile over the full 3-year period is constructed using representative days. Each representative day includes 24 hourly solar generation values and an associated weight, indicating how many actual days it represents. The complete 3-year profile is assembled by repeating each representative day's hourly values according to its weight and concatenating them sequentially.

E.0.2. Heating transition existing buildings

This section explains how hourly heating energy consumption is simulated for existing houses, broken down by building block and year. The mix of heating systems evolves over time and includes gas boilers, hybrid heat pumps (HHPs), electric heat pumps (eHPs), heat networks, and air conditioning systems.

The model assumes constant hourly energy consumption (in kW) for each heating system type per house:

- Gas boiler = 8 kW
- HHP = 6 kW

- eHP = 4 kW
- Heat network = 3 kW
- Airco = 2 kW

Before 2028, the shares of each heating technology are taken directly from the attributes of each building block. From 2028 onward, a portion of the existing gas boilers transition to other heating technologies. This transition depends on the number of gas boilers present three years earlier, a yearly heat factor that determines what share of those gas boilers transition, and a hybrid factor that specifies what fraction of the transitioning systems become hybrid heat pumps. Additionally, there is a lifespan-based logic to handle replacements of hybrid heat pumps once they reach the end of their service life. The remaining transitioned systems — those not becoming hybrids — are distributed among electric heat pumps, heat networks, and air conditioning systems. If a building block does not have heat network infrastructure, the share allocated to heat networks is redistributed proportionally between electric heat pumps and air conditioning. Previously installed hybrid heat pumps are tracked over time and replaced at the end of their lifespan; these replacements are assumed to convert into electric heat pumps.

To calculate hourly heating energy demand, the model uses a normalized 24-hour heating demand profile (values sum to 1). This profile is scaled based on the number of each technology type and their energy consumption:

$$\text{Hourly Heating (kWh)} = \sum_i N_i \times E_i \times \text{Profile}_{\text{hour}}$$

Where: N_i = Number of houses using technology i
E_i = Hourly energy consumption of technology i
$\text{Profile}_{\text{hour}}$ = Normalized hourly demand pattern

Electricity and gas consumption are calculated separately: the energy consumption from electric-based heating systems (hybrid heat pumps, electric heat pumps, heat networks, and air conditioning) contributes to electricity use, while only gas boilers contribute to gas use.

Finally, to build the full three-year hourly heating profile, the model concatenates the weighted profiles of the representative days. Each weight corresponds to the number of real days that a representative day stands for.

E.0.3. Cooling transition existing buildings

This section describes how hourly cooling energy consumption is modeled for existing residential buildings, broken down by building block and year. The adoption of cooling systems evolves over time, focusing on two categories of air conditioning units: small air conditioners and large (or “big”) air conditioners. The model tracks the number of houses using each cooling system type within each building block for every simulation year. Before 2028, the number of air conditioners in each building block is fixed, based on the existing installations recorded in the building attributes. All of these airco’s are put as big air conditioners.

Starting from 2028, cooling adoption increases as more houses install air conditioning systems. The model identifies eligible houses for cooling adoption based on their heating system types. Houses currently using air conditioning for heating and those with hybrid heat pumps or heat network heating are considered eligible. A yearly adoption factor determines the share of these eligible houses that adopt new cooling systems. New small air conditioners are assigned to houses already using air conditioning for heating. Remaining eligible houses, mostly those with hybrid or heat network heating, are assigned new large air conditioners. Existing large air conditioners from before 2028 are included in the total count of big air conditioners.

To estimate the total hourly cooling energy consumption for a building block, the model assumes that small air conditioners consume half the energy of large ones, leading to:

$$E_{\text{cooling}} = N_{\text{small}} \times \frac{1}{2} E_{\text{airco}} + N_{\text{big}} \times E_{\text{airco}}$$

where E_{airco} is the hourly energy consumption per air conditioning unit (typically 2 kW).

Hourly cooling demand profiles are based on representative days with normalized 24-hour cooling demand patterns, which sum to 1 over the day. The hourly cooling energy for each representative day is obtained by scaling the total block cooling energy with this profile. Finally, these hourly profiles are repeated according to the weight (number of actual days represented) of each representative day and concatenated to form a full-year hourly cooling energy profile for each building block.

E.0.4. E-vehicles

The model estimates hourly EV charging demand by following several key steps. First, it estimates the total number of vehicles for each building block and year. For years before 2028, this number is predefined. From 2028 onwards, a growth factor is applied. An EV adoption factor is then used to determine what share of the total vehicles are electric. These EVs are divided into categories (cars, vans, buses, and trucks) based on fixed annual shares.

For each vehicle category, an average distance driven over 3 years is calculated as:

$$D_{b,y}^{(c)} = \text{EV}_{b,y}^{(c)} \times \text{km\_per\_vehicle}^{(c)}$$

where:

- $D_{b,y}^{(c)}$ is the total distance (in km) driven by electric vehicles of category c in building block b during year y,
- $\text{EV}_{b,y}^{(c)}$ is the number of electric vehicles of category c in block b and year y,
- $\text{km\_per\_vehicle}^{(c)}$ is the average annual driving distance (in km) for one vehicle of category c, assumed to be constant across time and location.

This distance is then converted into energy demand using a static energy consumption rate (in kWh/km). To convert energy demand into charging hours, it is divided by a known charging power level (in kW). This yields the total annual charging hours required per vehicle category.

Next, the total annual charging hours $H_{b,y}^{(c)}$ are distributed among three behavior groups: grid-aware, average, and grid-unaware. This is done using predefined behavior shares α_y^{beh}, where the sum of all shares equals 1:

$$H_{b,y,\text{beh}}^{(c)} = H_{b,y}^{(c)} \times \alpha_y^{\text{beh}}, \quad \text{with} \quad \sum_{\text{beh}} \alpha_y^{\text{beh}} = 1$$

To estimate daily charging needs, the annual hours are divided by the number of days in the representative 3-year period:

$$h_{b,y,\text{beh}}^{(c)} = \frac{H_{b,y,\text{beh}}^{(c)}}{\text{days}_{3y}}$$

The daily charging hours are then distributed across the 24 hours of a day, depending on the user's behavior:

- **Grid-unaware** users charge during **peak hours** (typically 17:00–19:00),
- **Grid-aware** and **average** users charge during **non-peak hours** (all other hours).

For each group, the total charging time is evenly spread across their allowed hours. The hourly charging load for hour h is calculated as:

$$\text{Load}_{b,y,h}^{(c)} = \frac{\text{DailyHours}_{b,y,\text{group}}^{(c)}}{\text{Hours}_{\text{group}}} \times P^{(c)}$$

where:

- $\text{DailyHours}_{b,y,\text{group}}^{(c)}$ is the number of daily charging hours for behavior group `group`,
- $\text{Hours}_{\text{group}}$ is the number of hours allocated for charging (e.g., 3 for peak hours),
- $P^{(c)}$ is the charging power (in kW) for vehicle category c.

The result is a daily charging profile consisting of 24 hourly values per vehicle category and behavior group. These profiles are assumed to remain constant across the 3-year representative period and are scaled using representative day counts to produce a complete hourly charging demand for the year.

E.0.5. New buildings

For each simulation year and for each building block classified as a building sector, the model calculates the electricity consumption and solar energy production associated with newly constructed buildings.

The number of new buildings in a given year and building block is determined by comparing the projected total building count against the base year (2025) count. These new buildings are assigned heating technologies according to predefined shares, which can only be electric heat pumps (eHP) or district heating networks. Then, a fraction of the buildings connected to the heating network adopt air conditioning systems (airco) for cooling.

The hourly electricity demand for each technology is calculated by:

$$E_{\text{eHP},y,b,h} = N_{\text{eHP},y,b} \times P_{\text{heat},h}$$

$$E_{\text{heat\_network},y,b,h} = N_{\text{heat\_network},y,b} \times P_{\text{heat},h}$$

$$E_{\text{airco},y,b,h} = N_{\text{airco},y,b} \times P_{\text{cool},h}$$

where

$P_{\text{heat},h}$ is the normalized heating demand profile at hour h,

$P_{\text{cool},h}$ is the normalized cooling demand profile at hour h.

The total hourly electricity demand from new buildings is then the sum of these three components:

$$E_{\text{demand},y,b,h} = E_{\text{eHP},y,b,h} + E_{\text{heat\_network},y,b,h} + E_{\text{airco},y,b,h}$$

Every new building is assumed to be equipped with solar panels of the same capacity per building as existing buildings. The hourly solar energy generation for these panels is calculated by scaling the normalized solar generation profile by the total installed solar capacity of the new buildings.

Finally, the net electricity demand from new buildings at each hour is calculated by subtracting the solar generation from the total electricity demand:

$$E_{\text{net},y,b,h} = E_{\text{demand},y,b,h} - E_{\text{solar},y,b,h}$$

This approach provides an hourly time series of net electricity demand for new buildings that accounts for heating, cooling, and on-site solar generation.

E.0.6. Industry

The model calculates the electricity consumption of industrial sectors by projecting changes in industry stock and their energy source mix over time, incorporating electrification, biogas/hydrogen adoption, industry inactivity, and a complete phase-out of methane.

For each simulation year, the total industrial building stock within each industry block is estimated. Before 2028, the model uses the baseline stock as-is from 2025. After 2028, the stock is adjusted by applying an industry-specific growth factor to the 2025 baseline, reflecting growth, stagnation, or decline.

The energy source mix for industry evolves as follows:

- Methane share declines linearly from 100% in 2025 to 0% in 2049.
- No industry share (representing closures or no industrial activity) is a fixed factor from inputs.
- The remaining share is divided between electrification and biogas/hydrogen according to their projected shares.

The remaining shares are normalized within the remaining portion of the industry stock to ensure they sum to 100%:

$$S_{\text{electrification},y} = \frac{s_{\text{electrification},y}}{s_{\text{electrification},y} + s_{\text{biogas/hydrogen},y}} \times S_{\text{remaining},y}$$

$$S_{\text{biogas/hydrogen},y} = \frac{s_{\text{biogas/hydrogen},y}}{s_{\text{electrification},y} + s_{\text{biogas/hydrogen},y}} \times S_{\text{remaining},y}$$

where $s_{\text{electrification},y}$ and $s_{\text{biogas/hydrogen},y}$ are the projected shares calculated as increasing functions of time (starting at 30% electrification and 10% biogas/hydrogen in 2025, increasing by 5% and 3% per interval, respectively, capped at 100%).

The annual energy consumption per heat source, per unit of industry stock, is fixed as:

- Electrification: 900,000 kWh/year
- Biogas/Hydrogen: 750,000 kWh/year
- Methane: 850,000 kWh/year
- No industry: 0

To convert these annual values to hourly consumption rates, each is divided by the total number of hours per simulation period (26,280 hours). Finally, the hourly energy use of each heat source in an industry block during a given year is calculated by multiplying the heat source's stock size by its hourly consumption rate.

E.0.7. Greenhouses

The calculation of electricity use for greenhouses follows the same methodology as that for industrial electricity consumption. The primary difference lies in the specific energy use assumptions for greenhouses, which are as follows:

- Electrification: 1200 kWh/m^2/year
- Biogas/Hydrogen: 1000 kWh/m^2/year
- Methane: 1350 kWh/m^2/year
- No greenhouses: 0 kWh/m^2/year

E.0.8. Solar park

The model estimates solar park electricity production by projecting the available solar surface area and applying efficiency and time-profile factors to generate hourly energy outputs.

The initial solar surface area in 2025 is set to a base value of 1 square meter. This base allows the model to simulate growth over time. From 2025 until 2028, the solar surface area remains constant at this base level. Starting in 2028, the surface area increases every 3 years by applying a growth factor specific to each year:

$$A_y = A_{y-3} + (A_{y-3} \times g_y)$$

where g_y is the solar park growth factor for year y, and A_{y-3} is the surface area three years prior.

The energy yield per square meter over a 3-year period is fixed at 360 kWh/m². This means that the total electricity production by the solar park in 3-year span is:

$$E_y = A_y \times 360 \times \eta_y$$

where η_y represents the solar panel efficiency for year y. For years before 2028, the efficiency is held constant at the 2028 value.

To convert this 3-year total energy into hourly production, the model uses representative days weighted by their occurrence within the year. Each representative day has an hourly solar production profile normalized (value between 0 and 1). These hourly profiles are repeated according to their weights, representing the number of days each profile stands for, and concatenated to form a fully hourly time series for the year.

From 2040 onwards, the model includes building block-specific solar production. Certain building sectors have fixed solar surfaces assigned (for example, Sector 2.1 has 400,000 m²). For Sector 2.2, solar surface growth can be enabled by overrides after a defined year, with a surface area of 60,000 m² when active. The production for these blocks is calculated with the same energy yield and efficiency parameters, applying the representative day profiles to generate their respective hourly outputs.

E.0.9. Shore power

The electricity demand from shore power is estimated for industrial building blocks starting from the year 2028. For all years before 2028, no shore power usage is assumed, and both the number of connections and energy use are set to zero. From 2028 onward, the number of shore power connections increases in steps every three years. The number of connections in block b and year y, denoted $C_{b,y}$, is calculated as:

$$C_{b,y} = C_{b,y-3} + \Delta C_y$$

where ΔC_y is the stepwise increase defined externally per year. If a block is not classified as industrial (i.e., its name does not start with `Industry`), it is excluded from the calculation entirely.

Once the number of connections is known, the total annual energy demand from shore power, $E_{b,y}$, is calculated by combining two components: the hotel load and the charging load. The hotel load represents the non-propulsion energy needs of ships while docked and is assumed to be a fixed value per connection. The charging load accounts for electric ships that require energy while at shore. Let s_y be the share of electric (shore power-compatible) ships in year y. Then, the annual energy use becomes:

$$E_{b,y} = C_{b,y} \times E_{\text{hotel}} + C_{b,y} \times s_y \times E_{\text{charge}}$$

where E_{hotel} is the annual energy use per ship for hotel load (in kWh), and E_{charge} is the daily charging energy required per electric ship (also in kWh). This means that the total energy use is made up of the total number of ships using shore power multiplied by the hotel load, plus the number of electric ships times the charging energy required over the year.

To convert this annual energy demand into an hourly profile, a fixed daily load shape is used. This shape, represented by values p_h for each hour, defines the relative share of energy consumed in each hour of the day. These 24 values are normalized over the full 3-year period. Let days_{3y} be the total number of days in the representative 3-year period. The hourly energy demand for hour h on any day is given by:

$$e_{b,y,d,h} = E_{b,y} \times \frac{p_h}{\sum_{h'=0}^{23} p_{h'} \times \text{days}_{3y}}$$

This results in a consistent 24-hour load shape that is repeated for each day of the 3-year period. The same daily profile is assumed for all industrial blocks and does not vary across days or seasons. Consequently, the hourly shore power usage is evenly distributed across the 3-year period according to this fixed daily shape.

E.0.10. Solar panels on large roofs

The calculation for solar panels on large roofs follows the same approach as for solar panels on existing buildings. The key difference is that this calculation is applied exclusively to building blocks classified as Industry. Additionally, each roof is assumed to have 20 solar panels, with each panel generating 500 W. Apart from these distinctions, the methodology remains identical.

E.0.11. Total hourly demand

The total hourly demand for each building block and year is computed by aggregating various components of electricity use and generation on an hourly basis. This includes electricity consumption from heating, cooling, electric vehicle charging, new buildings, industrial electrification, greenhouses, shore power usage, and subtracting local solar energy generation from different solar sources. Some components, like industrial electrification and greenhouse electricity use, are assumed constant over all hours in the simulation period, while others vary hourly according to representative profiles. Since all created data dictionaries already contain hourly values per building block, implementing this aggregation is straightforward. This calculation is performed for every hour over the simulation period, for each building block and year, producing a comprehensive time series of combined electricity demand.

F

Hourly value 2025 per building block

This appendix presents the hourly power (kW) values for various building blocks throughout the year 2025. Each figure illustrates the electricity consumption or feed-in patterns on an hourly basis. The x-axis represents the time (datetime) spanning the full year of 2025, while the y-axis represents the power in kilowatts (kW). Positive values indicate electricity consumption, while negative values indicate instances where electricity is being fed back into the grid (i.e., net generation exceeds consumption). First there will be looked at all the building sectors.

Figure F.1 illustrates relatively stable electricity demand throughout the year. While minor fluctuations are present, the overall pattern does not show a strong seasonal trend. During the summer months, a few instances of negative values appear, indicating limited feed-in to the grid. However, these are rare, suggesting that this sector is primarily a net consumer of electricity. Among all sectors, this building exhibits the lowest overall electricity consumption.

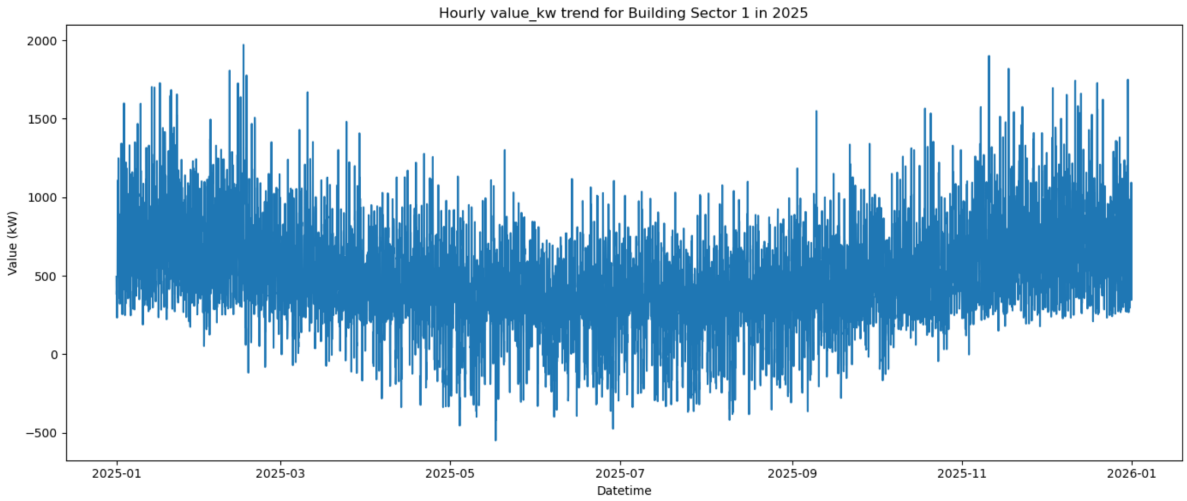

Figure F.1: Building sector 1 hourly value 2025

Figure F.2 displays a clear seasonal pattern, with significantly higher electricity consumption in the winter and lower demand during the summer months. Notably, the electricity values fall well below zero in spring and summer, suggesting that this building sector regularly feeds electricity back into the grid—likely due to on-site generation such as solar PV. This sector also exhibits the highest peak hourly electricity values among all analyzed sectors.

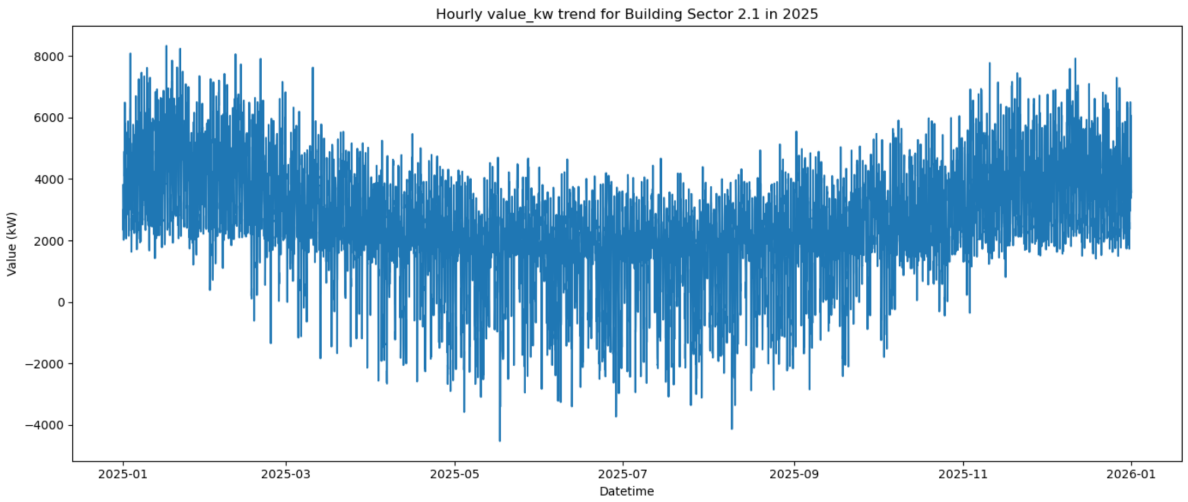

Figure F.2: Building sector 2.1 hourly value 2025

Figure F.3 shows a similar seasonal trend: electricity use is highest in winter and decreases during summer. There are numerous negative values, especially during the warmer months, indicating frequent instances of electricity being fed back into the grid, likely from renewable generation sources.

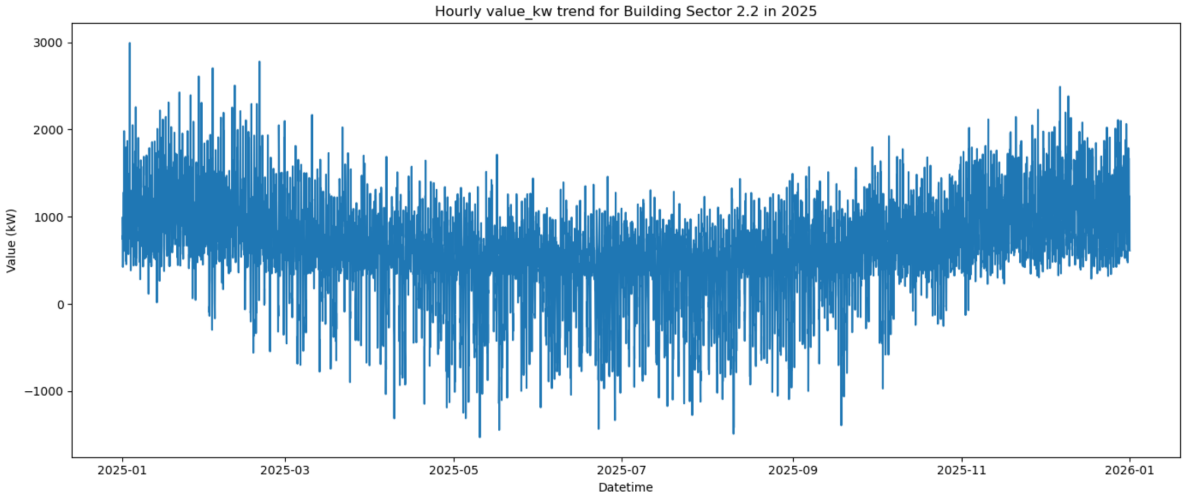

Figure F.3: Building sector 2.2 hourly value 2025

Figure F.4 closely resembles the pattern in Figure F.3. It features a pronounced seasonal load profile, with reduced demand during the summer and higher consumption in winter. Several instances of negative values occur, particularly in the summer, again indicating periodic feed-in to the grid.

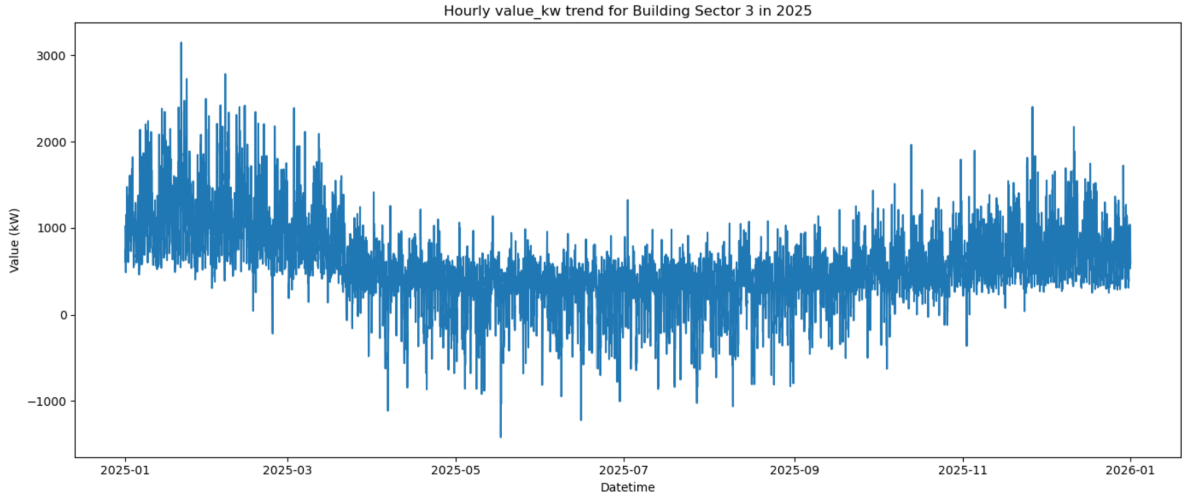

Figure F.4: Building sector 3 hourly value 2025

Following the analysis of the building sectors, the focus shifts to the greenhouse sectors. Figure F.5 displays the hourly power values for Greenhouse 3 in 2025. Notably, the data for this greenhouse was incomplete—several data points were missing throughout the year. To address this, the available data from the first three months of the year was repeated to fill the remainder of the timeline. As a result, the trend shown in the plot reflects a repeating pattern that mimics the initial period, rather than representing actual measurements for the entire year. The power values fluctuate significantly, with both large consumption peaks and notable periods of feed-in (negative values), suggesting intermittent operation.

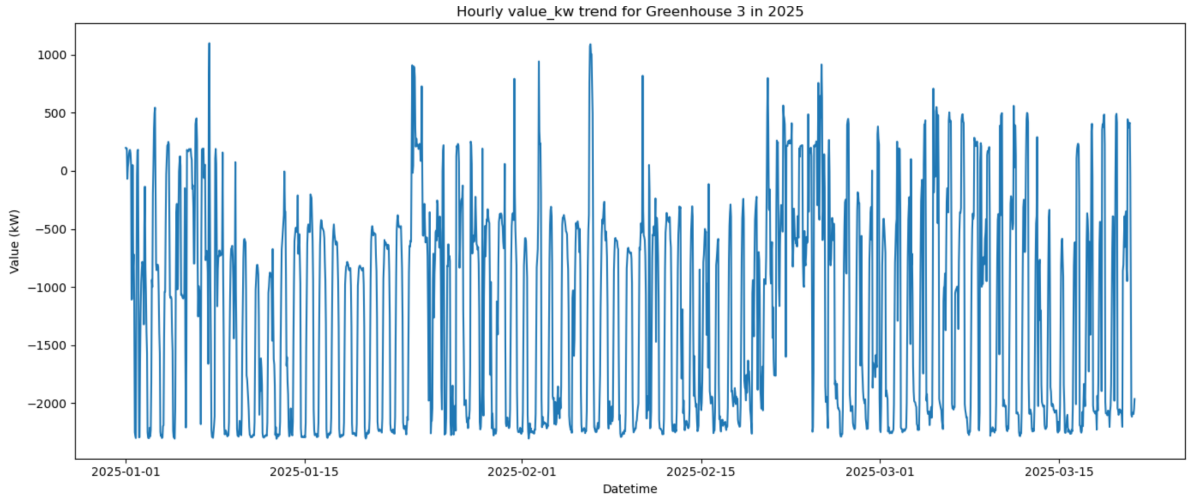

Figure F.5: Greenhouse 3 hourly value 2025

In contrast, Figure F.6 illustrates a relatively stable pattern over time, with frequent fluctuations. However, there is a distinct and notable dip in power values during March, where the data drops sharply and frequently into negative values. This deviation suggests an unusual operational period or anomaly during that time. After this dip, the power values stabilize into a more consistent pattern for the remainder of the year. During the colder months towards the end of the year, the power consumption increases and remains consistently positive, indicating higher electricity demand likely due to heating requirements, with no instances of feed-in observed during that period.

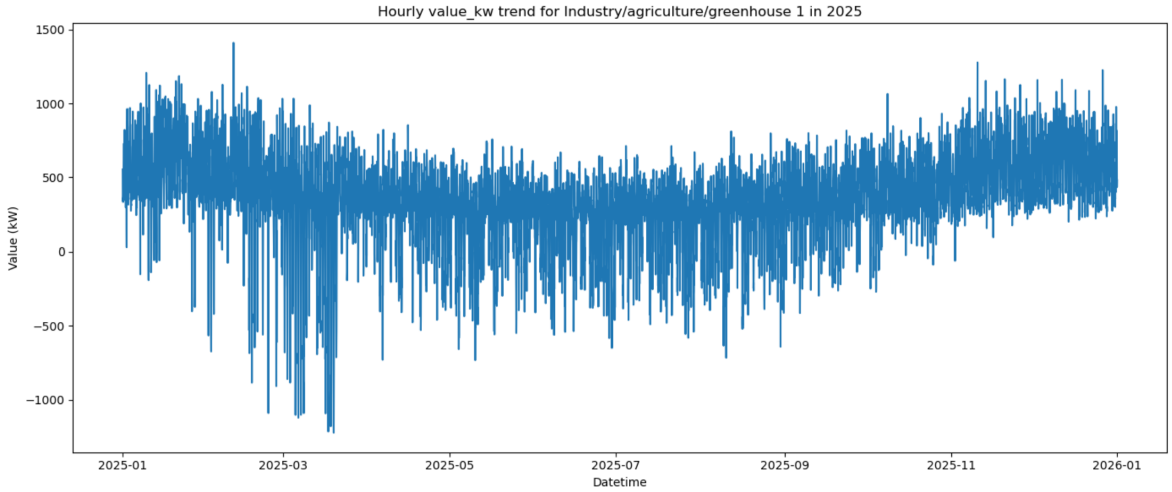

Figure F.6: Industry/agriculture/greenhouse 1 hourly value 2025

Next, the industry sectors will be discussed. The plot for Industry Sector 1.1 shows a consistent hourly power pattern over 2025, with values generally ranging between 0 and 300 kW. There's a slight decline in usage leading into mid-year, followed by a gradual increase toward the end of the year. While fluctuations are frequent, the power remains mostly positive with few instances dipping below zero, indicating continuous consumption with very limited or no feed-in.

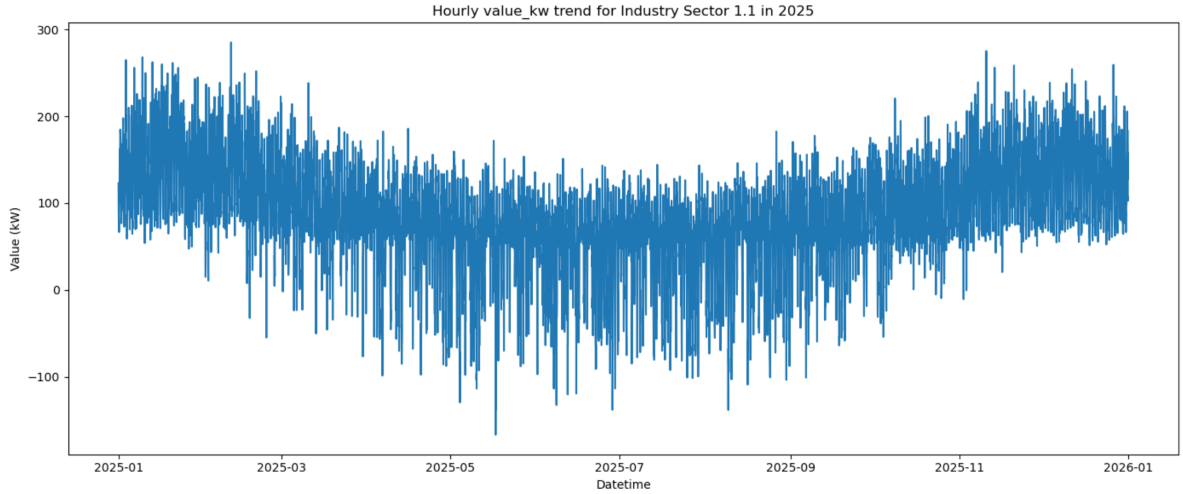

Figure F.7: Industry sector 1.1 hourly value 2025

Figure F.8 shows a much higher power range than sector 1.1, with values peaking above 1500 kW. A distinct drop in power consumption begins around March and continues into the middle of the year, after which the trend stabilizes at a lower level until consumption increases again in the final months. The middle period even includes occasional negative values, suggesting brief feed-in events. The pattern clearly follows a seasonal cycle.

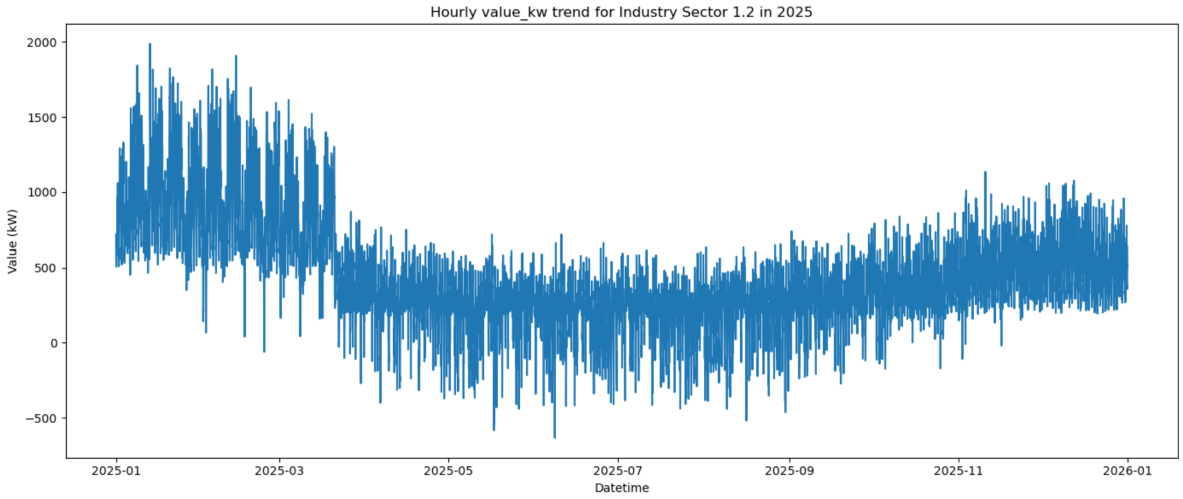

Figure F.8: Industry sector 1.2 hourly value 2025

Industry Sector 1.3 reveals a dramatic shift. The early part of the year shows high variability and extreme swings, including strong feed-in values (down to -1000 kW). Around March, there is a significant and abrupt decline in both positive and negative extremes, after which the pattern becomes more stable but flatter. Toward the year's end, power usage begins to increase again, though more gradually.

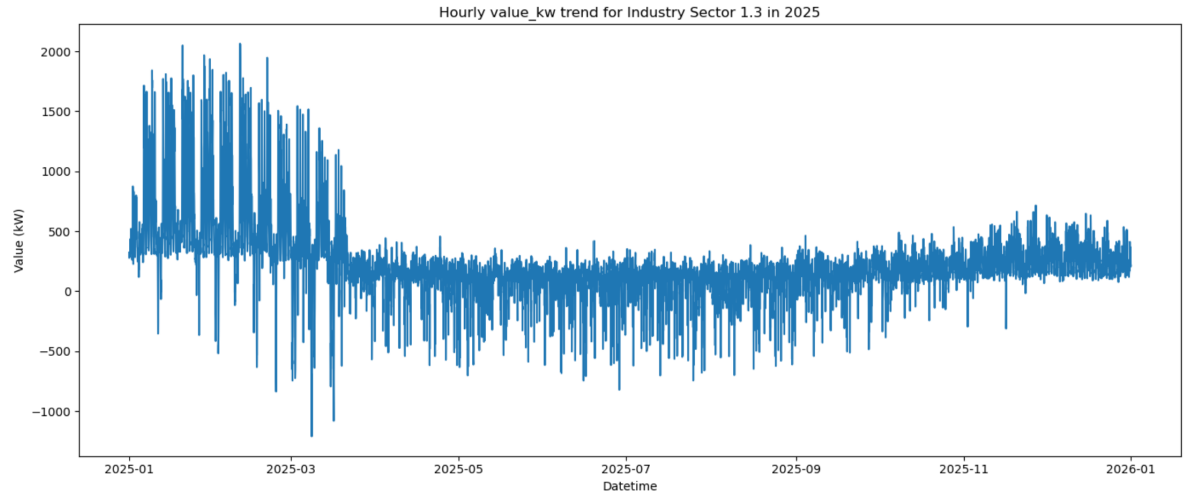

Figure F.9: Industry sector 1.3 hourly value 2025

In Industry Sector 2.1, the pattern is similar to sector 1.3. Early in the year, power values vary widely, often ranging between -3000 kW and +3000 kW. After March, there's a pronounced stabilization with much lower fluctuations. As with the other industrial plots, a slow increase in power consumption is visible in the final months. This sector appears to switch from volatile usage and feed-in to more consistent demand.

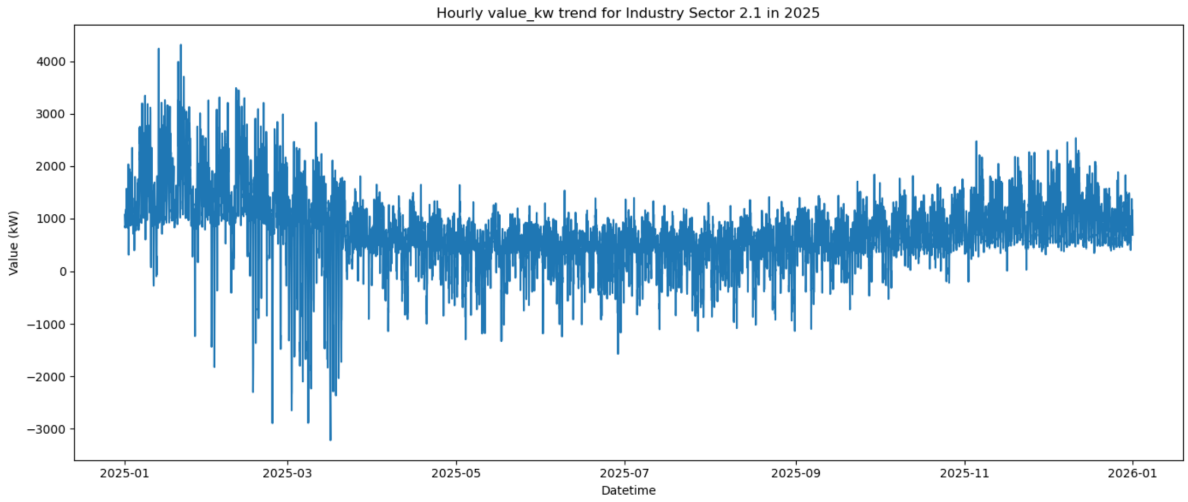

Figure F.10: Industry sector 2.1 hourly value 2025

Industry Sector 2.2 exhibits the same overall shape: intense variability early in the year, followed by stabilization through summer and an upward trend into the winter months. Negative values (feed-in) dominate the early months, indicating possible on-site generation, while later in the year, consumption overtakes and remains stable.

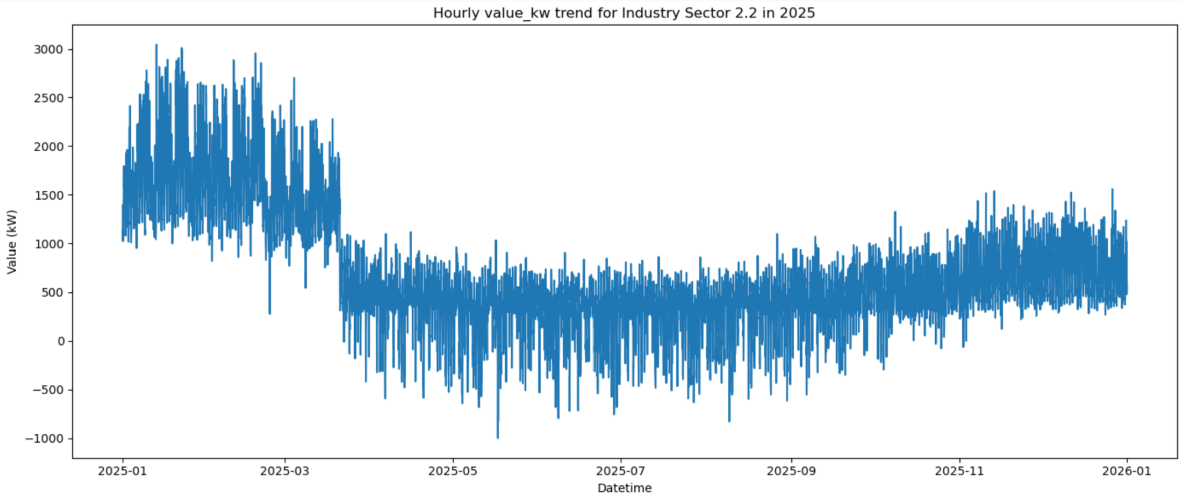

Figure F.11: Industry sector 2.2 hourly value 2025

Figure F.12 shows the hourly power values for Industry Sector 2.3 in 2025. Like Greenhouse 3, the data for this sector was incomplete, with substantial portions of the year missing. To address this issue, the available data from the first three months was repeated to fill the remainder of the year. As a result, the visualized trend reflects a looping pattern rather than actual continuous measurements. The recorded values range from approximately 2500 kW to 3750 kW, with several notable dips that likely reflect operational pauses or fluctuations in production demand. Despite the artificial repetition, the data suggests a relatively stable consumption profile without instances of feed-in, indicating the sector primarily consumes electricity.

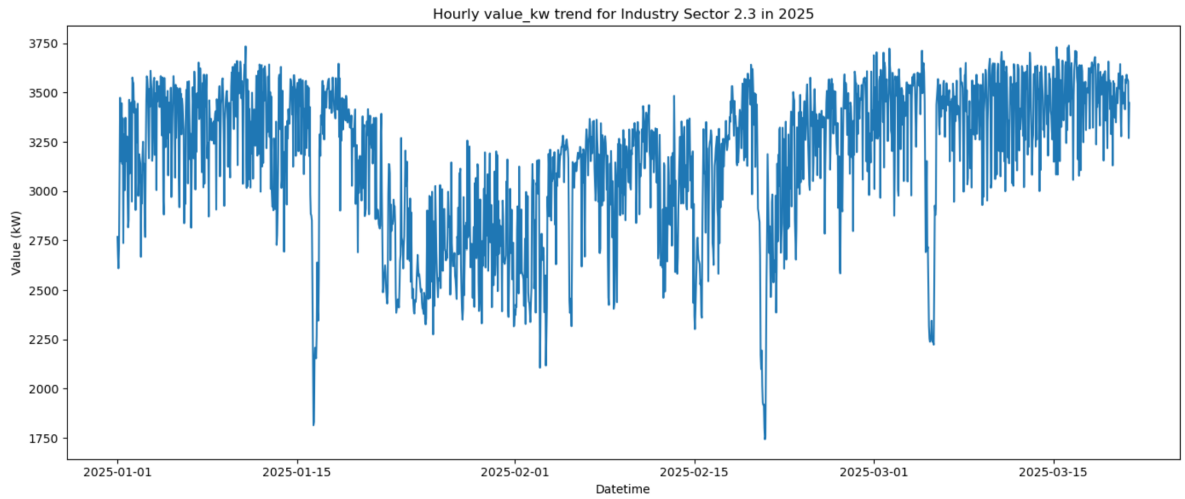

Figure F.12: Industry sector 2.3 hourly value 2025

Industry Sector 2.4, depicted in Figure F.13, shows a full year of hourly power data and exhibits a clear seasonal consumption pattern. Power usage peaks in the early months and declines steadily through spring and summer, during which negative values (feed-in) are frequent—suggesting active on-site generation, likely solar. The trend begins to rise again toward the end of the year, although the magnitude of fluctuation remains high throughout. The sector transitions between being a net generator and a net consumer depending on the season.

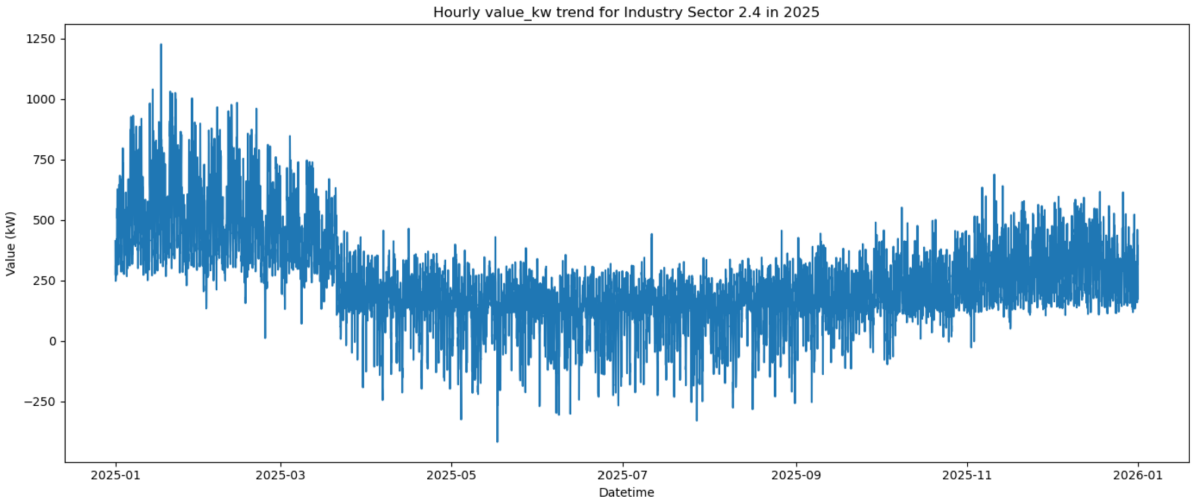

Figure F.13: Industry sector 2.4 hourly value 2025

Figure F.14 presents the hourly power trend for Industry Sector 3 in 2025. Like sector 2.3, the data for this sector was incomplete. To create a full-year representation, the available data from the first three months was repeated for the remaining months. This repetition results in a recurring pattern that reflects the characteristics of the initial period rather than actual variation across the year. The power profile shows extreme fluctuations with sharp peaks reaching above 2000 kW and near-zero troughs, consistent with an intermittent or batch-based operational process. No feed-in is observed, implying that the sector is strictly a power consumer.

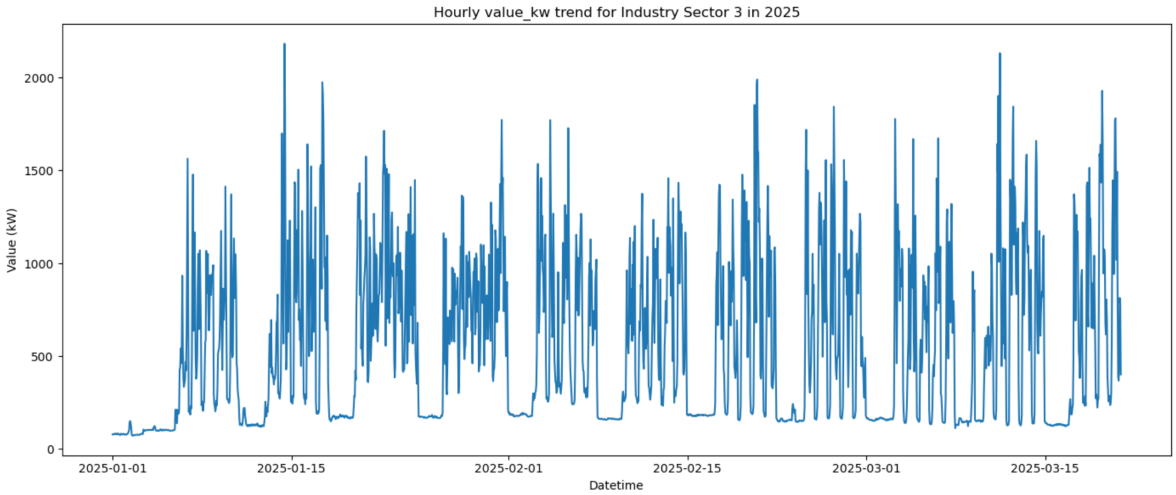

Figure F.14: Industry sector 3 hourly value 2025

Lastly, there will be looked at the Train networks. The plots for Train Network 1 and Train Network 3 (Figures F.15 and F.16) display nearly identical patterns, both in shape and in absolute power levels. These networks exhibit by far the lowest electricity consumption and production across all sectors considered in the analysis, with values mostly fluctuating between -50 kW and +120 kW. A faint seasonal trend is visible: higher power values appear at the beginning and end of the year, while the summer months show a modest decline in both magnitude and variability. Despite the noise in the data, both networks demonstrate relatively stable, small-scale operation with occasional instances of negative values—suggesting minor feed-in events. The similarity between the two trends implies they serve comparable functions or operate under nearly identical schedules and usage profiles.

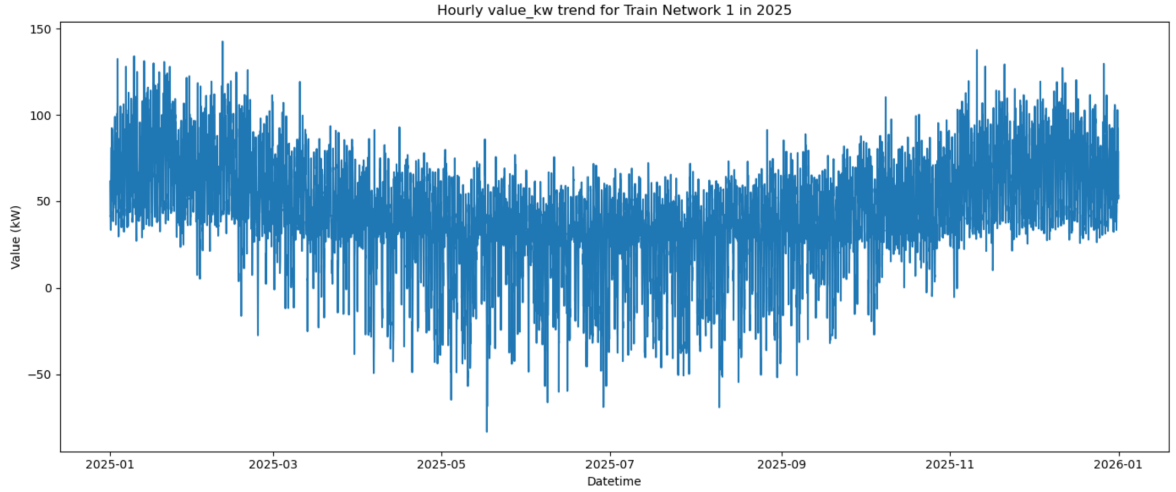

Figure F.15: Train network 1 hourly value 2025

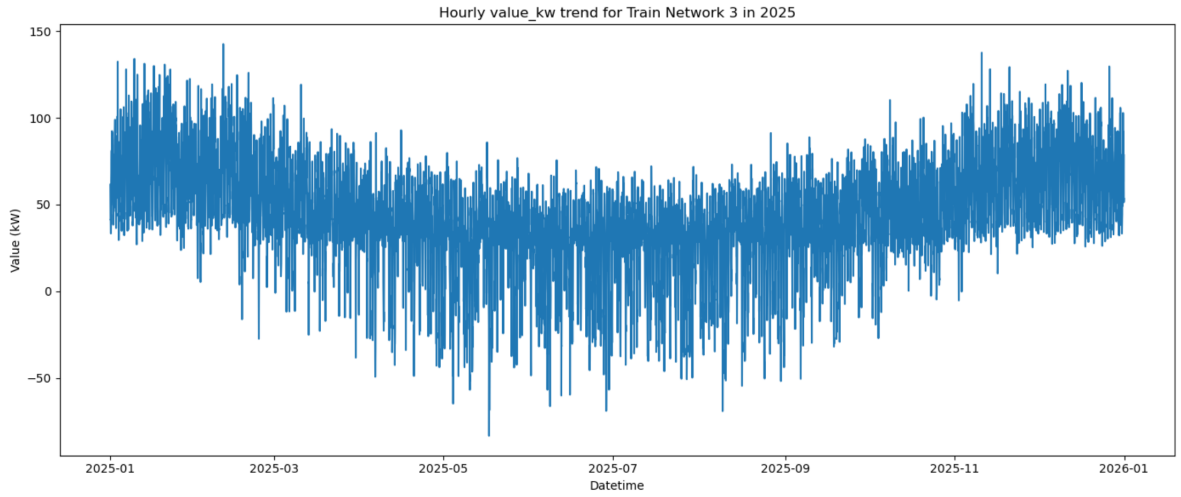

Figure F.16: Train network 3 hourly value 2025

All in all, the hourly power data for 2025 show clear differences between the building blocks. Most building sectors use more electricity in winter and occasionally feed power back into the grid during summer, likely due to solar panels. Among them, Building Sector 2.1 stands out with both the highest overall consumption and frequent feed-in. In the industry category, Industry Sector 2.1 recorded the highest power peaks, reaching up to 4000 kW early in the year. Some other industry sectors and greenhouse profiles showed incomplete data, which was filled by repeating the first three months—these patterns should be interpreted with caution. Greenhouses generally displayed variable demand, with some feed-in during certain periods, but overall they remained electricity consumers. In contrast, the train networks showed the lowest overall power values with nearly identical seasonal patterns and very limited feed-in, indicating a relatively small and stable electricity footprint.